



QUANTUM
COMPUTING
AND
SIMULATION
CENTER



TENSOR NETWORK ALGORITHMS FOR HIGH-DIMENSIONAL HEP SIMULATIONS

Simone Montangelo
University of Padova



Dipartimento
di Fisica
e Astronomia
Galileo Galilei



QUANTUM
FLAGSHIP



UNIVERSITÀ
DI PADOVA

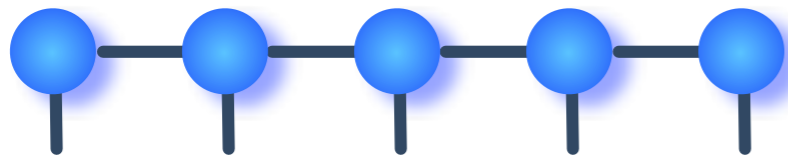
TENSOR NETWORKS STATES

$$\psi_{\alpha_1, \alpha_2, \dots, \alpha_N} \quad \mathcal{O}(d^N)$$



TENSOR NETWORKS STATES

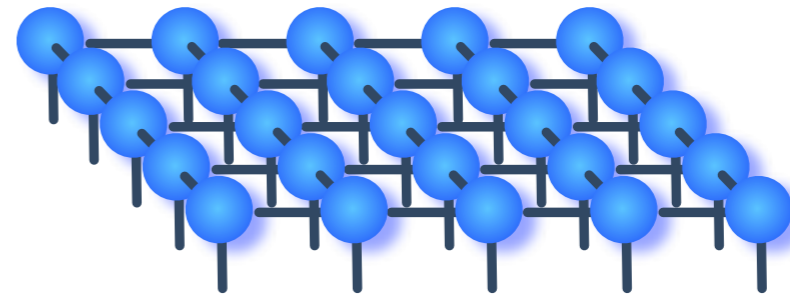
$$\psi_{\alpha_1, \alpha_2, \dots, \alpha_N} \quad \mathcal{O}(d^N)$$



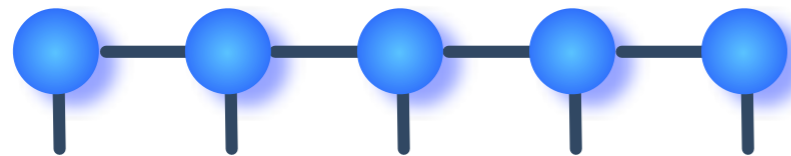
$$A_{\alpha_1}^{\beta_1} A_{\alpha_2}^{\beta_1 \beta_2} \dots A_{\alpha_N}^{\beta_{N-1}} \quad \mathcal{O}(N d m^2)$$

TENSOR NETWORK STATES

$$\psi_{\alpha_1, \alpha_2, \dots, \alpha_N} \quad \mathcal{O}(d^N)$$



PEPS

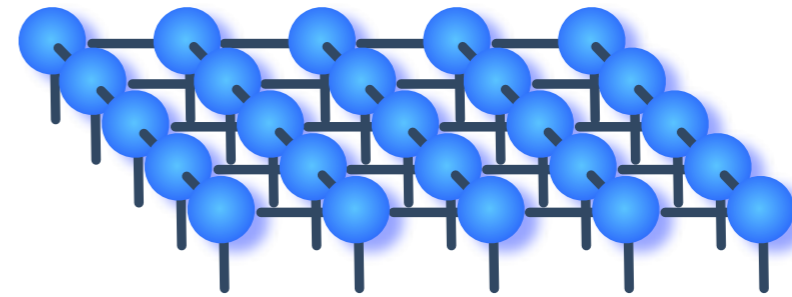


$$A_{\alpha_1}^{\beta_1} A_{\alpha_2}^{\beta_1 \beta_2} \dots A_{\alpha_N}^{\beta_{N-1}}$$

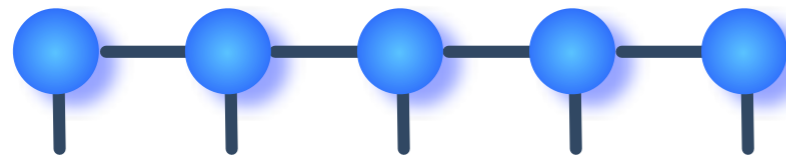
$\mathcal{O}(Ndm^2)$

TENSOR NETWORK STATES

$$\psi_{\alpha_1, \alpha_2, \dots, \alpha_N} \quad \mathcal{O}(d^N)$$

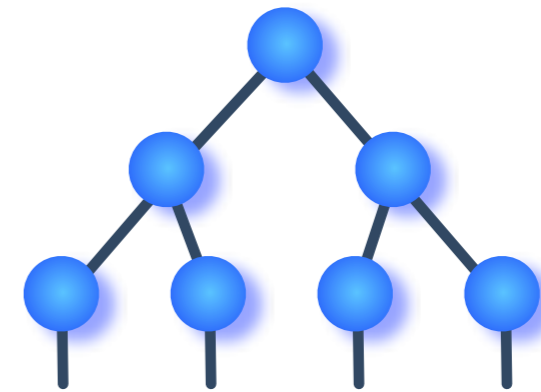


PEPS



$$A_{\alpha_1}^{\beta_1} A_{\alpha_2}^{\beta_1 \beta_2} \dots A_{\alpha_N}^{\beta_{N-1}}$$

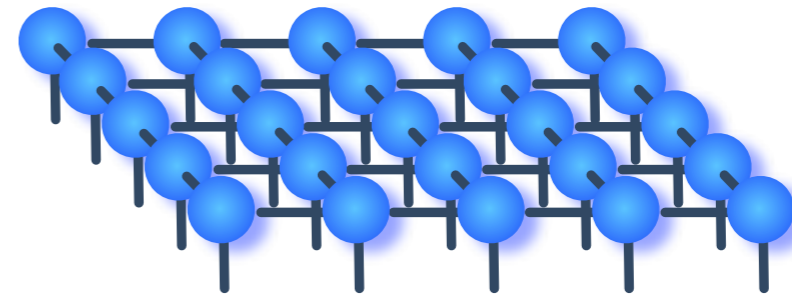
$\mathcal{O}(Ndm^2)$



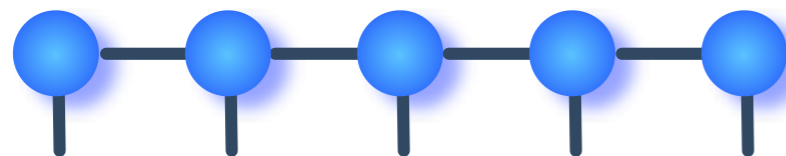
Tree Tensor Network

TENSOR NETWORKS STATES

$$\psi_{\alpha_1, \alpha_2, \dots, \alpha_N} \quad \mathcal{O}(d^N)$$

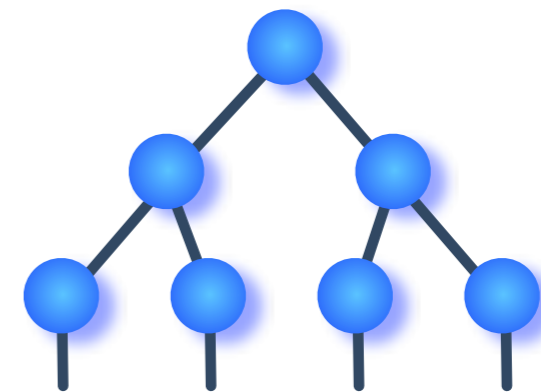


PEPS



$$A_{\alpha_1}^{\beta_1} A_{\alpha_2}^{\beta_1 \beta_2} \dots A_{\alpha_N}^{\beta_{N-1}}$$

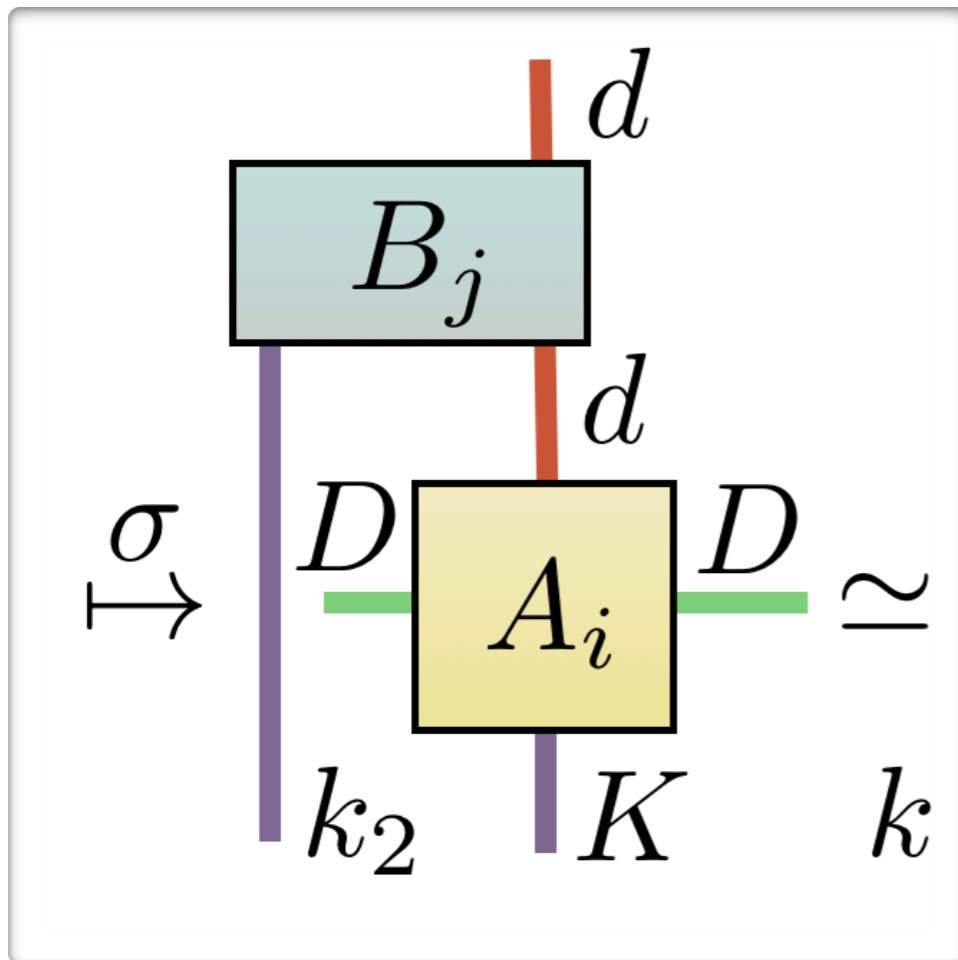
$\mathcal{O}(N d m^2)$



Tree Tensor Network

Tensor networks states are a compressed description of the system tunable between mean field and exact

TENSOR NETWORK ALGORITHMS

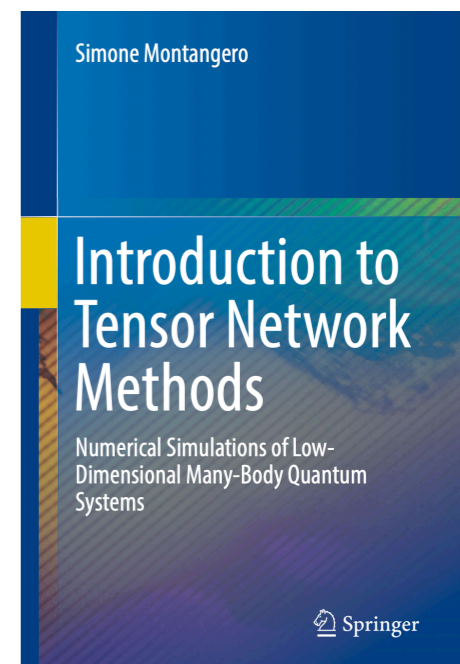


- *State of the art in 1D (poly effort)*
- *No sign problem*
- *Extended to open quantum systems*
- *Machine Learning & Big Data*
- *Compression of LLM*
- *Extended to lattice gauge theories*
- *Thousands of low-entangled qubits*

U. Schollwock, RMP (2005)

I. Glasser, et al. PRX (2018)

A. Cichocki, ECM (2013)



ENTANGLEMENT OF PURE MANY-BODY QUANTUM SYSTEMS

For pure states:

$$\mathcal{S} = -\text{Tr} \rho \log \rho$$

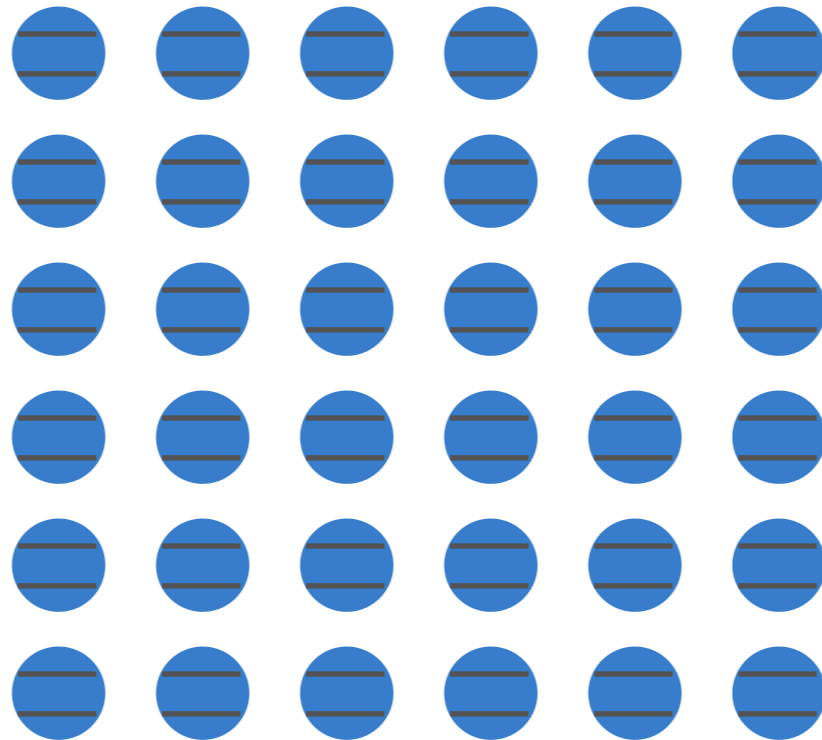
Von Neumann Entropy

ENTANGLEMENT OF PURE MANY-BODY QUANTUM SYSTEMS

For pure states:

$$\mathcal{S} = -\text{Tr} \rho \log \rho$$

Von Neumann Entropy

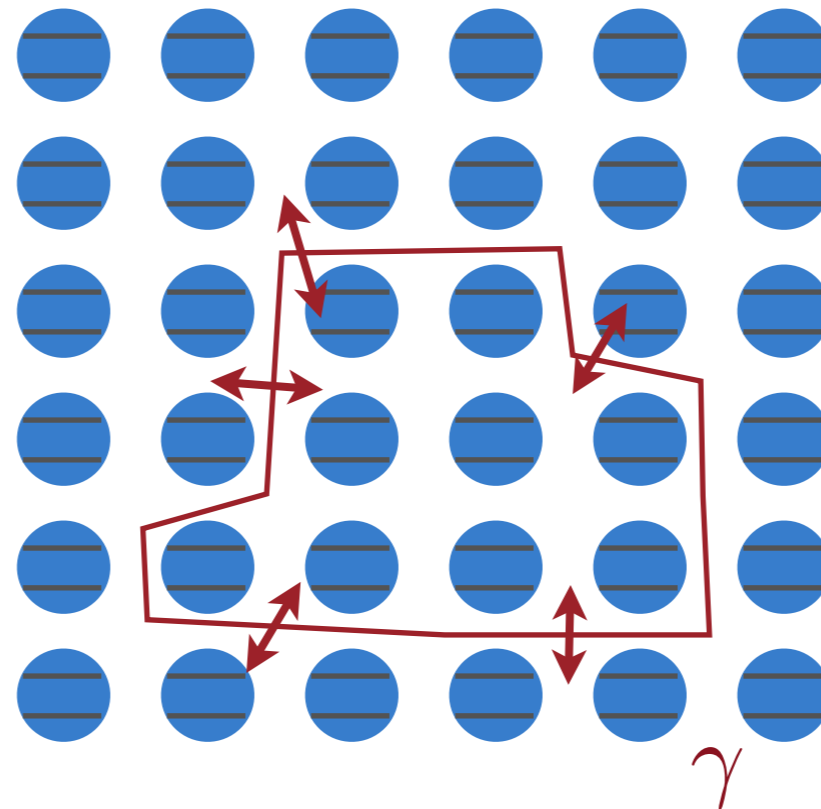


ENTANGLEMENT OF PURE MANY-BODY QUANTUM SYSTEMS

For pure states:

$$\mathcal{S} = -\text{Tr} \rho \log \rho$$

Von Neumann Entropy

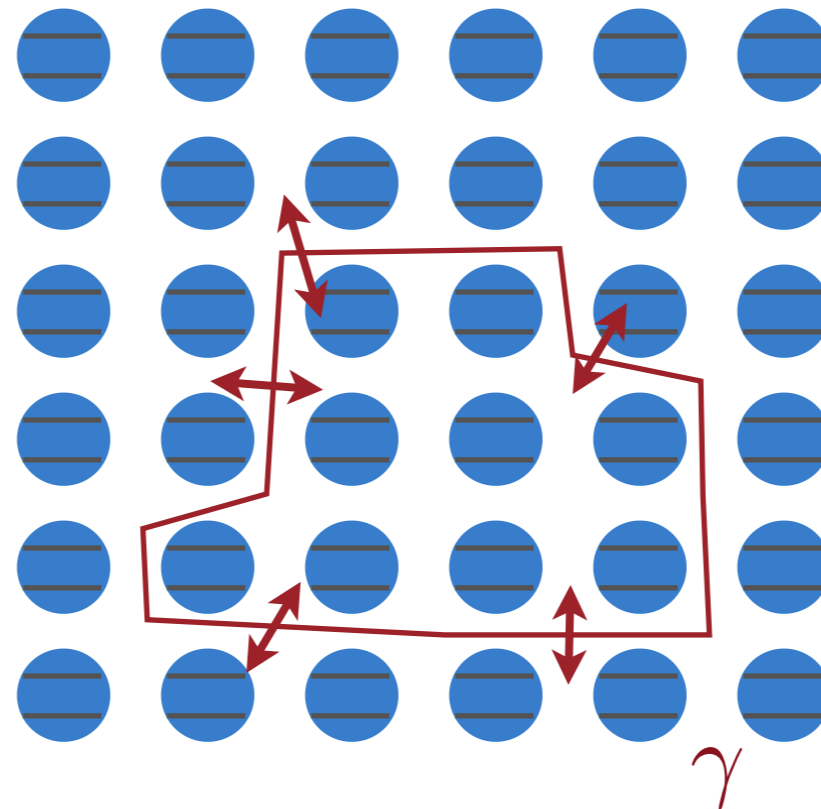


ENTANGLEMENT OF PURE MANY-BODY QUANTUM SYSTEMS

For pure states:

$$\mathcal{S} = -\text{Tr} \rho \log \rho$$

Von Neumann Entropy



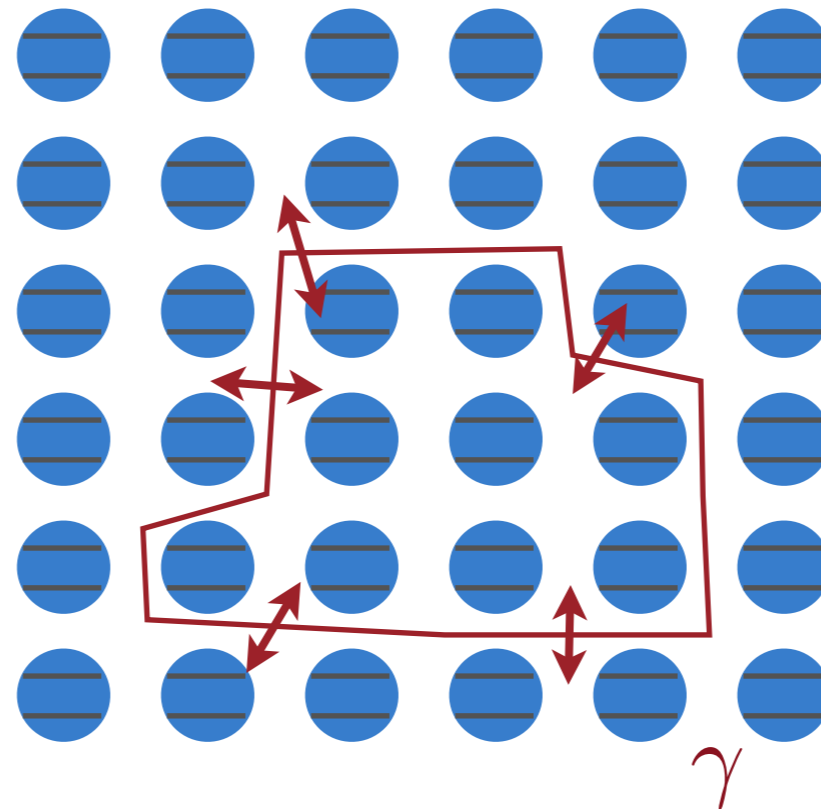
Area law

ENTANGLEMENT OF PURE MANY-BODY QUANTUM SYSTEMS

For pure states:

$$\mathcal{S} = -\text{Tr} \rho \log \rho$$

Von Neumann Entropy



Area law

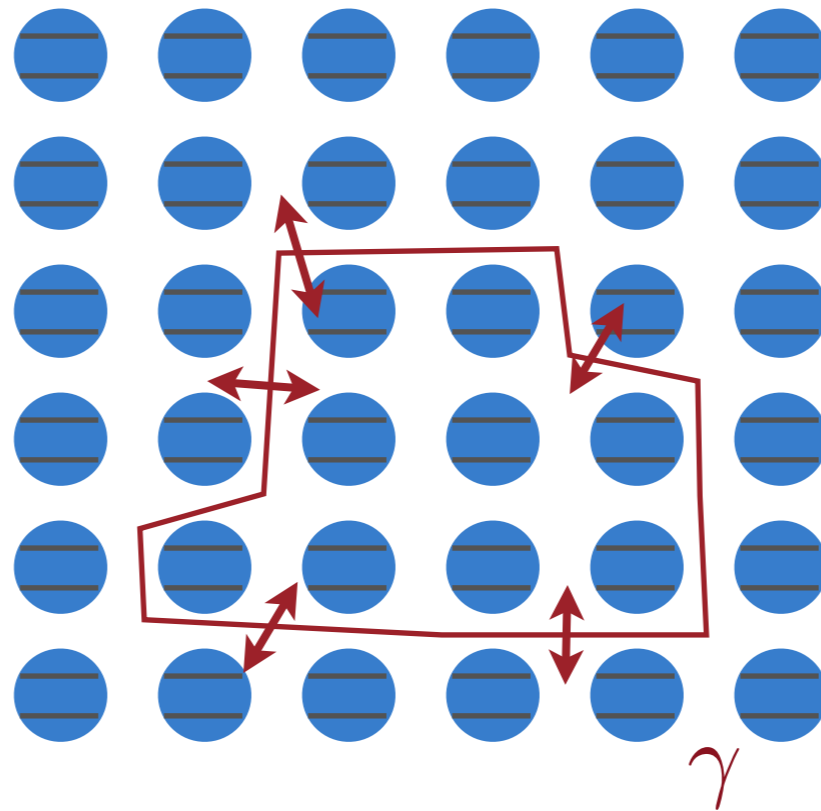
$$\mathcal{S} \propto \gamma$$

ENTANGLEMENT OF PURE MANY-BODY QUANTUM SYSTEMS

For pure states:

$$\mathcal{S} = -\text{Tr} \rho \log \rho$$

Von Neumann Entropy



Area law

$$\mathcal{S} \propto \gamma$$

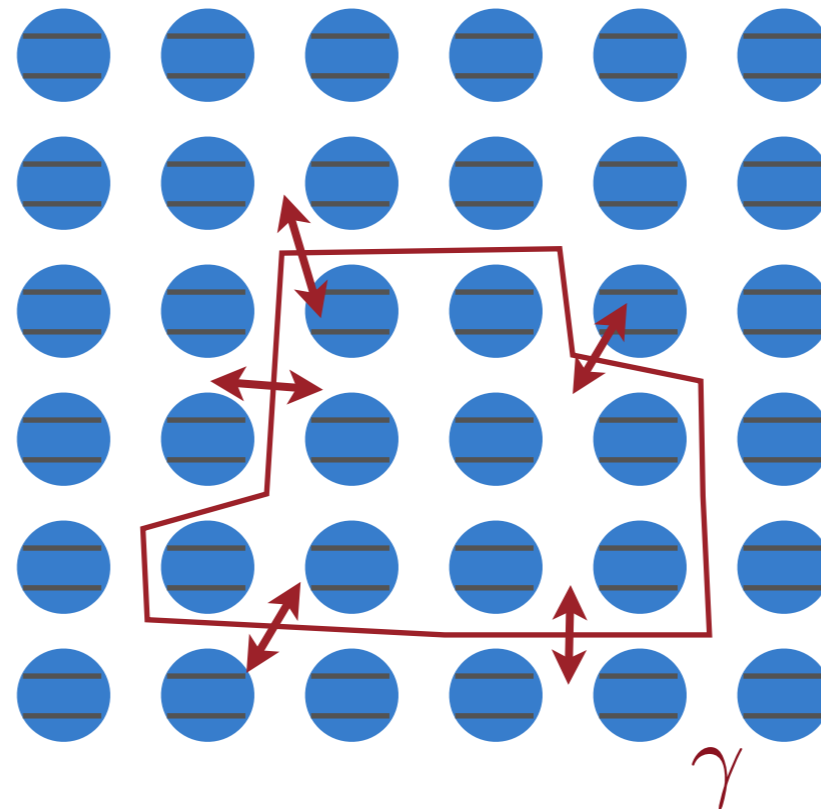
$$\mathcal{S} \propto N^{(D-1)}$$

ENTANGLEMENT OF PURE MANY-BODY QUANTUM SYSTEMS

For pure states:

$$\mathcal{S} = -\text{Tr} \rho \log \rho$$

Von Neumann Entropy



Area law

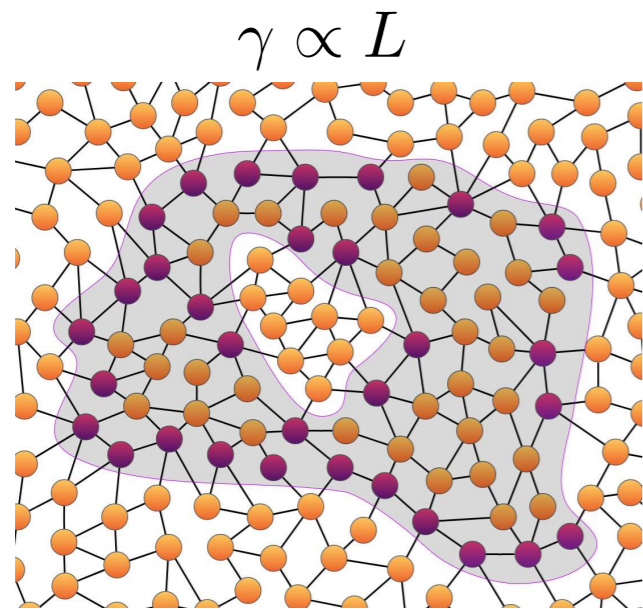
$$\mathcal{S} \propto \gamma$$

$$\mathcal{S} \propto N^{(D-1)}$$

1D critical systems:

$$\mathcal{S} = \frac{c}{3} \log N$$

AREA LAWS AND TENSOR NETWORKS

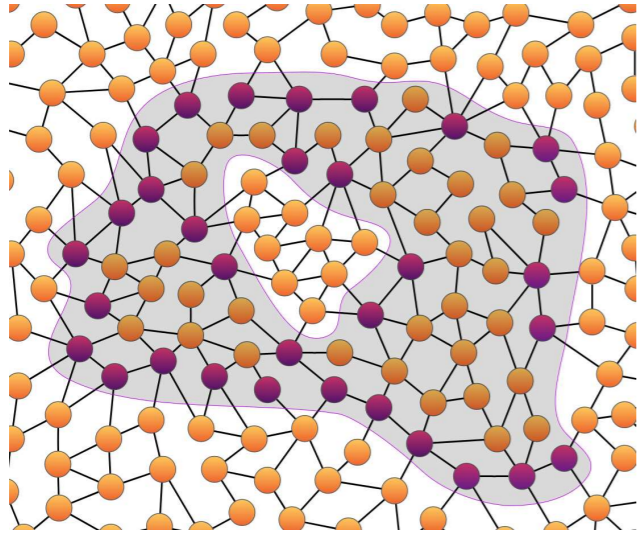


$$\gamma \propto L$$

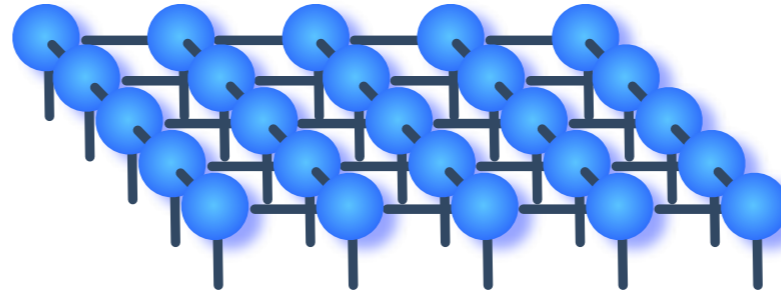
$$S \propto \gamma \propto L$$

AREA LAWS AND TENSOR NETWORKS

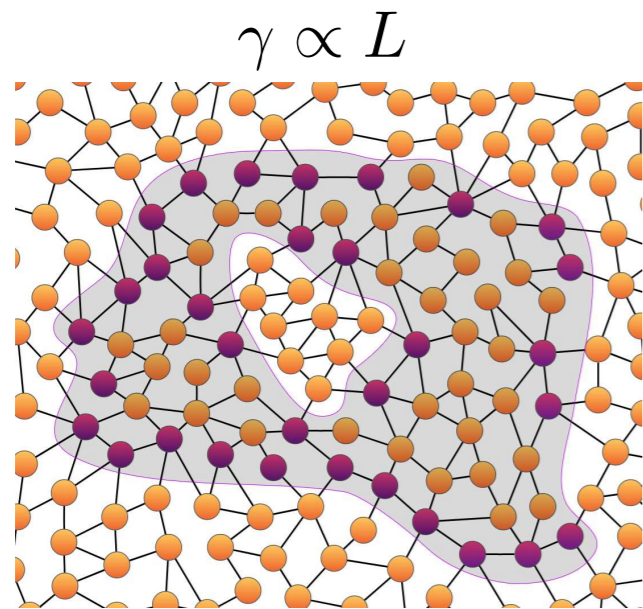
$$\gamma \propto L$$



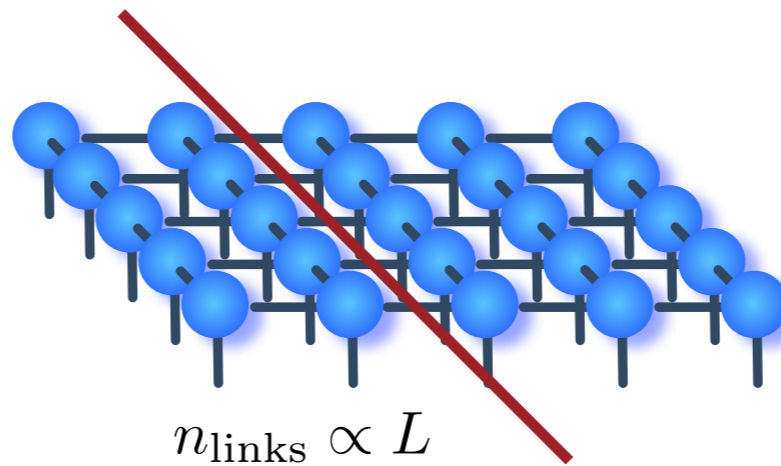
$$S \propto \gamma \propto L$$



AREA LAWS AND TENSOR NETWORKS

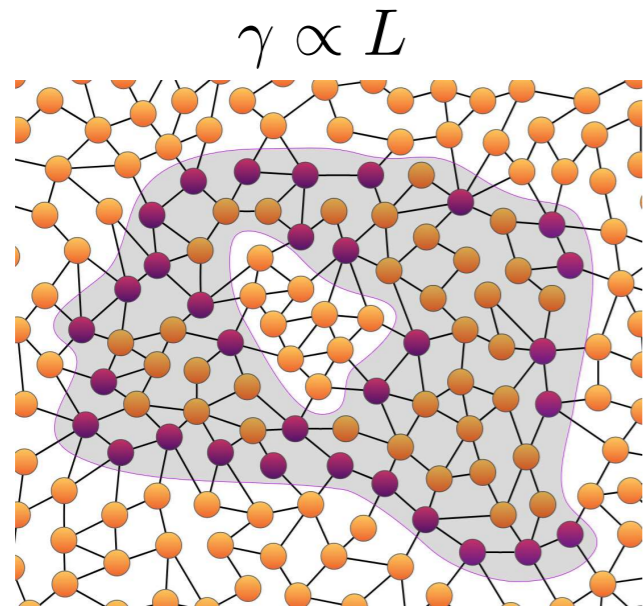


$S \propto \gamma \propto L$



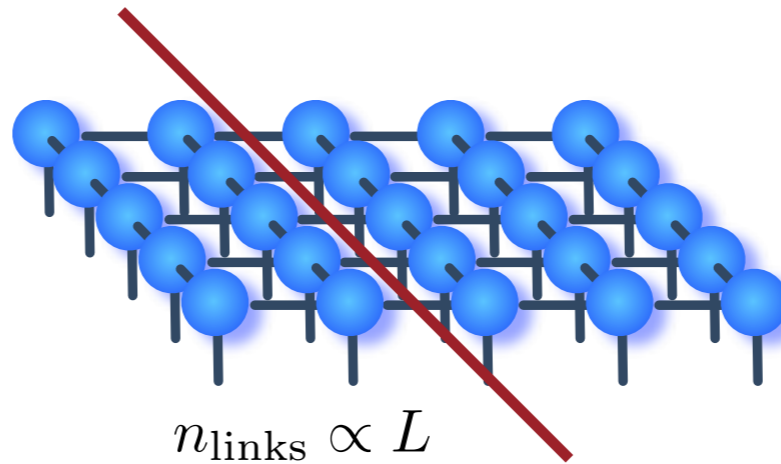
$n_{\text{links}} \propto L$

AREA LAWS AND TENSOR NETWORKS



$$\gamma \propto L$$

$$S \propto \gamma \propto L$$

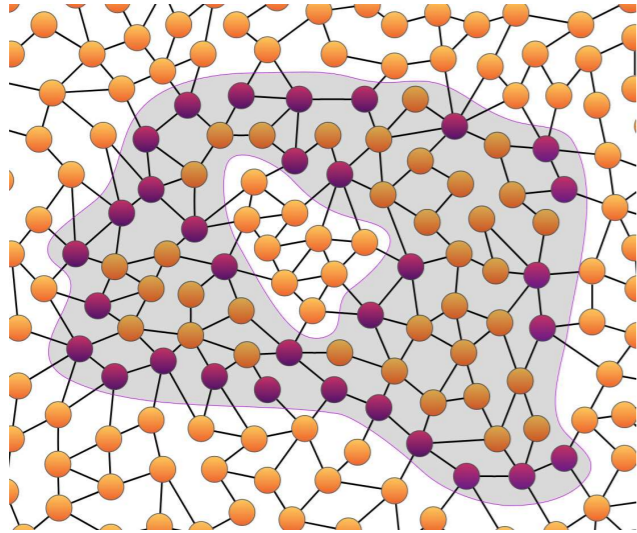


$$n_{\text{links}} \propto L$$

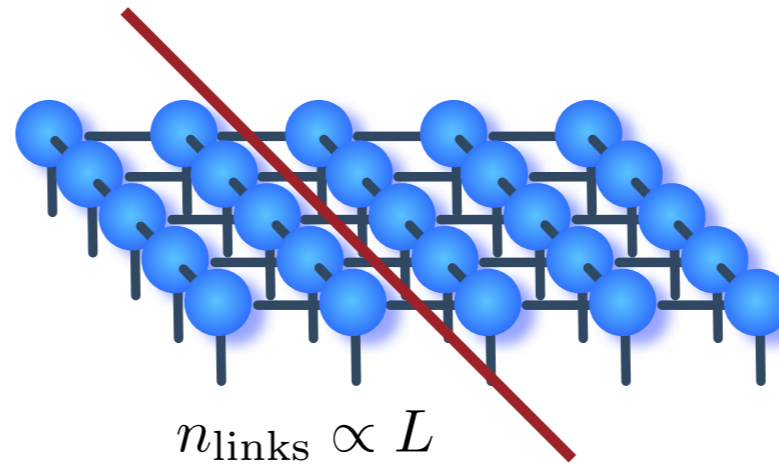
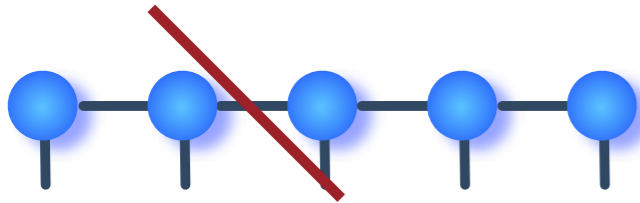
$$S_{\text{max}} \propto n_{\text{links}} \times \log m$$

AREA LAWS AND TENSOR NETWORKS

$$\gamma \propto L$$

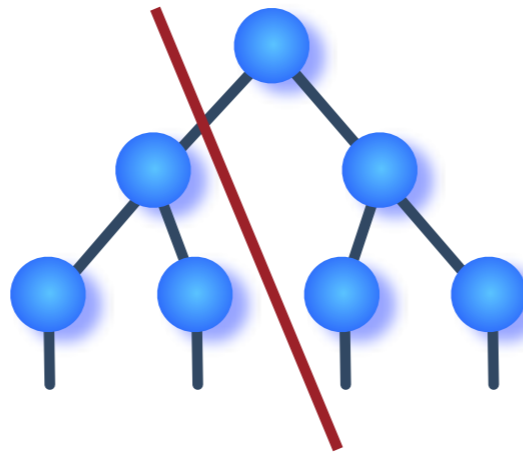


$$\mathcal{S} \propto \gamma \propto L$$

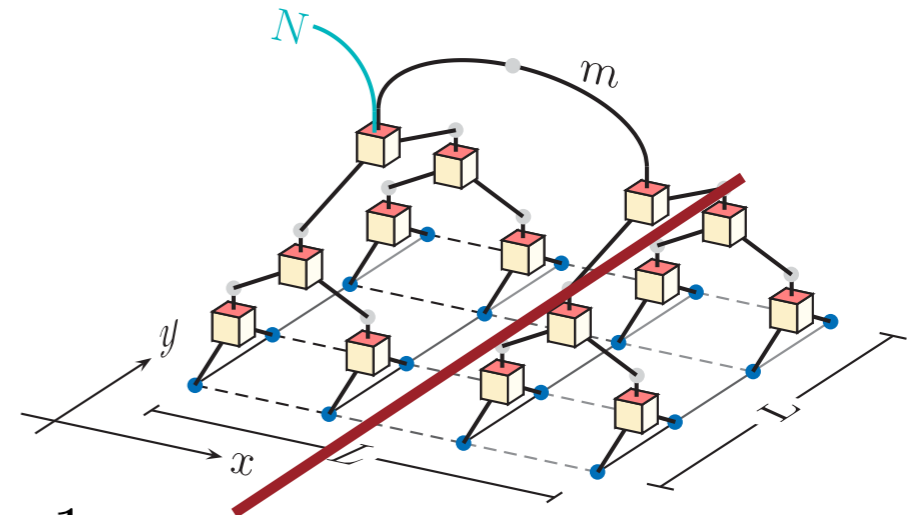


$$n_{\text{links}} \propto L$$

$$\mathcal{S}_{\text{max}} \propto n_{\text{links}} \times \log m$$

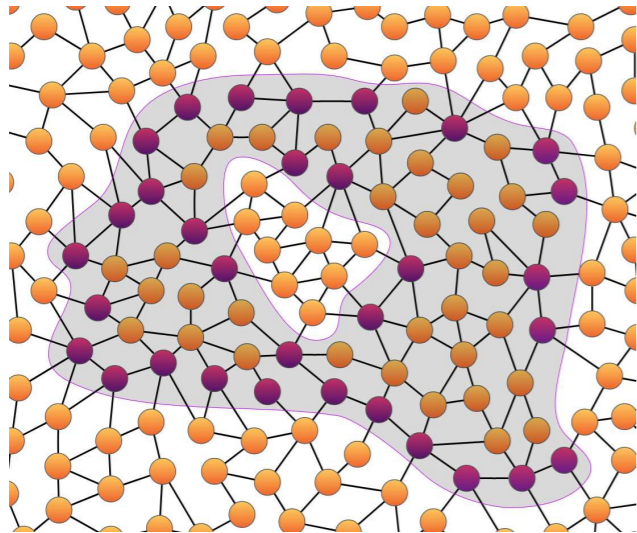


$$n_{\text{links}} = 1$$

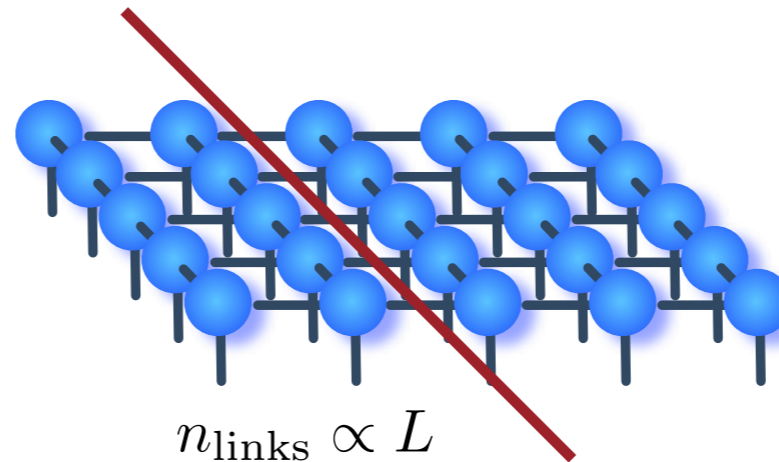
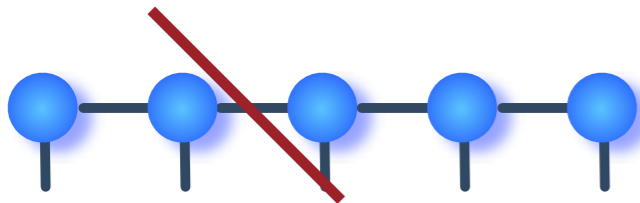


AREA LAWS AND TENSOR NETWORKS

$$\gamma \propto L$$



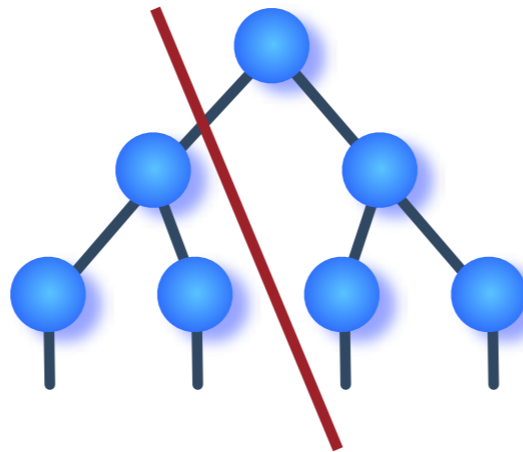
$$S \propto \gamma \propto L$$



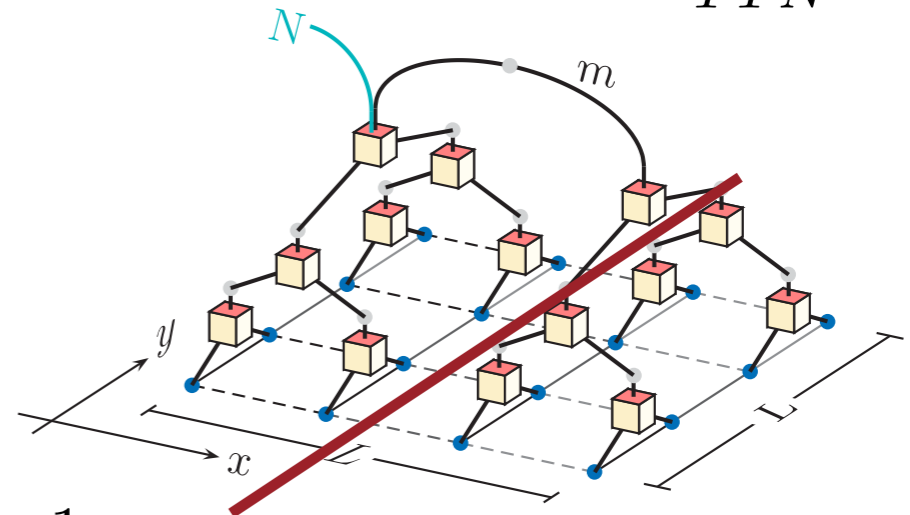
$$n_{\text{links}} \propto L$$

$$S_{\text{max}} \propto n_{\text{links}} \times \log m$$

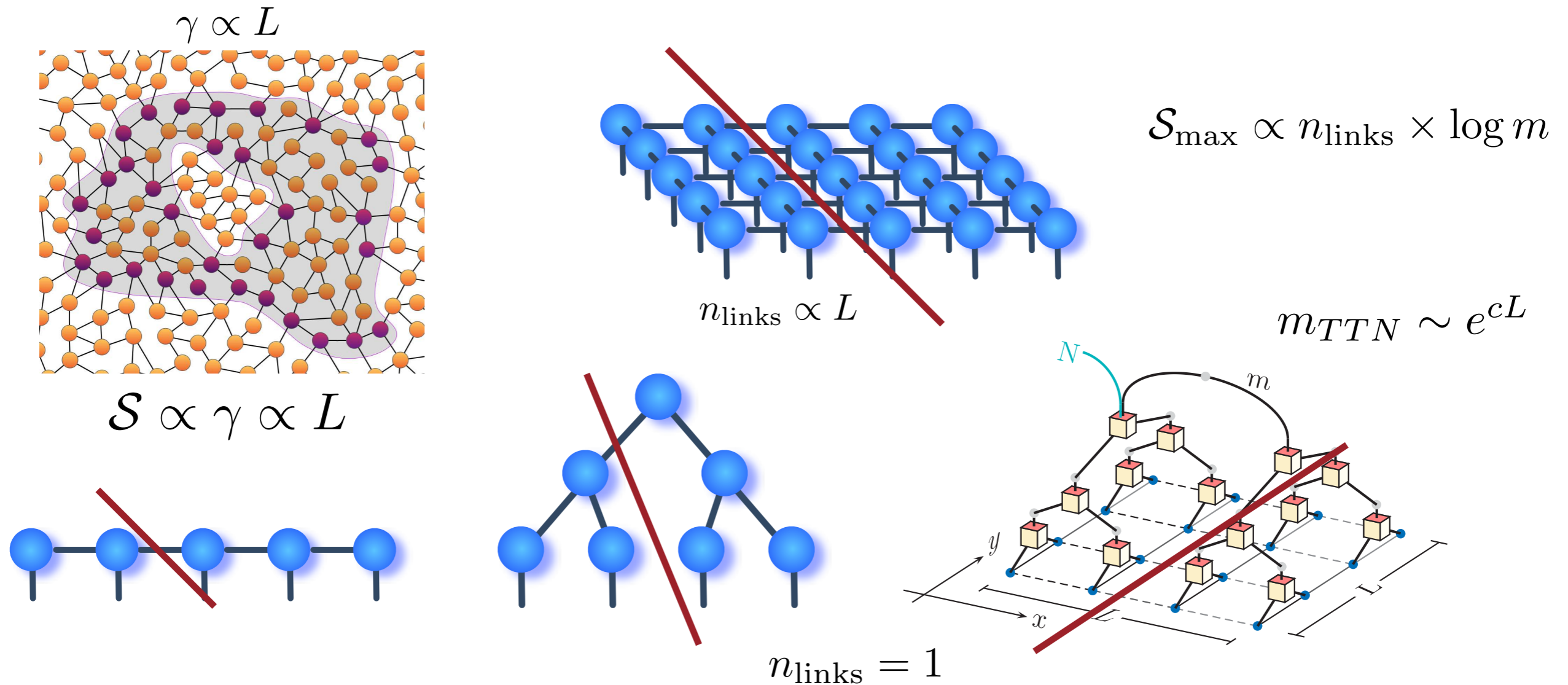
$$m_{TTN} \sim e^{cL}$$



$$n_{\text{links}} = 1$$

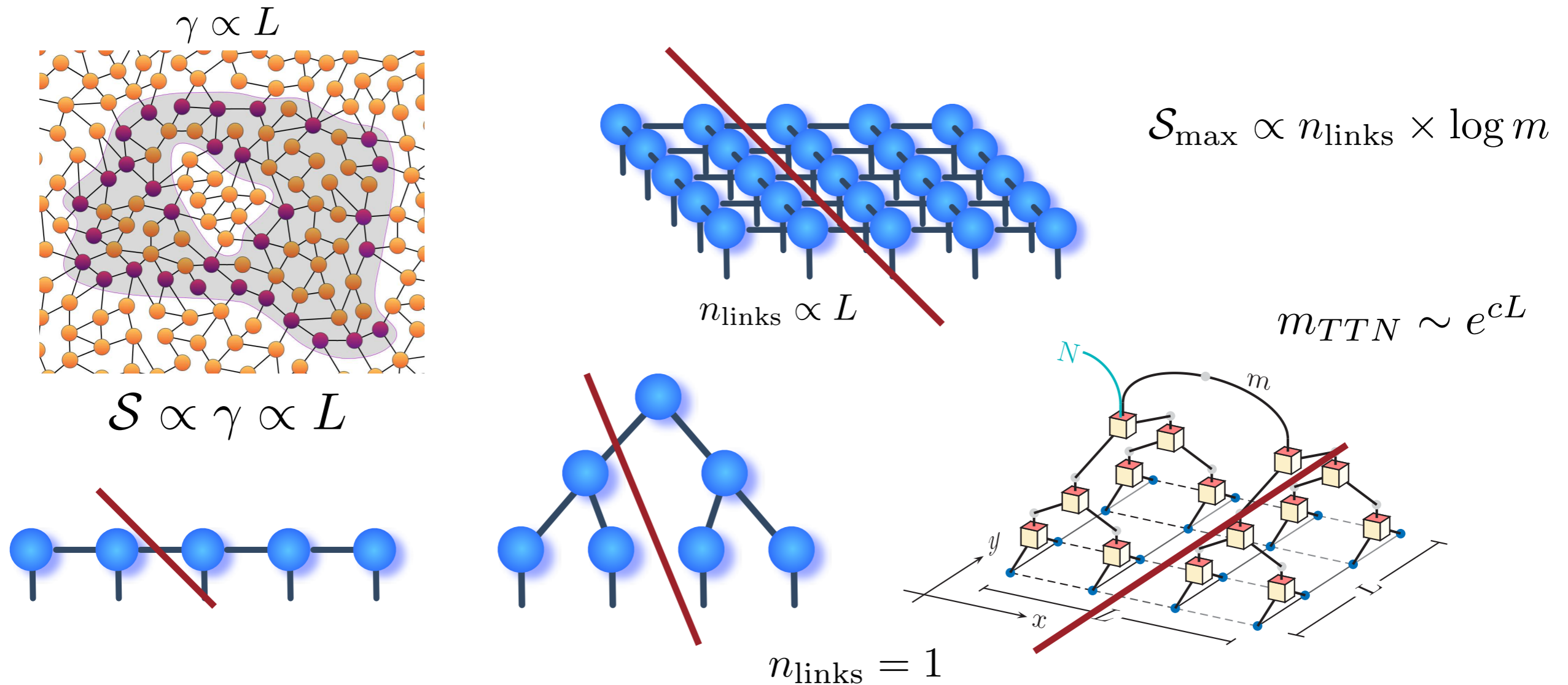


AREA LAWS AND TENSOR NETWORKS



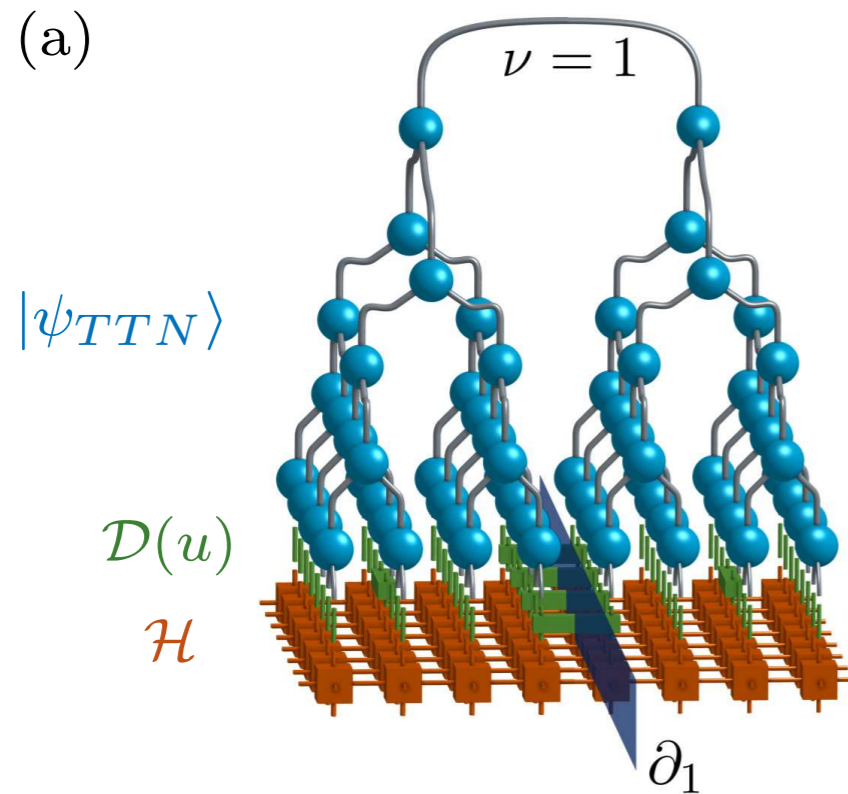
Tensor Network	Complexity	Area law in 2D	Typical Bond dimensions	Exact contractable
MPS / DMRG	$\mathcal{O}\{\chi^3\}$	No (Only in 1D)	> 10.000	Yes ($\mathcal{O}\{\chi^3\}$)
TTN	$\mathcal{O}\{\chi^4\}$	No (Only in 1D)	$\approx 1.000 - 2.000$	Yes ($\mathcal{O}\{\chi^4\}$)
PEPS	$\mathcal{O}\{\chi^{10}\}$	Yes	~ 10	No ($\mathcal{O}\{\chi^L\}$)
MERA	$\mathcal{O}\{\chi^8\}$ (1D), $\mathcal{O}\{\chi^{16}\}$ (2D)	Yes	~ 10	Yes ($\mathcal{O}\{\chi^8\}$)

AREA LAWS AND TENSOR NETWORKS

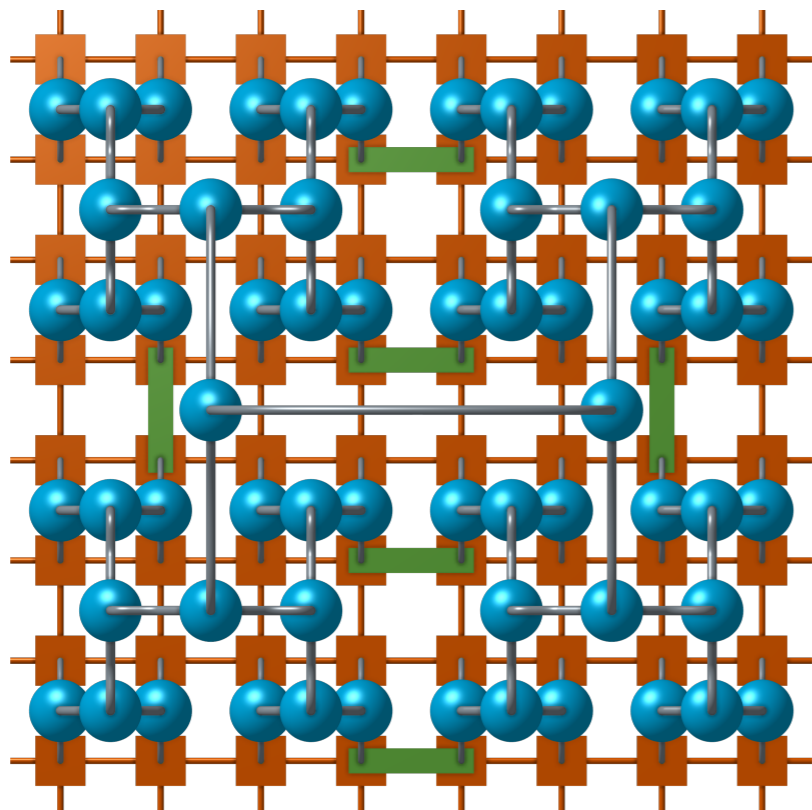


Tensor Network	Complexity	Area law in 2D	Typical Bond dimensions	Exact contractable
MPS / DMRG	$\mathcal{O}\{\chi^3\}$	No (Only in 1D)	> 10.000	Yes ($\mathcal{O}\{\chi^3\}$)
TTN	$\mathcal{O}\{\chi^4\}$	No (Only in 1D)	$\approx 1.000 - 2.000$	Yes ($\mathcal{O}\{\chi^4\}$)
PEPS	$\mathcal{O}\{\chi^{10}\}$	Yes	~ 10	No ($\mathcal{O}\{\chi^L\}$)
MERA	$\mathcal{O}\{\chi^8\}$ (1D), $\mathcal{O}\{\chi^{16}\}$ (2D)	Yes	~ 10	Yes ($\mathcal{O}\{\chi^8\}$)
aTTN	$\mathcal{O}\{\chi^4\}$	Yes*	≈ 500	Yes ($\mathcal{O}\{\chi^4\}$)

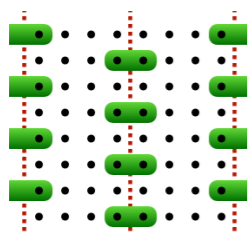
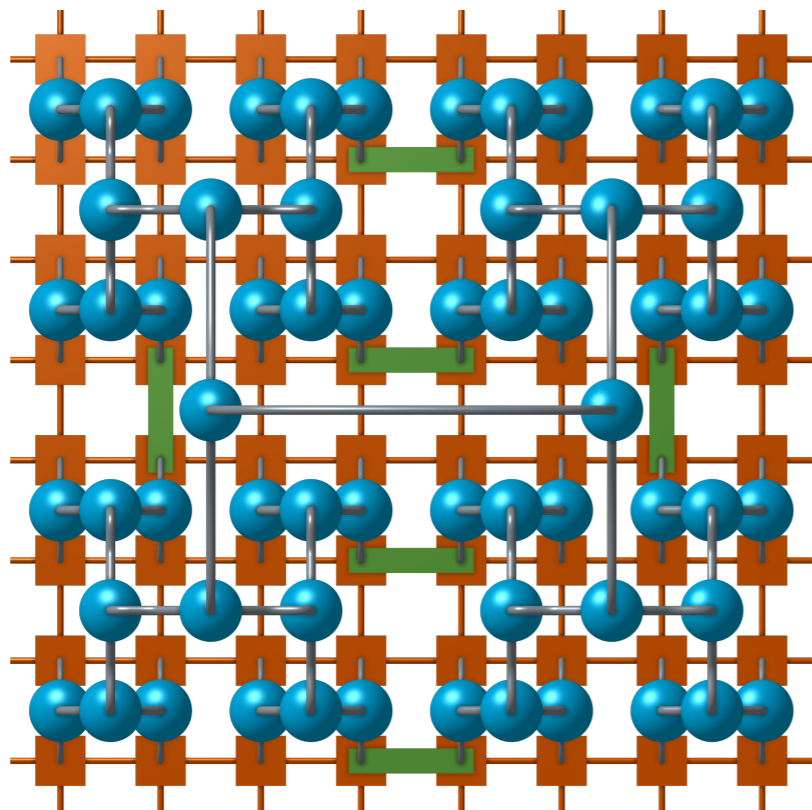
AUGMENTED TREE TENSOR NETWORKS



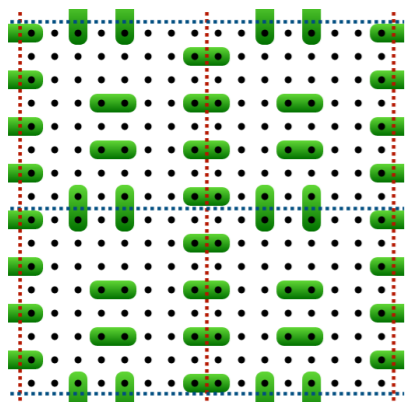
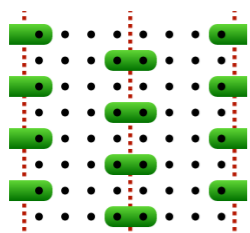
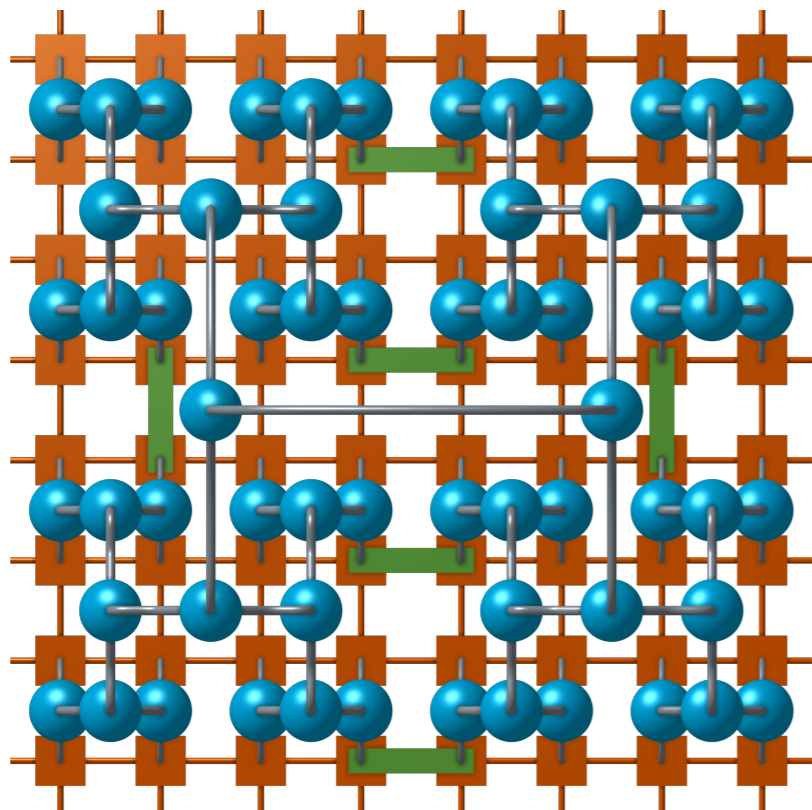
AUGMENTED TREE TENSOR NETWORKS



AUGMENTED TREE TENSOR NETWORKS

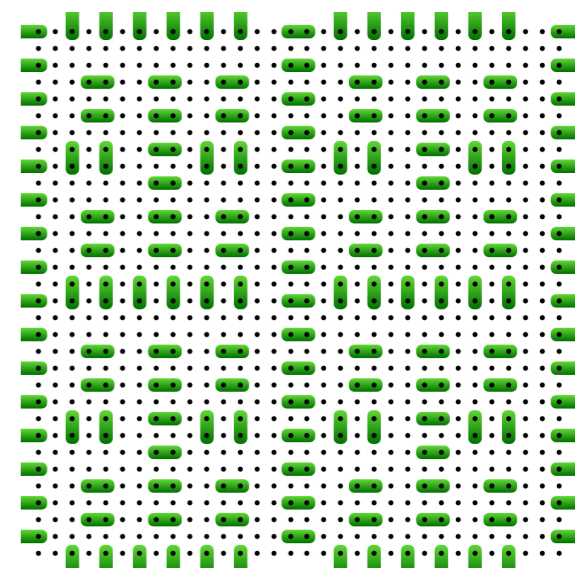
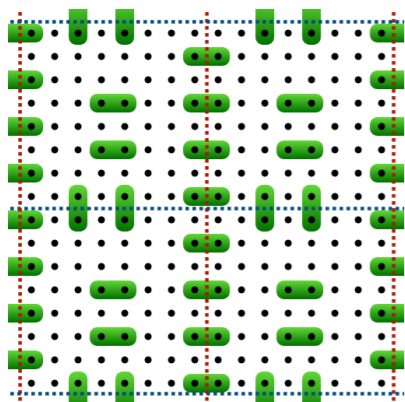
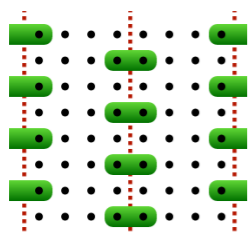
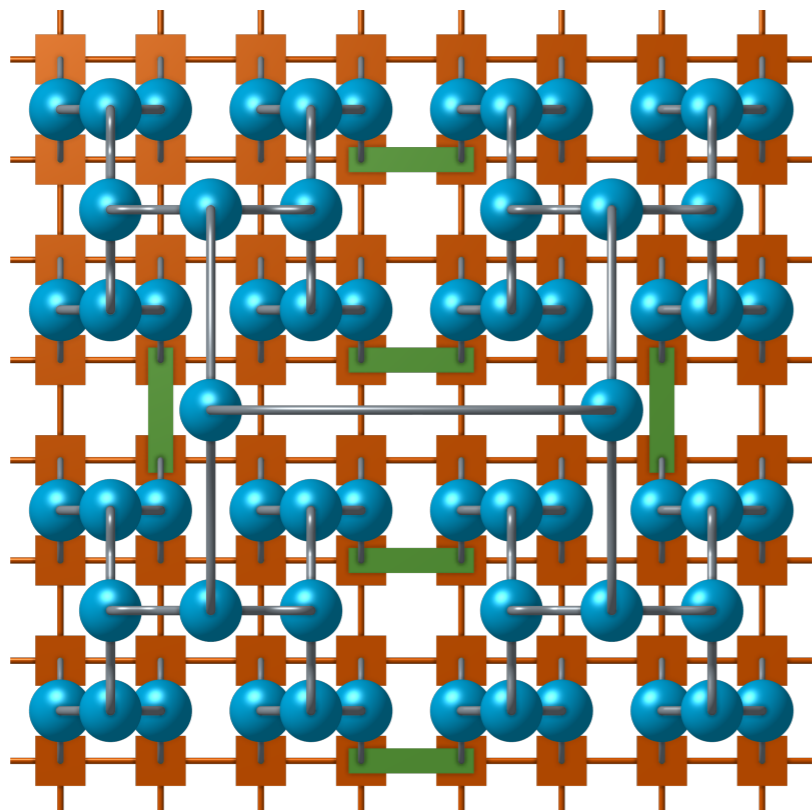


AUGMENTED TREE TENSOR NETWORKS



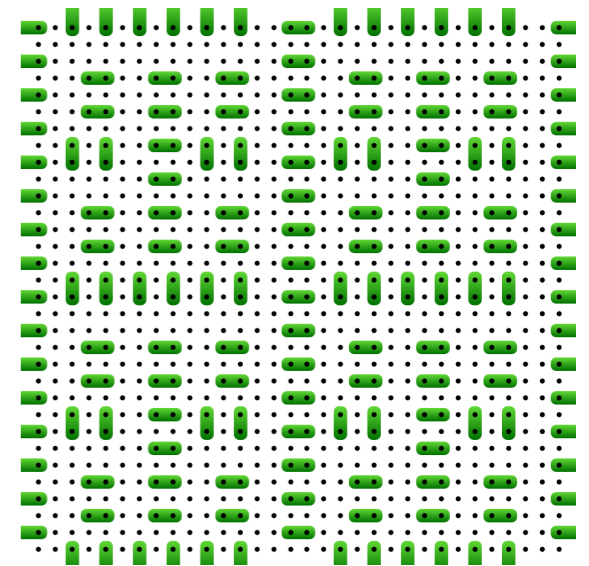
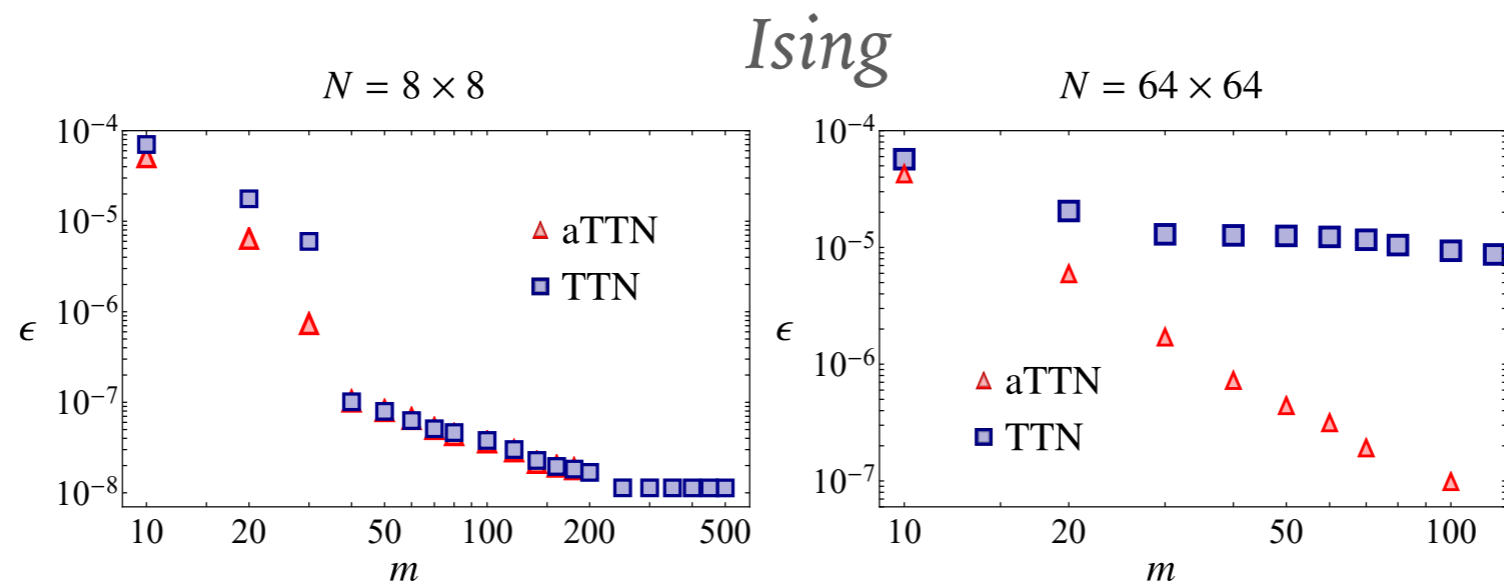
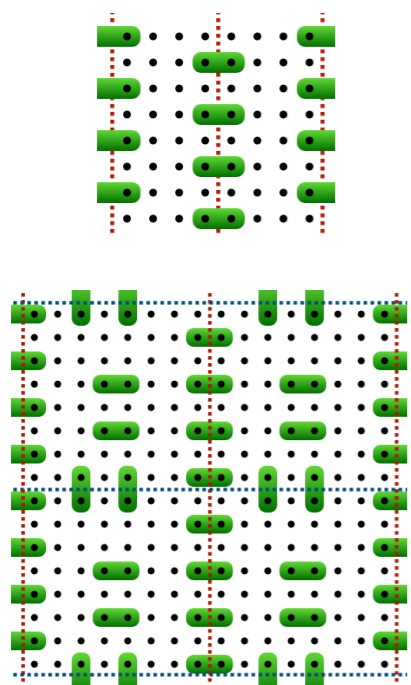
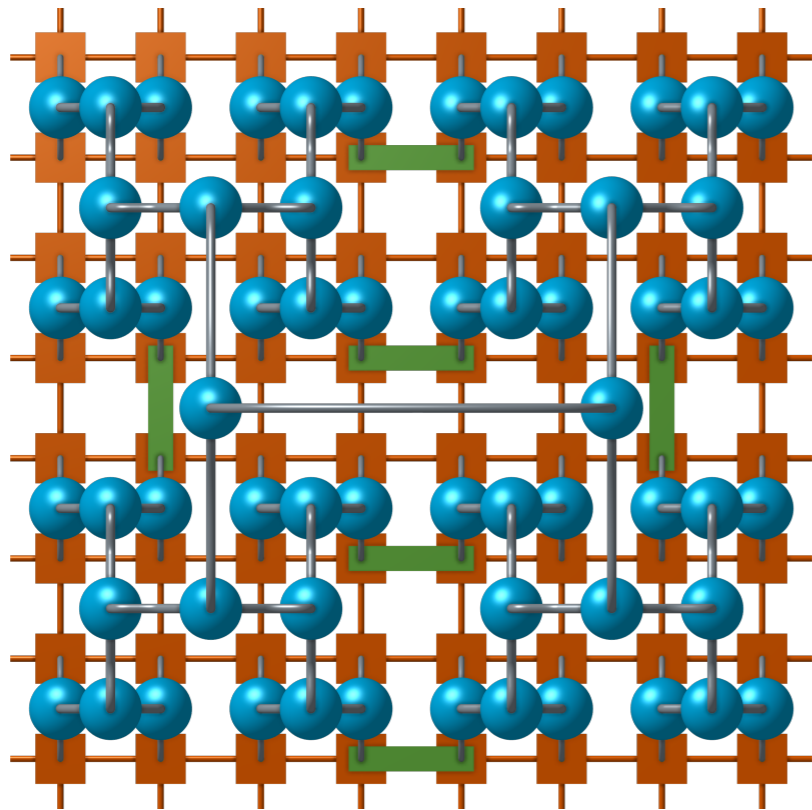
T. Felser, S. Notarnicola, S. Montangero PRL (2021)

AUGMENTED TREE TENSOR NETWORKS



T. Felser, S. Notarnicola, S. Montangero PRL (2021)

AUGMENTED TREE TENSOR NETWORKS



AUGMENTED TREE TENSOR NETWORKS

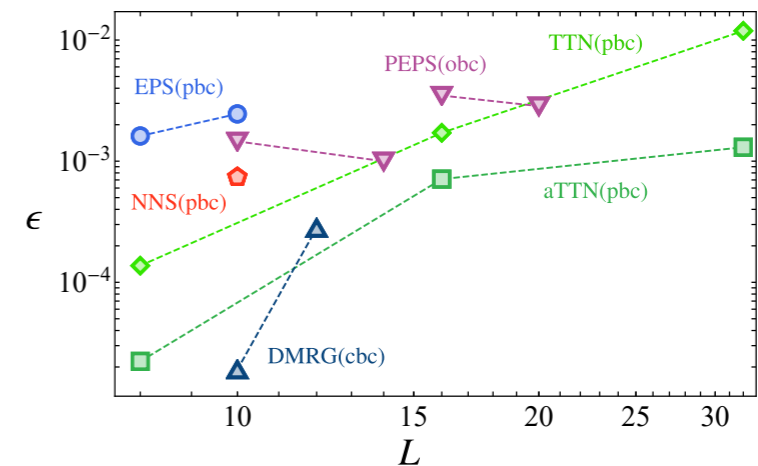
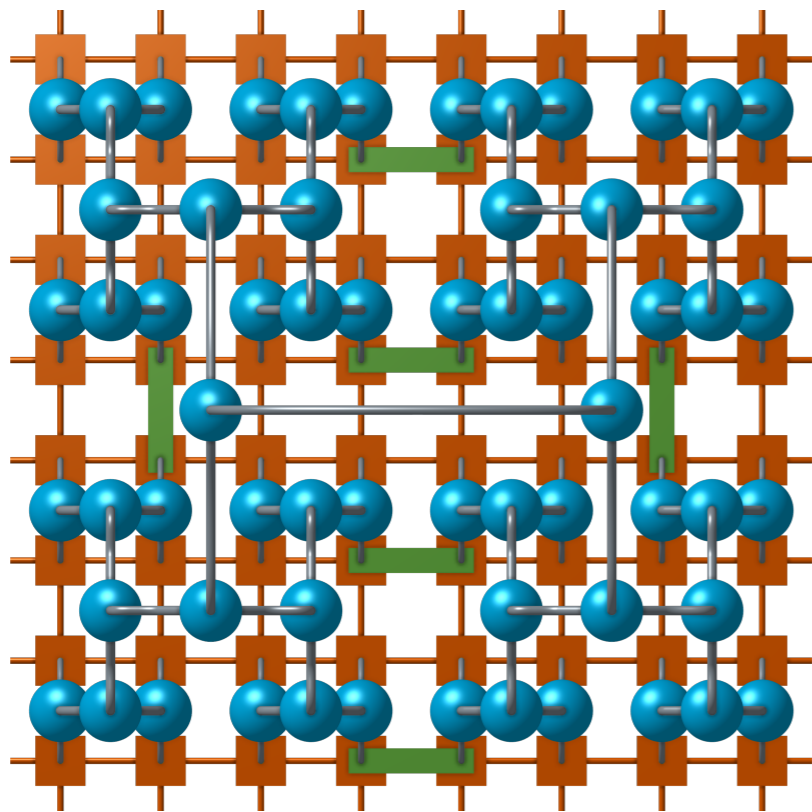
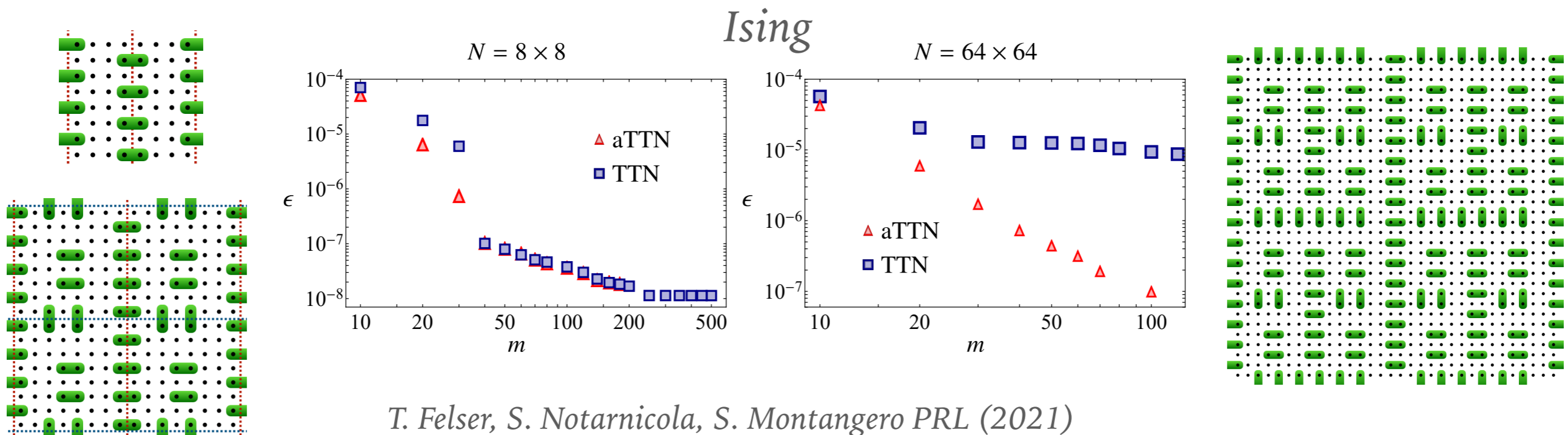


FIG. 2: Relative error ϵ of the 2D Heisenberg ground-state energy as a function of the system linear size L compared with the best available estimates obtained by MC [21] for the TTN, aTTN, NNS [59], EPS [60], PEPS [61], 2D-DMRG [57]. Depending on the method open (obic), cylindrical (cbc) or periodic (pbc) boundary conditions have been chosen. For each datapoint, we compare the Monte Carlo result with the same boundary conditions.



Overview Quantum TEA



Quantum Tensor network Emulator Applications

Can I just have tensor networks for quantum information?



How to emulate a digital quantum circuits?



+



www.quantumtea.it

baltig.infn.it/quantum_tea

Overview Quantum TEA



Quantum Tensor network Emulator Applications

Can I just have tensor networks for quantum information?



How to emulate a digital quantum circuits?



+



How to solve the Schrödinger equation?



+



www.quantumtea.it

baltig.infn.it/quantum_tea

Overview Quantum TEA



Quantum Tensor network Emulator Applications

Can I just have tensor networks for quantum information?



How to emulate a digital quantum circuits?



+



How to solve the Schrödinger equation?



+



Can we do tensor network machine learning? ... soon:



+



www.quantumtea.it

baltig.infn.it/quantum_tea

Overview Quantum TEA



Quantum Tensor network Emulator Applications

Can I just have tensor networks for quantum information?



How to emulate a digital quantum circuits?



+



How to solve the Schrödinger equation?



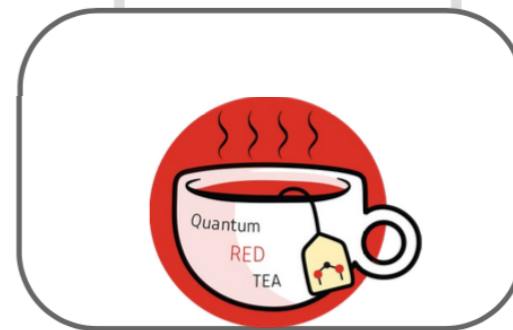
+



Can we do tensor network machine learning? ... soon:



+



www.quantumtea.it

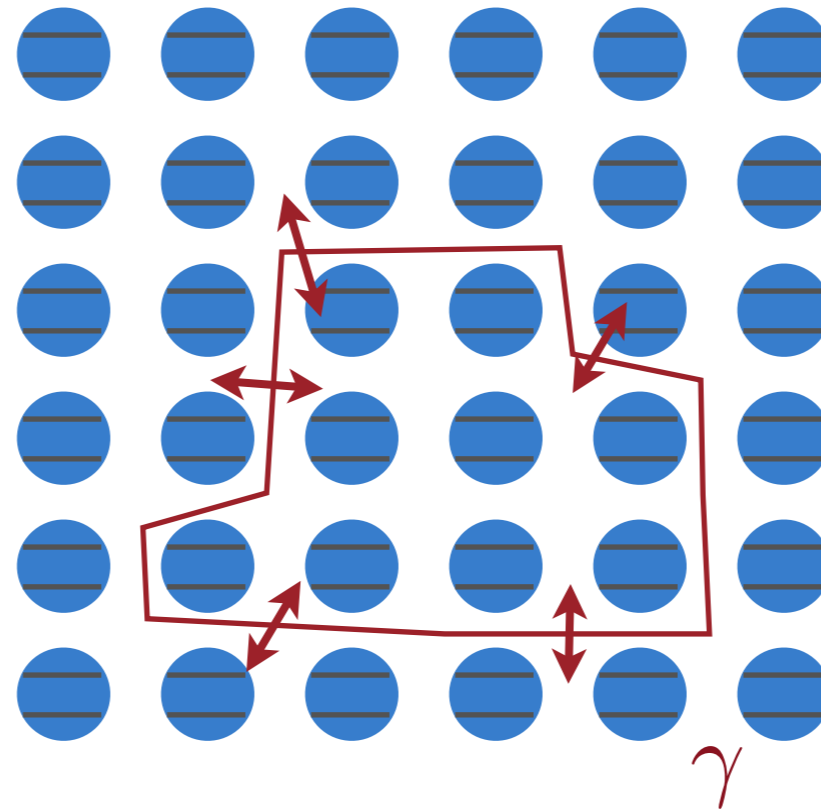
baltig.infn.it/quantum_tea

ENTANGLEMENT OF MIXED MANY-BODY QUANTUM SYSTEMS

For pure states:

$$\mathcal{S} = -\text{Tr} \rho \log \rho$$

Von Neumann Entropy



$$\rho = \sum p_j |\psi_j\rangle\langle\psi_j|$$

Area law

$$\mathcal{S} \propto \gamma$$

$$\mathcal{S} \propto N^{(D-1)}$$

1D critical systems:

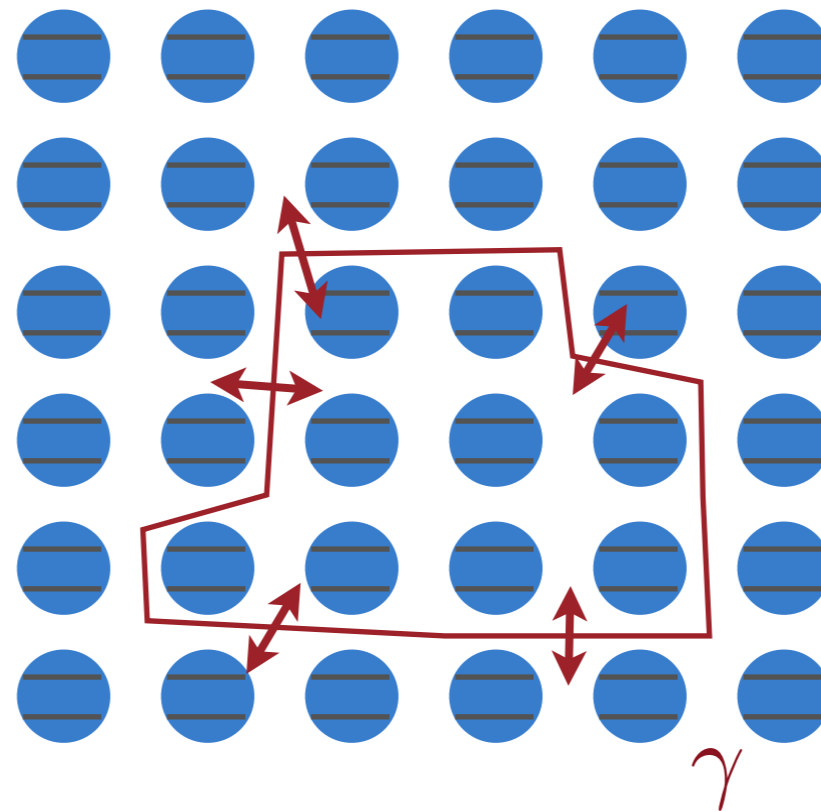
$$\mathcal{S} = \frac{c}{3} \log N$$

ENTANGLEMENT OF MIXED MANY-BODY QUANTUM SYSTEMS

For pure states:

$$\mathcal{S} = -\text{Tr} \rho \log \rho$$

Von Neumann Entropy



Area law

$$\mathcal{S} \propto \gamma$$

$$\mathcal{S} \propto N^{(D-1)}$$

1D critical systems:

$$\mathcal{S} = \frac{c}{3} \log N$$

For mixed states:

$$\rho = \sum p_j |\psi_j\rangle\langle\psi_j|$$

$$E_F(\rho) = \inf_{\{p_j, \psi_j\}} \left\{ \sum_j p_j \mathcal{S}(|\psi_j\rangle) : \rho = \sum_j p_j |\psi_j\rangle\langle\psi_j| \right\}$$

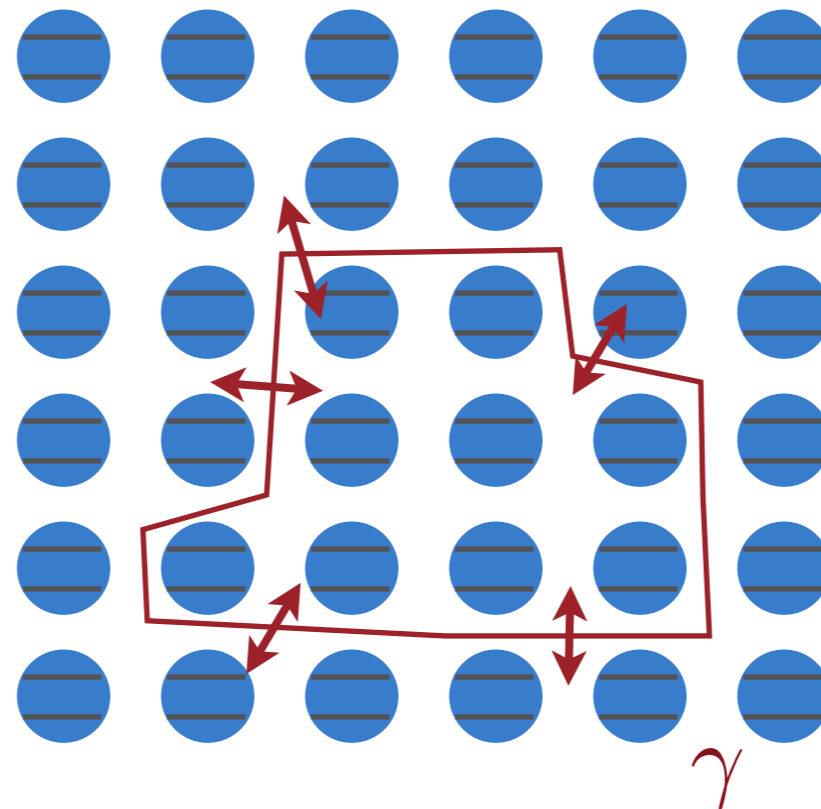
Entanglement of formation

ENTANGLEMENT OF MIXED MANY-BODY QUANTUM SYSTEMS

For pure states:

$$\mathcal{S} = -\text{Tr} \rho \log \rho$$

Von Neumann Entropy



Area law

$$\mathcal{S} \propto \gamma$$

$$\mathcal{S} \propto N^{(D-1)}$$

1D critical systems:

$$\mathcal{S} = \frac{c}{3} \log N$$

For mixed states:

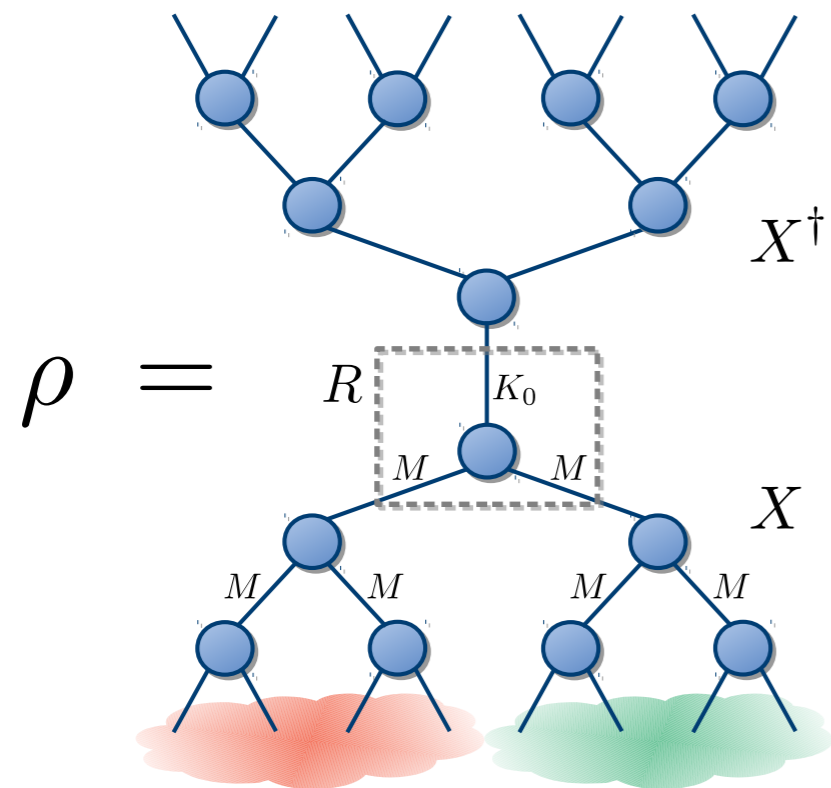
$$\rho = \sum p_j |\psi_j\rangle\langle\psi_j|$$

$$E_F(\rho) = \inf_{\{p_j, \psi_j\}} \left\{ \sum_j p_j \mathcal{S}(|\psi_j\rangle) : \rho = \sum_j p_j |\psi_j\rangle\langle\psi_j| \right\}$$

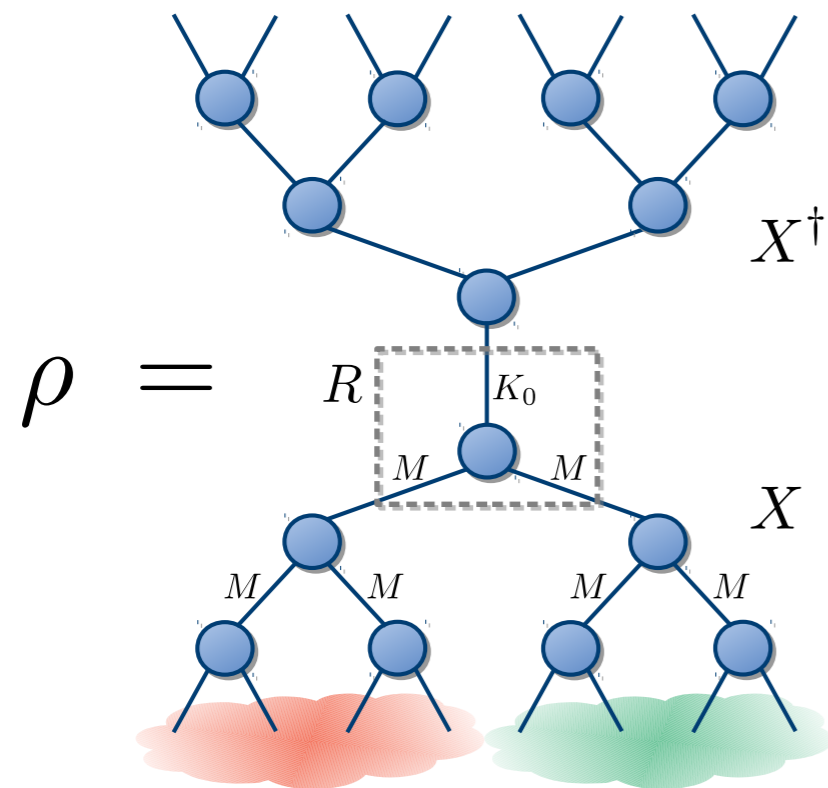
$$E_F(\rho, T) \stackrel{?}{\propto} \log N^{c/3}$$

Entanglement of formation

TREE TENSOR OPERATORS

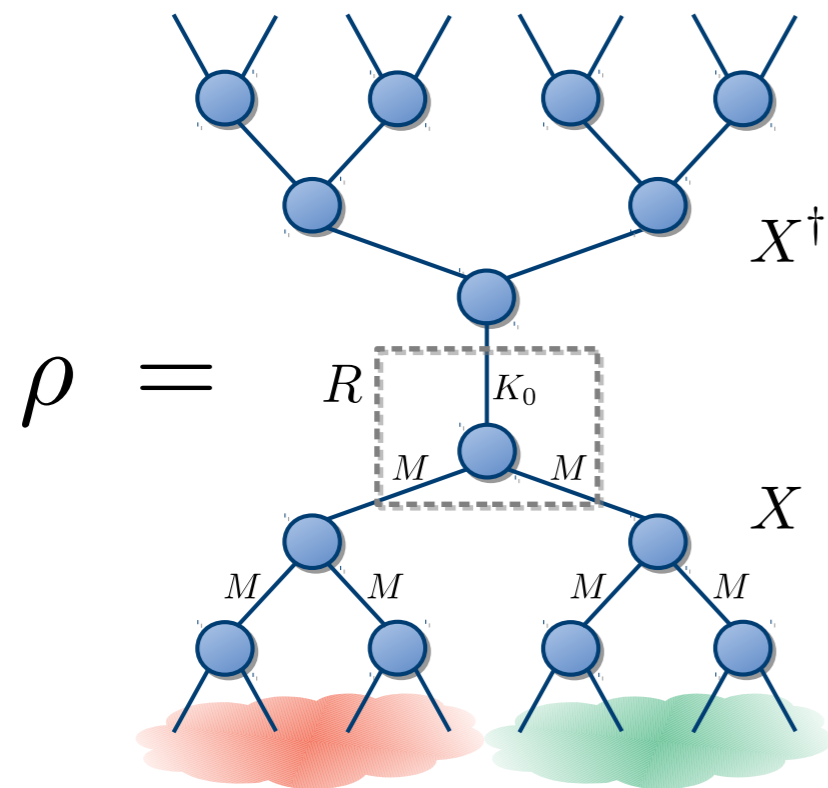


TREE TENSOR OPERATORS



$$E_F(\rho) = \min_{K \geq K_0} \inf_{\mathcal{U}} \left\{ \sum_{j=1}^K p_j \mathcal{S}(|\psi'_j\rangle) : X' = X\mathcal{U} \right\}$$

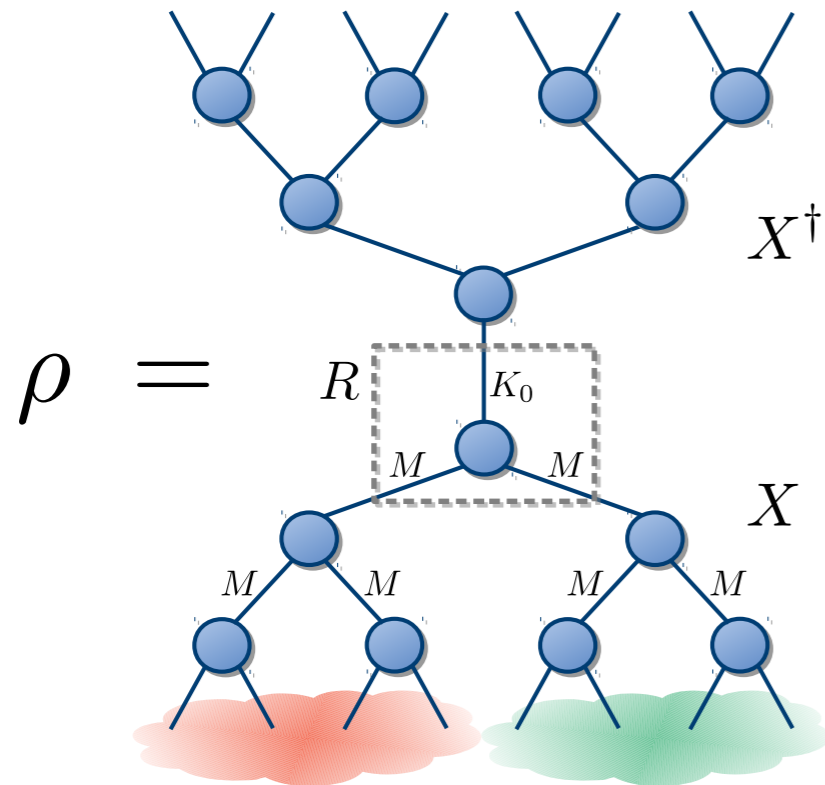
TREE TENSOR OPERATORS



$$E_F(\rho) = \min_{K \geq K_0} \inf_{\mathcal{U}} \left\{ \sum_{j=1}^K p_j \mathcal{S}(|\psi'_j\rangle) : X' = X\mathcal{U} \right\}$$

$$\hat{H}_{Ising} = J \sum_{i=1}^N (\hat{\sigma}_i^x \hat{\sigma}_{i+1}^x + h \hat{\sigma}_i^z)$$

TREE TENSOR OPERATORS

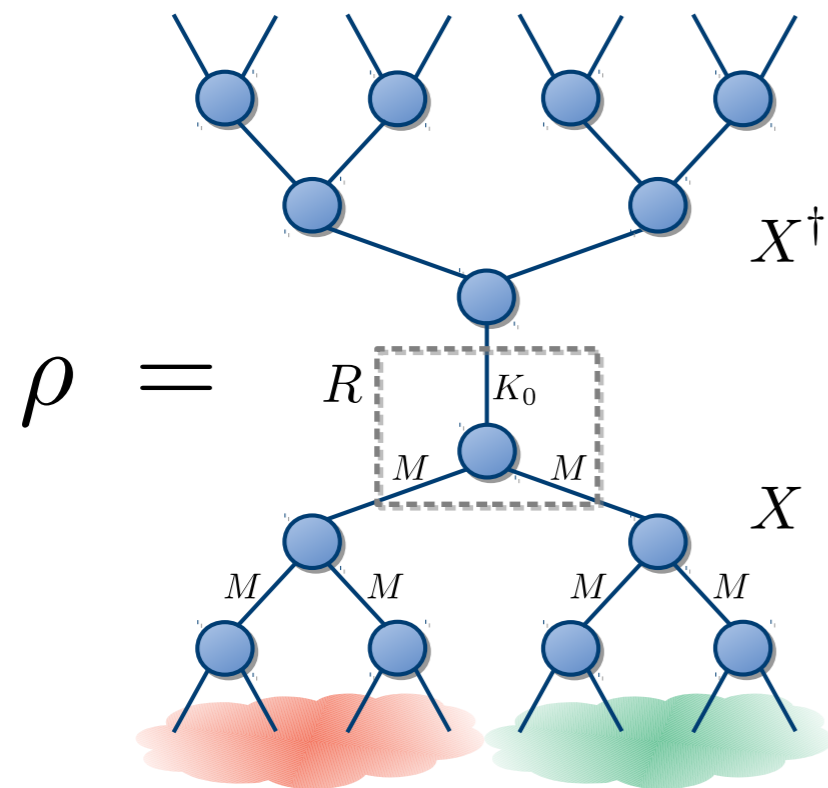


$$E_F(\rho) = \min_{K \geq K_0} \inf_{\mathcal{U}} \left\{ \sum_{j=1}^K p_j \mathcal{S}(|\psi'_j\rangle) : X' = X\mathcal{U} \right\}$$

$$\hat{H}_{Ising} = J \sum_{i=1}^N (\hat{\sigma}_i^x \hat{\sigma}_{i+1}^x + h \hat{\sigma}_i^z)$$

$$\hat{H}_{XXZ} = J \sum_{j=1}^N (\hat{\sigma}_j^x \hat{\sigma}_{j+1}^x + \hat{\sigma}_j^y \hat{\sigma}_{j+1}^y + \xi \hat{\sigma}_j^z \hat{\sigma}_{j+1}^z)$$

TREE TENSOR OPERATORS



$$E_F(\rho) = \min_{K \geq K_0} \inf_{\mathcal{U}} \left\{ \sum_{j=1}^K p_j \mathcal{S}(|\psi'_j\rangle) : X' = X\mathcal{U} \right\}$$

$$\hat{H}_{Ising} = J \sum_{i=1}^N (\hat{\sigma}_i^x \hat{\sigma}_{i+1}^x + h \hat{\sigma}_i^z)$$

$$\hat{H}_{XXZ} = J \sum_{j=1}^N (\hat{\sigma}_j^x \hat{\sigma}_{j+1}^x + \hat{\sigma}_j^y \hat{\sigma}_{j+1}^y + \xi \hat{\sigma}_j^z \hat{\sigma}_{j+1}^z)$$

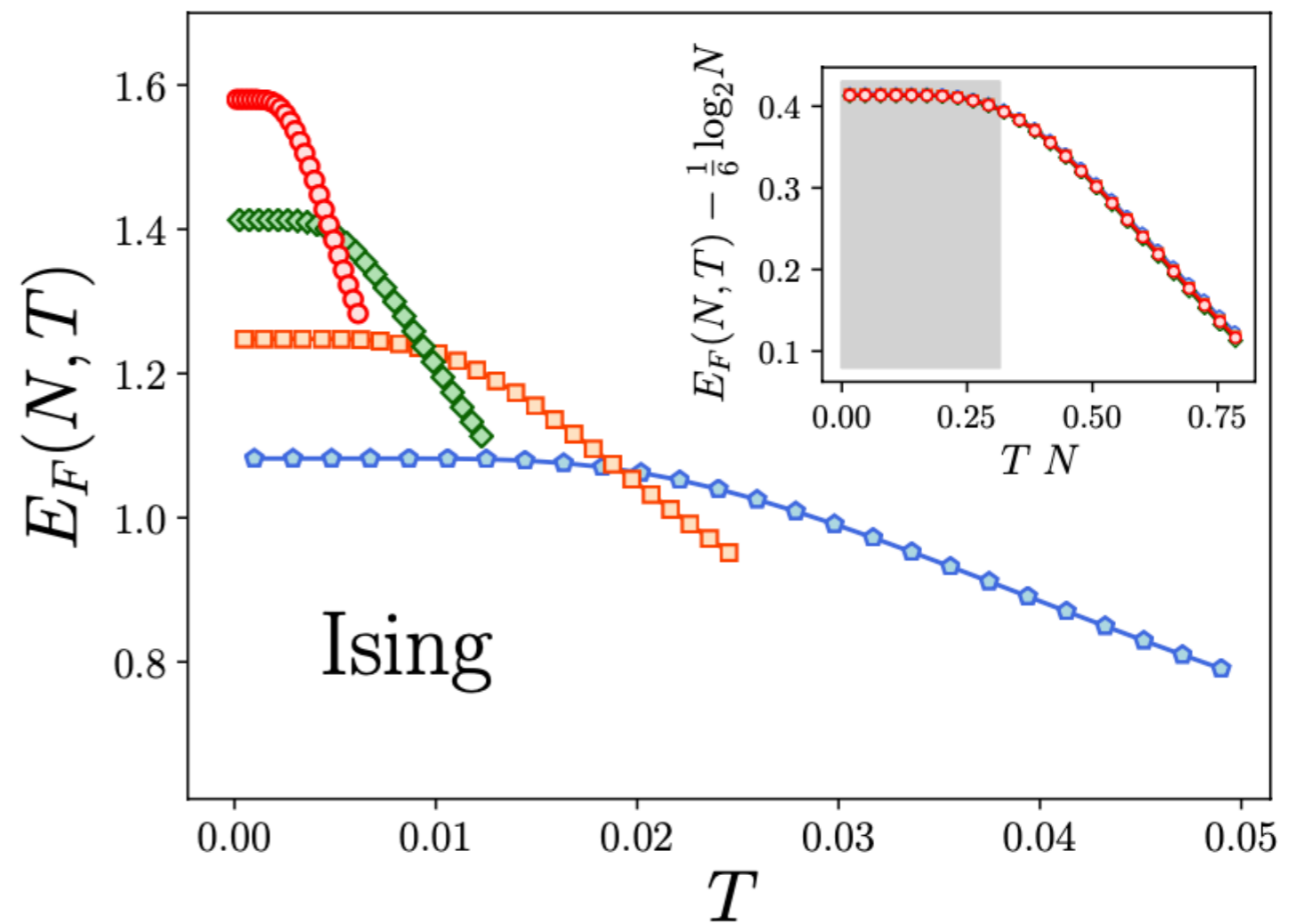
Thermal equilibrium state
(Mixture of K_0 Boltzmann factors)

$$X = \frac{1}{\sqrt{Z}} \sum_j^{K_0} e^{-E_j/2T} |\psi_j\rangle \langle j|$$

CONFORMAL SCALING OF ENTANGLEMENT OF FORMATION

CONFORMAL SCALING OF ENTANGLEMENT OF FORMATION

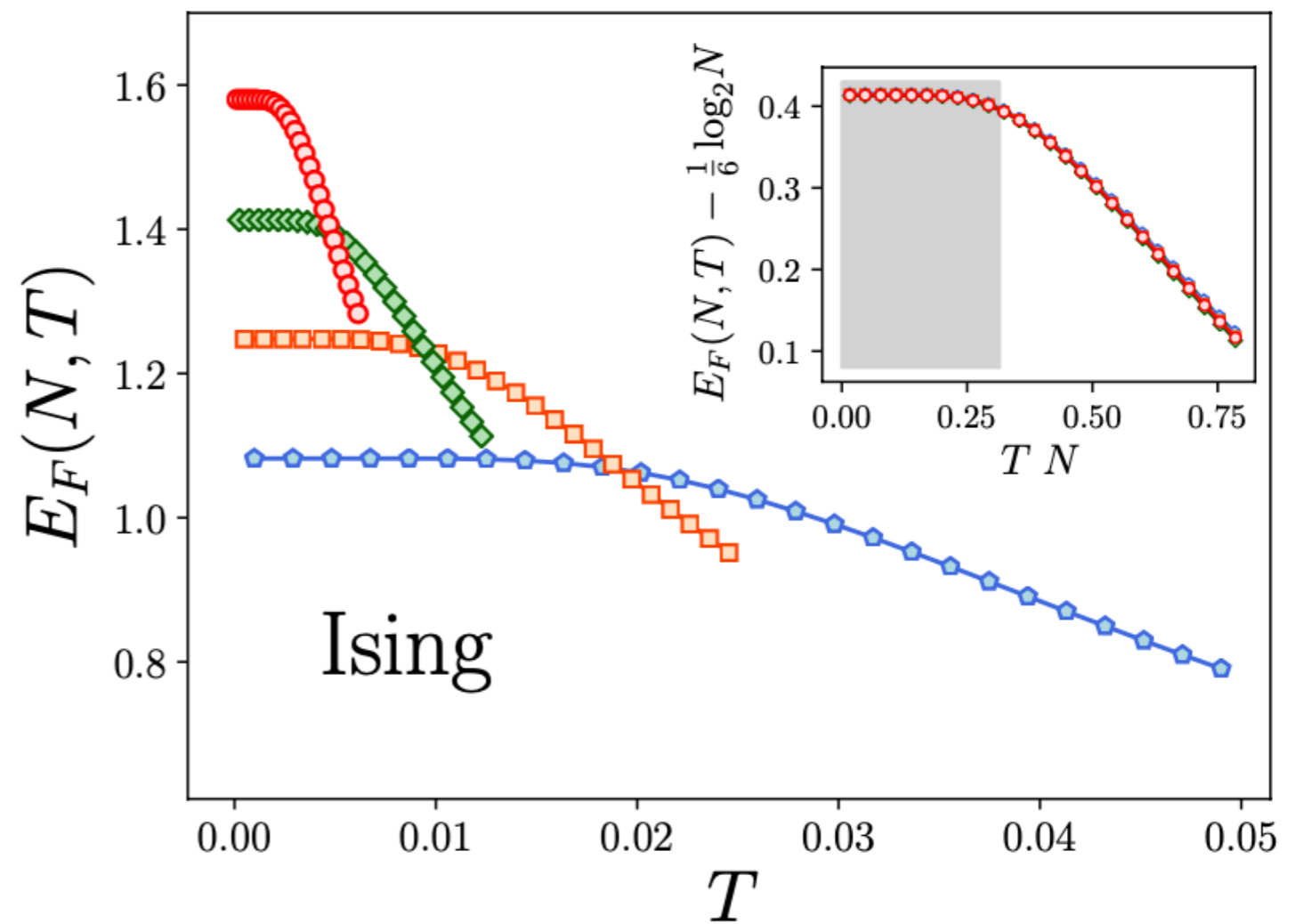
$N = 16, 32, 64, 128$



CONFORMAL SCALING OF ENTANGLEMENT OF FORMATION

$$E_F = \log(N^{c/3} f(TN^z))$$

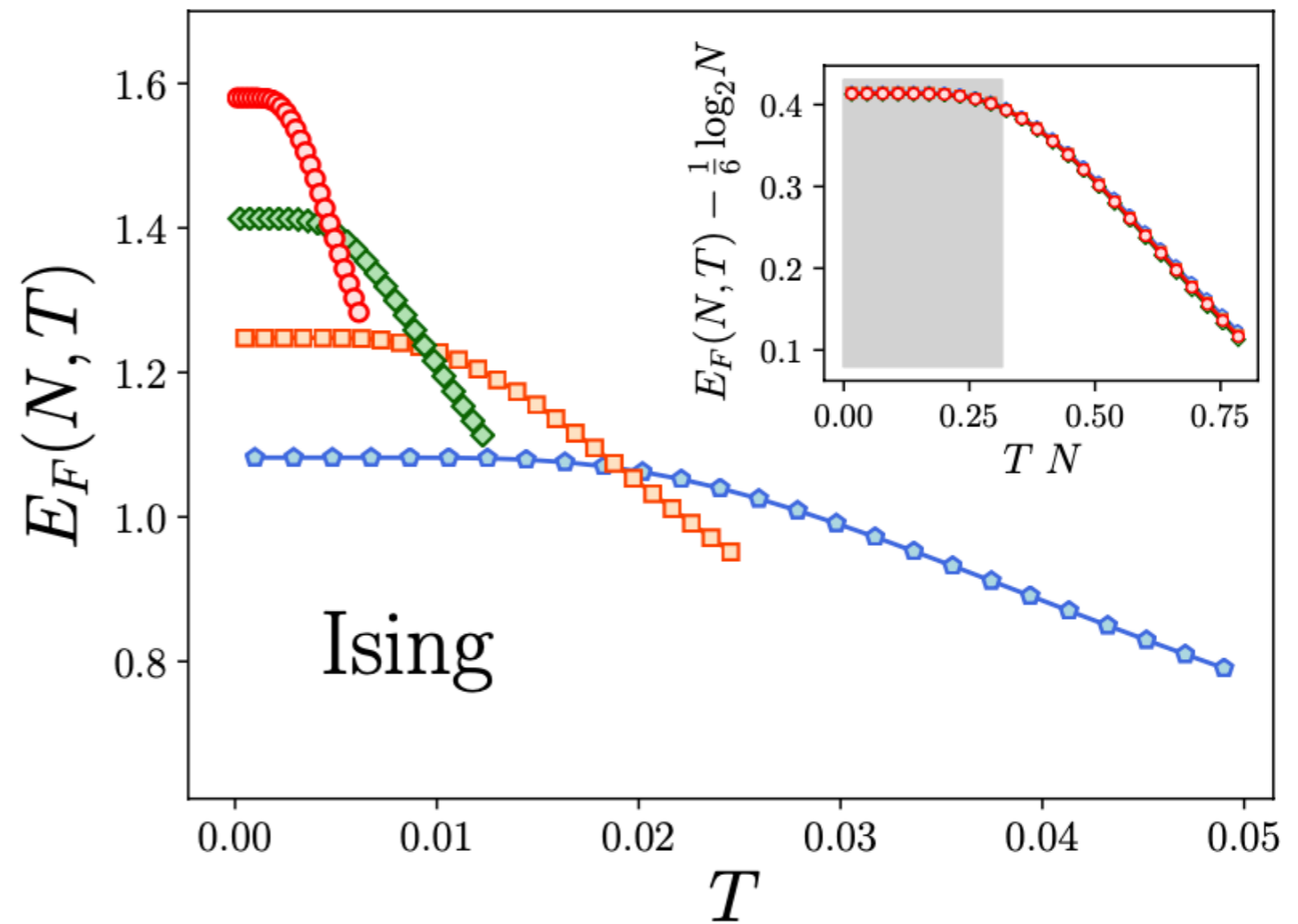
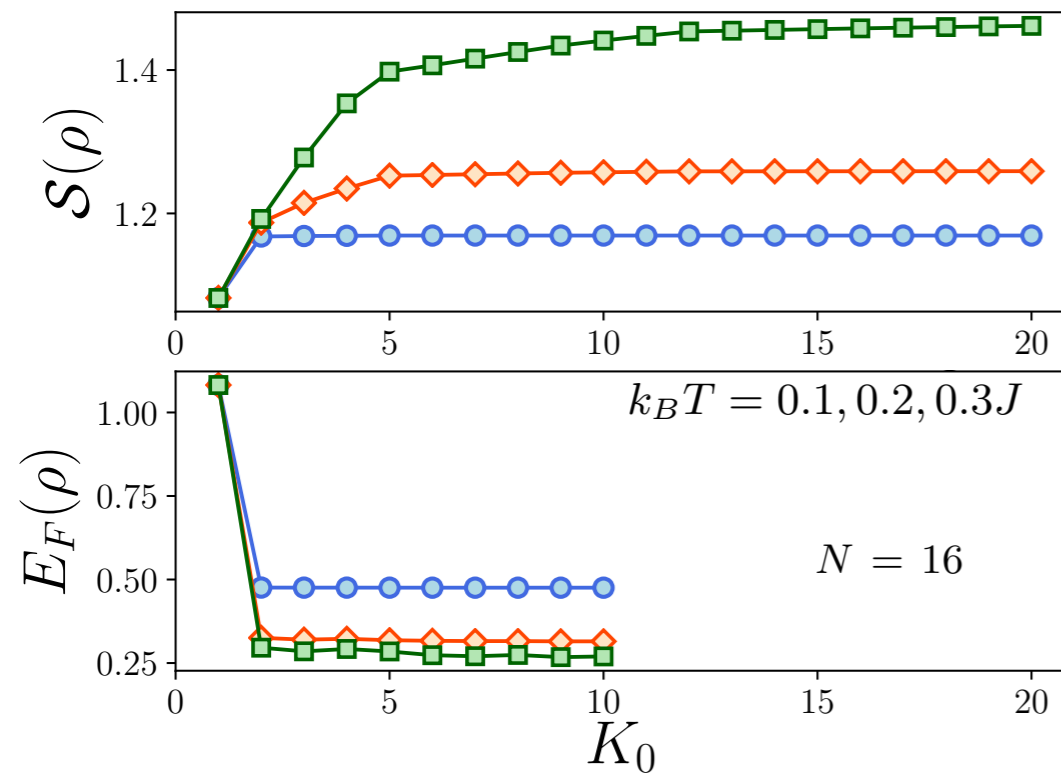
$$N = 16, 32, 64, 128$$



CONFORMAL SCALING OF ENTANGLEMENT OF FORMATION

$$E_F = \log(N^{c/3} f(TN^z))$$

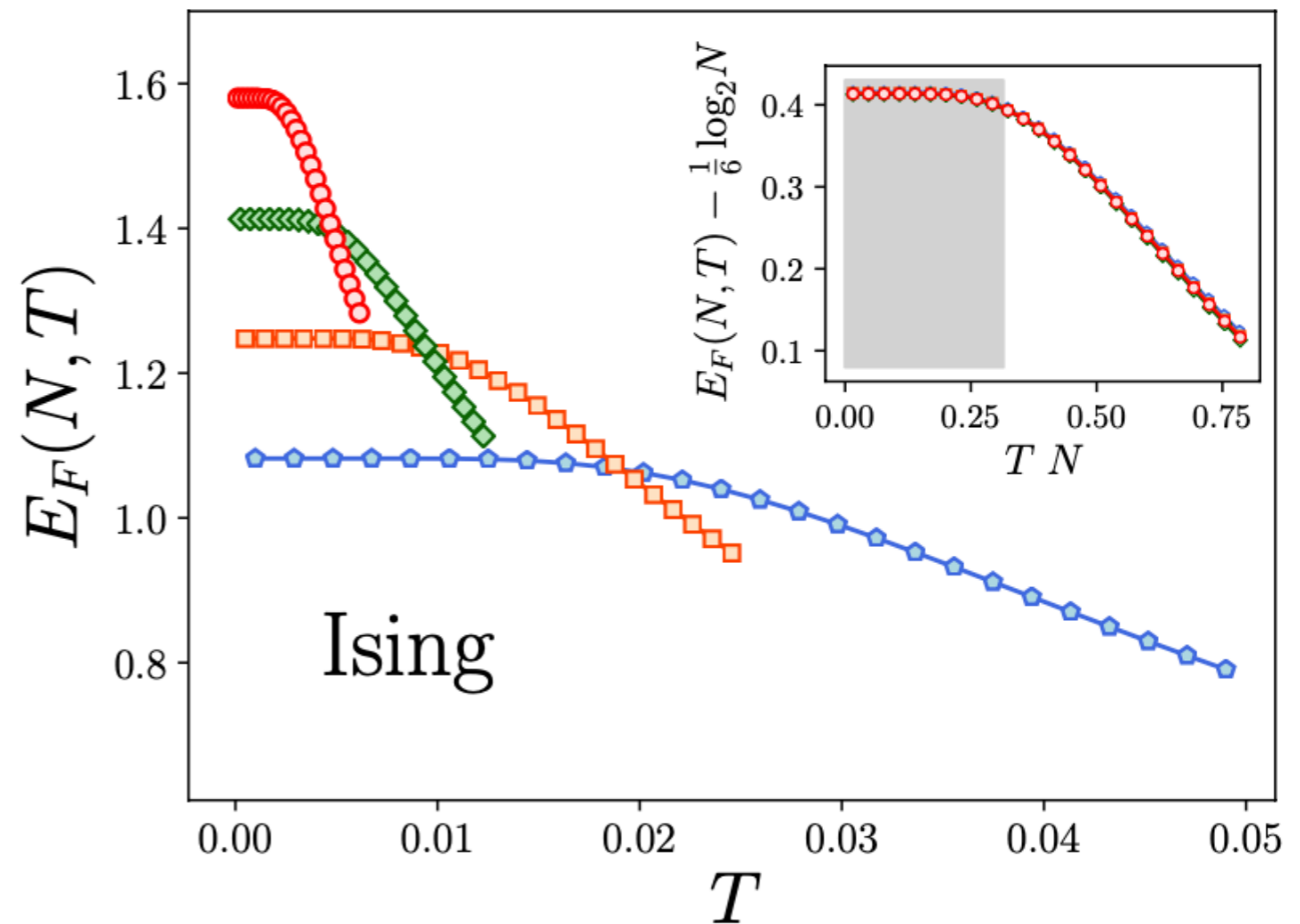
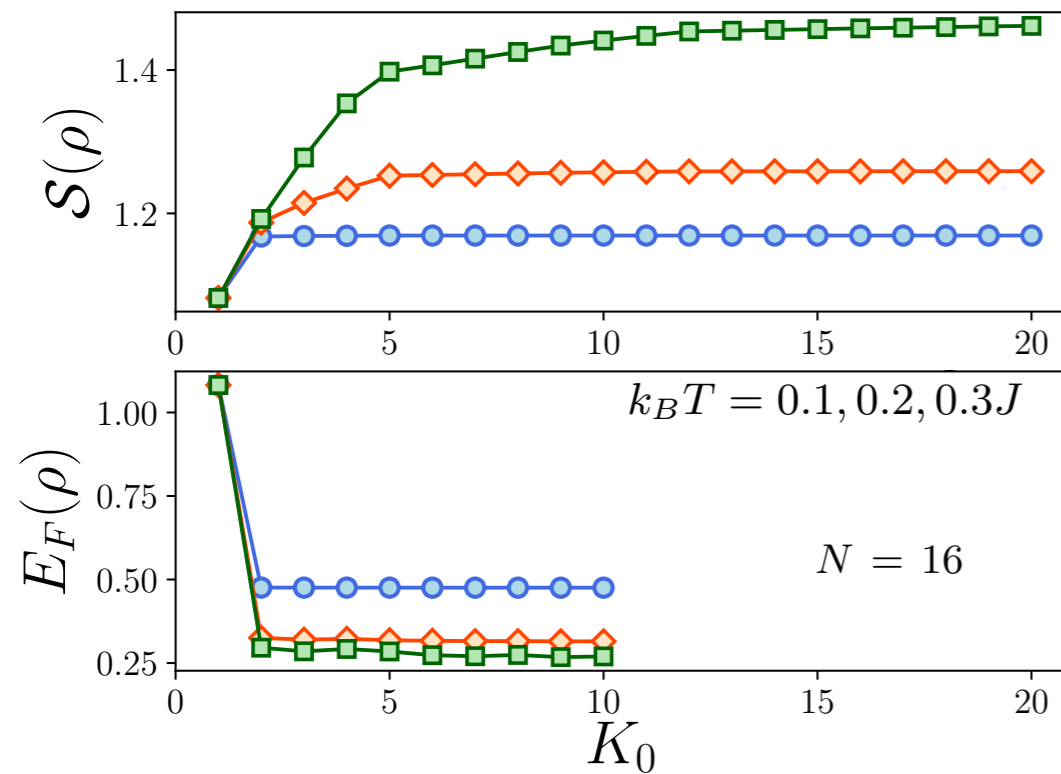
$$N = 16, 32, 64, 128$$



CONFORMAL SCALING OF ENTANGLEMENT OF FORMATION

$$E_F = \log(N^{c/3} f(TN^z))$$

$$N = 16, 32, 64, 128$$



*Numerical complexity depends
on entropy, not entanglement!*

ADIABATIC QUANTUM COMPUTING

- *Preparation of the system in an “easy” state*

ADIABATIC QUANTUM COMPUTING

- *Preparation of the system in an “easy” state*

$$H_0 = -h_0 \sum_{i=1}^N s_i \quad s_i = \{\uparrow, \downarrow\}$$

ADIABATIC QUANTUM COMPUTING

► Preparation of the system in an “easy” state



$$H_0 = -h_0 \sum_{i=1}^N s_i \quad s_i = \{\uparrow, \downarrow\}$$

ADIABATIC QUANTUM COMPUTING

➤ *Preparation of the system in an “easy” state*

↓↓↓ . . . ↓↓↓

➤ *Slowly change the system Hamiltonian to reach another ground state which encodes the solution of the problem*

↓↑↓ . . . ↓↓↑

$$H_0 = -h_0 \sum_{i=1}^N s_i \quad s_i = \{\uparrow, \downarrow\}$$

ADIABATIC QUANTUM COMPUTING

➤ Preparation of the system in an “easy” state

↓↓↓ . . . ↓↓↓

➤ Slowly change the system Hamiltonian to reach another ground state which encodes the solution of the problem

↓↑↓ . . . ↓↓↑

$$H_0 = -h_0 \sum_{i=1}^N s_i \quad s_i = \{\uparrow, \downarrow\}$$

$$H(t) = \left(1 - \frac{t}{T}\right) H_0 + \frac{t}{T} H_P$$

ADIABATIC QUANTUM COMPUTING

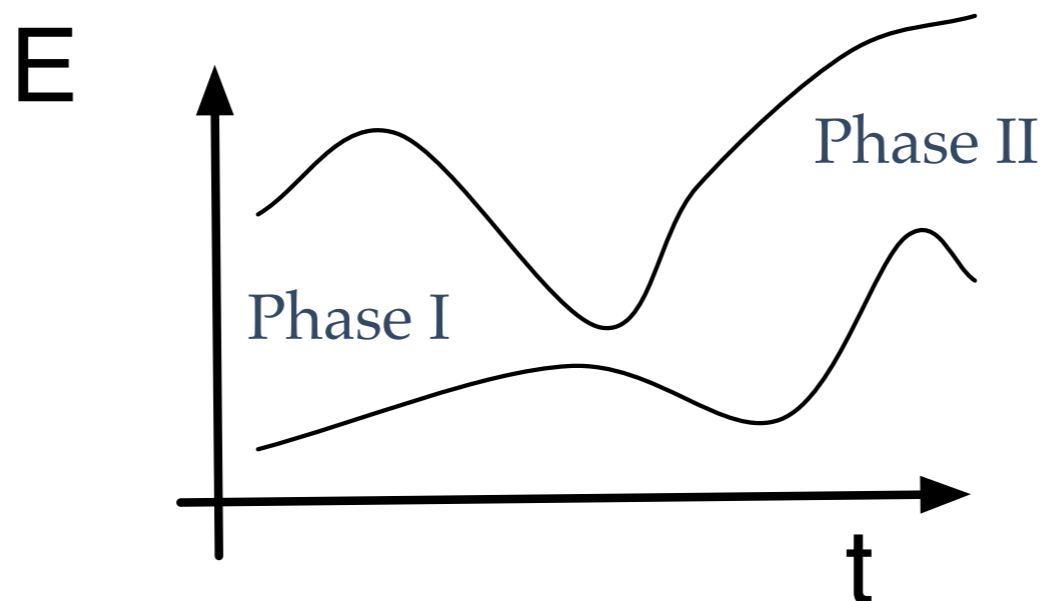
➤ Preparation of the system in an “easy” state

↓↓↓ . . . ↓↓↓

➤ Slowly change the system Hamiltonian to reach another ground state which encodes the solution of the problem

↓↑↓ . . . ↓↓↑

$$H_0 = -h_0 \sum_{i=1}^N s_i \quad s_i = \{\uparrow, \downarrow\} \quad H(t) = \left(1 - \frac{t}{T}\right) H_0 + \frac{t}{T} H_P$$



ADIABATIC QUANTUM COMPUTING

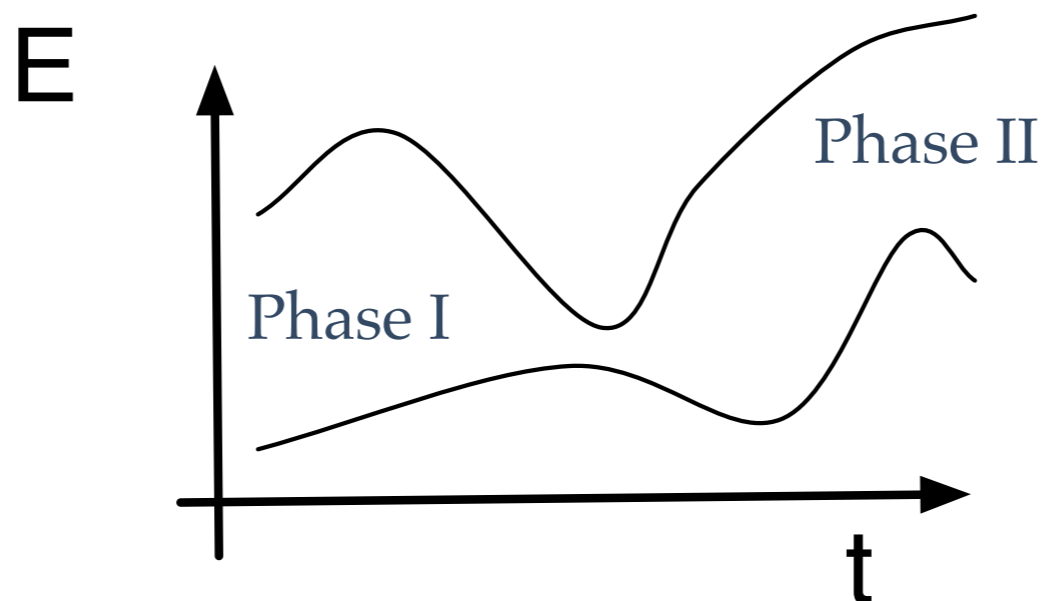
➤ Preparation of the system in an “easy” state

↓↓↓ . . . ↓↓↓

➤ Slowly change the system Hamiltonian to reach another ground state which encodes the solution of the problem

↓↑↓ . . . ↓↓↑

$$H_0 = -h_0 \sum_{i=1}^N s_i \quad s_i = \{\uparrow, \downarrow\} \quad H(t) = \left(1 - \frac{t}{T}\right) H_0 + \frac{t}{T} H_P$$



Adiabatic
strategy

ADIABATIC QUANTUM COMPUTING

➤ Preparation of the system in an “easy” state

↓↓↓ . . . ↓↓↓

➤ Slowly change the system Hamiltonian to reach another ground state which encodes the solution of the problem

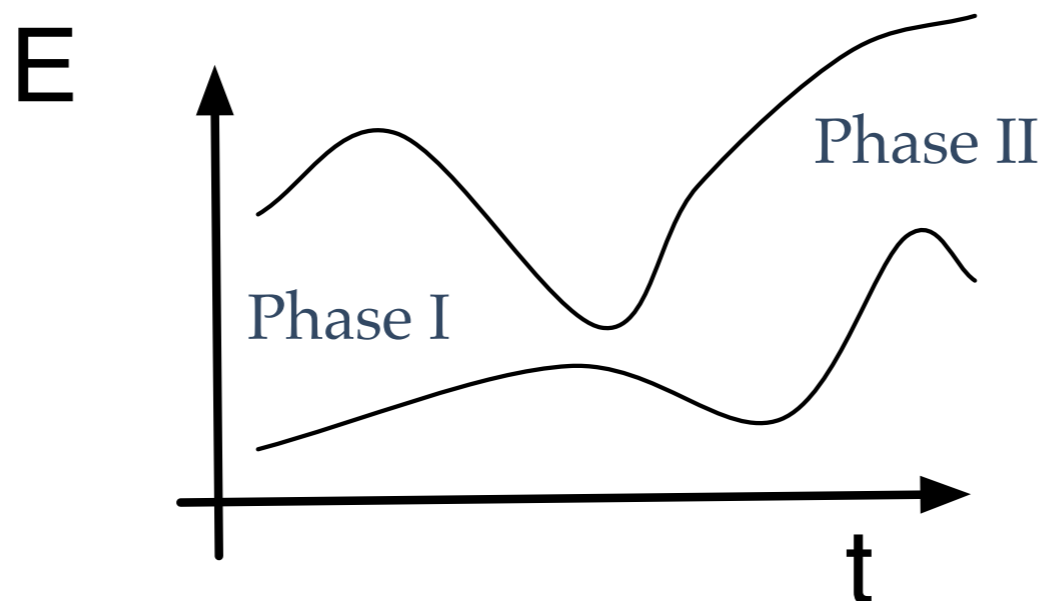
↓↑↓ . . . ↓↓↑

$$H_0 = -h_0 \sum_{i=1}^N s_i$$

$$s_i = \{\uparrow, \downarrow\}$$

$$H(t) = \left(1 - \frac{t}{T}\right) H_0 + \frac{t}{T} H_P$$

Slow



Adiabatic
strategy

ADIABATIC QUANTUM COMPUTING

➤ Preparation of the system in an “easy” state

↓↓↓ . . . ↓↓↓

➤ Slowly change the system Hamiltonian to reach another ground state which encodes the solution of the problem

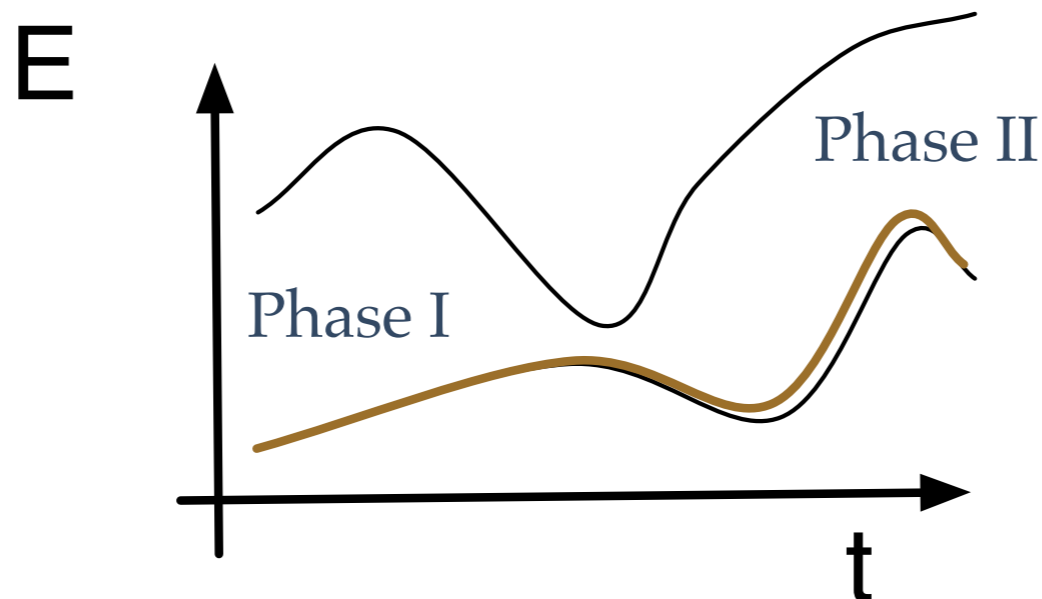
↓↑↓ . . . ↓↓↑

$$H_0 = -h_0 \sum_{i=1}^N s_i$$

$$s_i = \{\uparrow, \downarrow\}$$

$$H(t) = \left(1 - \frac{t}{T}\right) H_0 + \frac{t}{T} H_P$$

Slow



Adiabatic
strategy

OPTIMAL CROSSING OF QPT

RedCRAB

Optimal control

OPTIMAL CROSSING OF QPT

System

RedCRAB

Optimal control

OPTIMAL CROSSING OF QPT



RedCRAB

Optimal control

OPTIMAL CROSSING OF QPT

System

RedCRAB

Optimal control

OPTIMAL CROSSING OF QPT

System

RedCRAB

Optimal control

$$i\frac{\partial}{\partial t}|\psi(t)\rangle = (H_0 + f(t)H_1)|\psi(t)\rangle$$

OPTIMAL CROSSING OF QPT

System

RedCRAB

Optimal control

$$i\frac{\partial}{\partial t}|\psi(t)\rangle = (H_0 + f(t)H_1)|\psi(t)\rangle$$

$$\min_{f(t)} J(|\psi(T)\rangle)$$

OPTIMAL CROSSING OF QPT

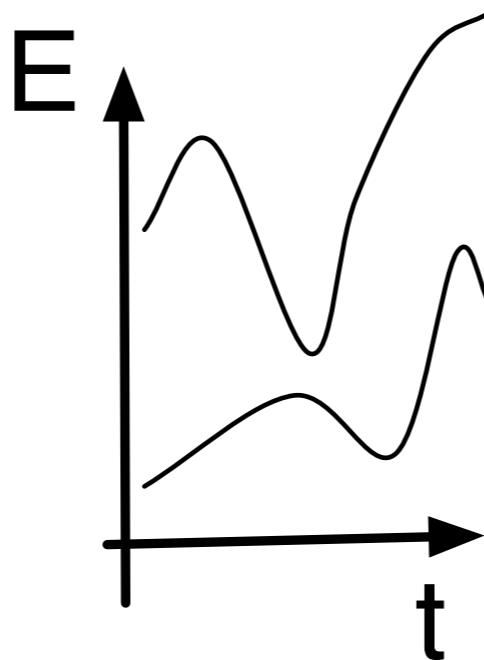
System

RedCRAB

Optimal control

$$i\frac{\partial}{\partial t}|\psi(t)\rangle = (H_0 + f(t)H_1)|\psi(t)\rangle$$

$$\min_{f(t)} J(|\psi(T)\rangle)$$



OPTIMAL CROSSING OF QPT

System

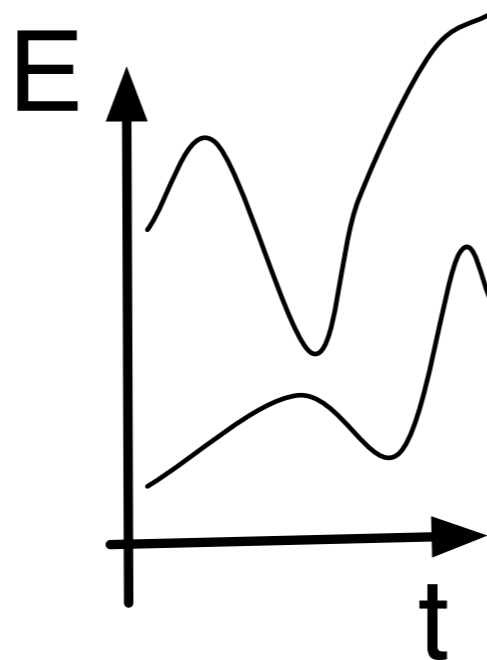
RedCRAB

Optimal control

$$i\frac{\partial}{\partial t}|\psi(t)\rangle = (H_0 + f(t)H_1)|\psi(t)\rangle$$

$$\min_{f(t)} J(|\psi(T)\rangle)$$

Fast



OPTIMAL CROSSING OF QPT

System

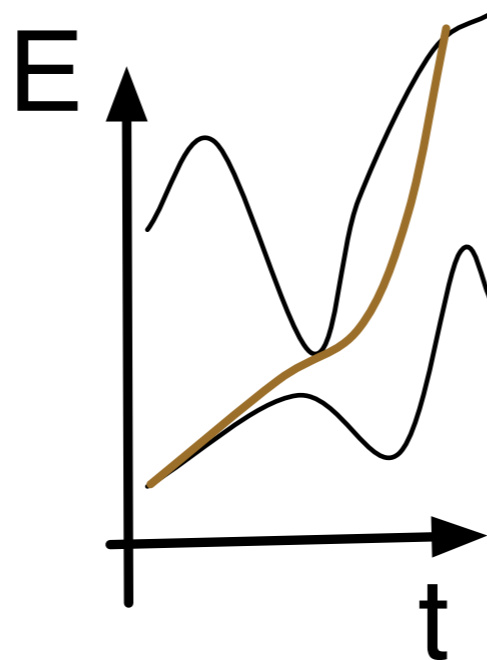
RedCRAB

Optimal control

$$i\frac{\partial}{\partial t}|\psi(t)\rangle = (H_0 + f(t)H_1)|\psi(t)\rangle$$

$$\min_{f(t)} J(|\psi(T)\rangle)$$

Fast



OPTIMAL CROSSING OF QPT

System

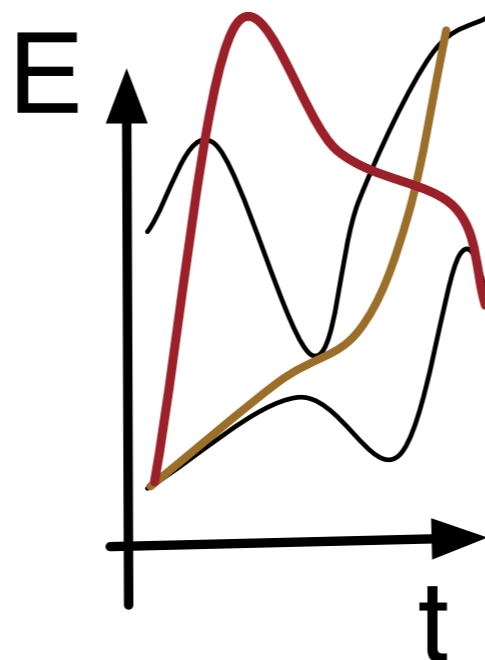
RedCRAB

Optimal control

$$i\frac{\partial}{\partial t}|\psi(t)\rangle = (H_0 + f(t)H_1)|\psi(t)\rangle$$

$$\min_{f(t)} J(|\psi(T)\rangle)$$

Fast



Optimal
control

OPTIMAL CROSSING OF QPT

Optimal control of complex atomic quantum systems

S. van Frank¹, M. Bonneau¹, J. Schmiedmayer¹,
S. Hild², C. Gross², M. Cheneau^{2,3}, I. Bloch²,
T. Pichler⁴, A. Negretti⁵, T. Calarco⁴, S. Montangero⁴

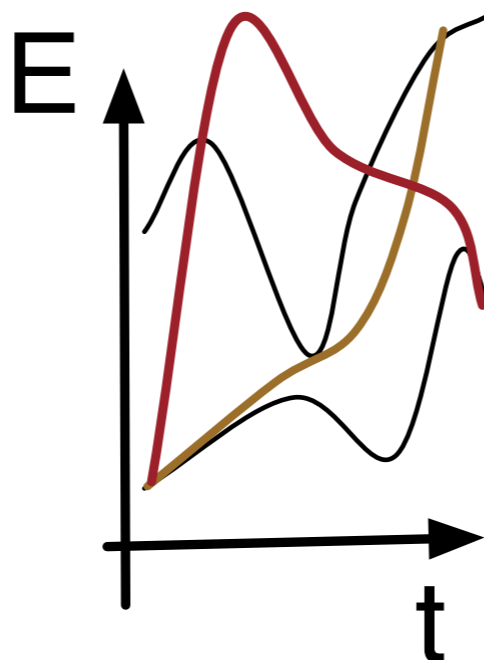
RedCRAB

Optimal control

$$i \frac{\partial}{\partial t} |\psi(t)\rangle = (H_0 + f(t)H_1) |\psi(t)\rangle$$

$$\min_{f(t)} J(|\psi(T)\rangle)$$

Fast



Optimal
control

OPTIMAL CROSSING OF QPT

Optimal control of complex atomic quantum systems

RedCRAB

S. van Frank¹, M. Bonneau¹, J. Schmiedmayer¹,
S. Hild², C. Gross², M. Cheneau^{2,3}, I. Bloch²,
T. Pichler⁴, A. Negretti⁵, T. Calarco⁴, S. Montangero⁴

Optimal control

Fast closed-loop optimal control of ultracold atoms in an optical lattice

S. Rosi¹, A. Bernard¹, N. Fabbri¹, L. Fallani^{1,2}, C. Fort¹, and M. Inguscio^{1,2}

¹*LENS and Dipartimento di Fisica e Astronomia,*

Università di Firenze and INO-CNR, 50019 Sesto Fiorentino, Italy

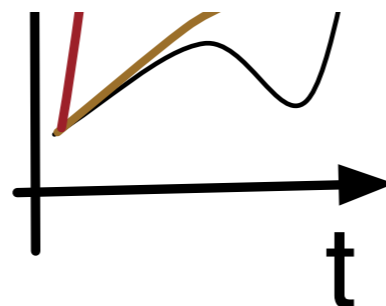
²*QSTAR Center for Quantum Science and Technology, Largo Enrico Fermi 2, I-50125 Arcetri, Italy*

T. Calarco³ and S. Montangero³

³*Institut für Quanteninformationsverarbeitung, Universität Ulm, D-89069 Ulm, Germany*

(Dated: July 30, 2019)

1430



control

OPTIMAL CROSSING OF QPT

Optimal control of complex atomic quantum systems

RedCRAB

S. van Frank¹, M. Bonneau¹, J. Schmiedmayer¹,
S. Hild², C. Gross², M. Cheneau^{2,3}, I. Bloch²,
T. Pichler⁴, A. Negretti⁵, T. Calarco⁴, S. Montangero⁴

Optimal control

Fast closed-loop optimal control of ultracold atoms in an optical lattice

S. Rosi¹, A. Bernard¹, N. Fabbri¹, L. Fallani^{1,2}, C. Fort¹, and M. Inguscio^{1,2}

¹*LENS and Dipartimento di Fisica e Astronomia,*

Università di Firenze and INO-CNR, 50019 Sesto Fiorentino, Italy

²*QSTAR Center for Quantum Science and Technology, Largo Enrico Fermi 2, I-50125 Arcetri, Italy*

T. Calarco³ and S. Montangero³

³*Institut für Quanteninformationsverarbeitung, Universität Ulm, D-89069 Ulm, Germany*

(Dated: July 30, 2019)

Generation and manipulation of Schrödinger cat states in Rydberg atom arrays

A. Omran,^{1,*} H. Levine,^{1,*} A. Keesling,¹ G. Semeghini,¹ T. T. Wang,^{1,2} S. Ebadi,¹ H. Bernien,³ A. S. Zibrov,¹ H. Pichler,^{1,4} S. Choi,⁵ J. Cui,⁶ M. Rossignolo,⁷ P. Rembold,⁶ S. Montangero,⁸ T. Calarco,^{6,9} M. Endres,¹⁰ M. Greiner,¹ V. Vuletić,¹¹ and M. D. Lukin^{1,†}

HIGHER DIMENSIONS

CONFINEMENT IN 2D ISING MODEL

$$H = -J \sum_{\langle i,j \rangle} \sigma_i^z \sigma_j^z - g \sum_i \sigma_i^x, \quad |\downarrow \dots \downarrow\rangle$$

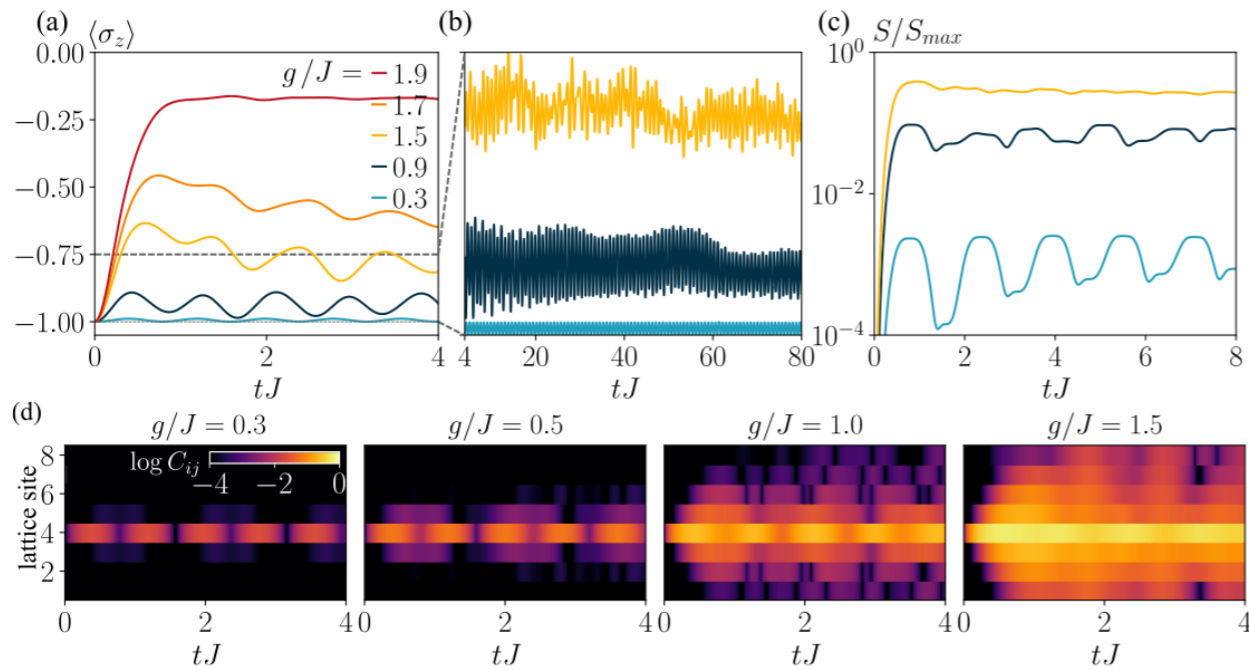


FIG. 1. Confinement in the 2D quantum Ising model. (a) Short time dependence of magnetization $\langle \sigma^z(t) \rangle$ for a set of g/J . (b) $\langle \sigma^z(t) \rangle$ for longer times and small g/J . (c) Time dependence of entanglement entropy S for a bipartition of two neighbouring spins and the rest of the system. S_{\max} is the maximal entanglement entropy of the bipartition (in this case $S_{\max} = 2 \ln 2$). (d) Time dependence of a horizontal cut of the connected correlation function C_{ij} where $i = 4$ for a set of g/J .

CONFINEMENT IN 2D ISING MODEL

$$H = -J \sum_{\langle i,j \rangle} \sigma_i^z \sigma_j^z - g \sum_i \sigma_i^x, \quad |\downarrow \dots \downarrow\rangle$$

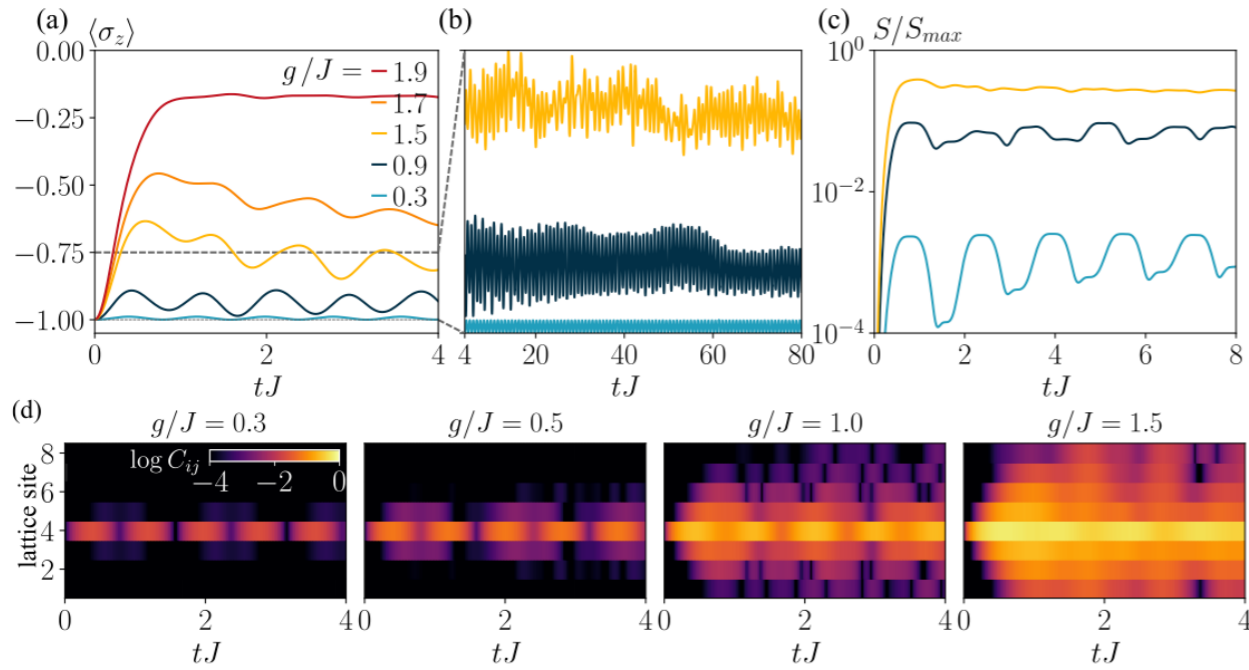


FIG. 1. Confinement in the 2D quantum Ising model. (a) Short time dependence of magnetization $\langle \sigma^z(t) \rangle$ for a set of g/J . (b) $\langle \sigma^z(t) \rangle$ for longer times and small g/J . (c) Time dependence of entanglement entropy S for a bipartition of two neighbouring spins and the rest of the system. S_{\max} is the maximal entanglement entropy of the bipartition (in this case $S_{\max} = 2 \ln 2$). (d) Time dependence of a horizontal cut of the connected correlation function C_{ij} where $i = 4$ for a set of g/J .

L. Pavešić et al. arxiv: 2406.11979, PRB (2025)

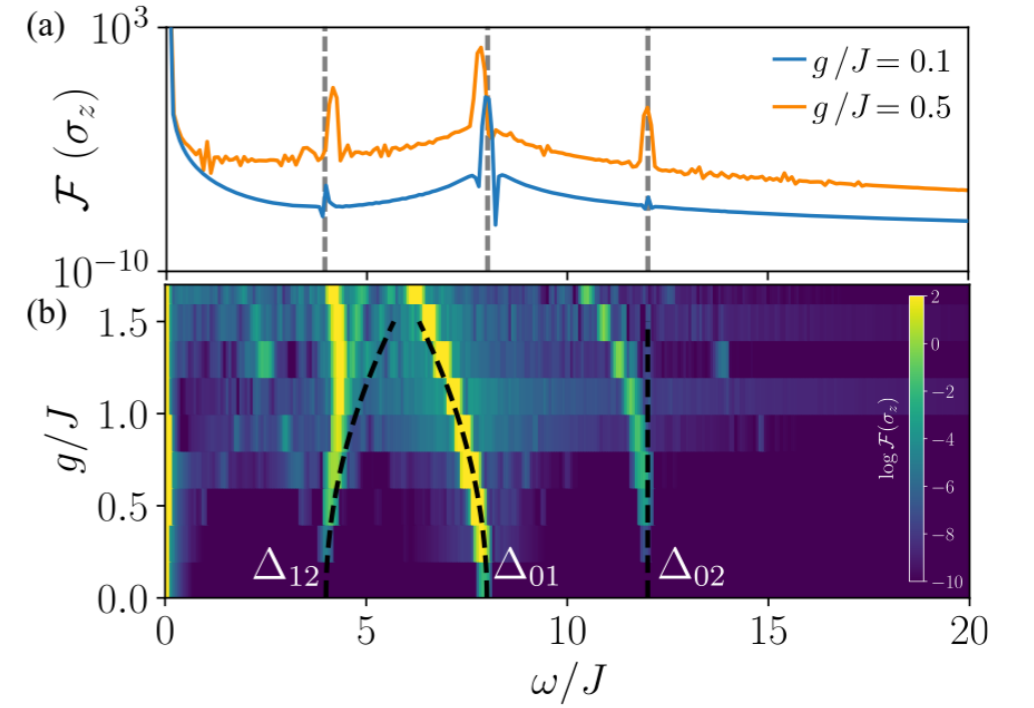


FIG. 2. Spectrum of σ^z , given by the Fourier transform $\mathcal{F}(\sigma^z)$. (a) Spectrum of magnetization for two cases of g/J . Dashed vertical lines correspond to $\omega/J = 4, 8, \text{ and } 12$. (b) Heatmap of the spectrum for a range of g/J . Black dashed lines correspond to the transition energies obtained by perturbation theory.

$$E_0 = -\frac{g^2}{8J} N^2 + \mathcal{O}(g^4),$$

$$E_1 = 8J - \frac{g^2}{8J} (N^2 + 6) + \mathcal{O}(g^4),$$

$$E_2 = 12J - \frac{g^2}{8J} N^2 + \mathcal{O}(g^4).$$

INTERFACE PHYSICS IN 2D ISING MODEL

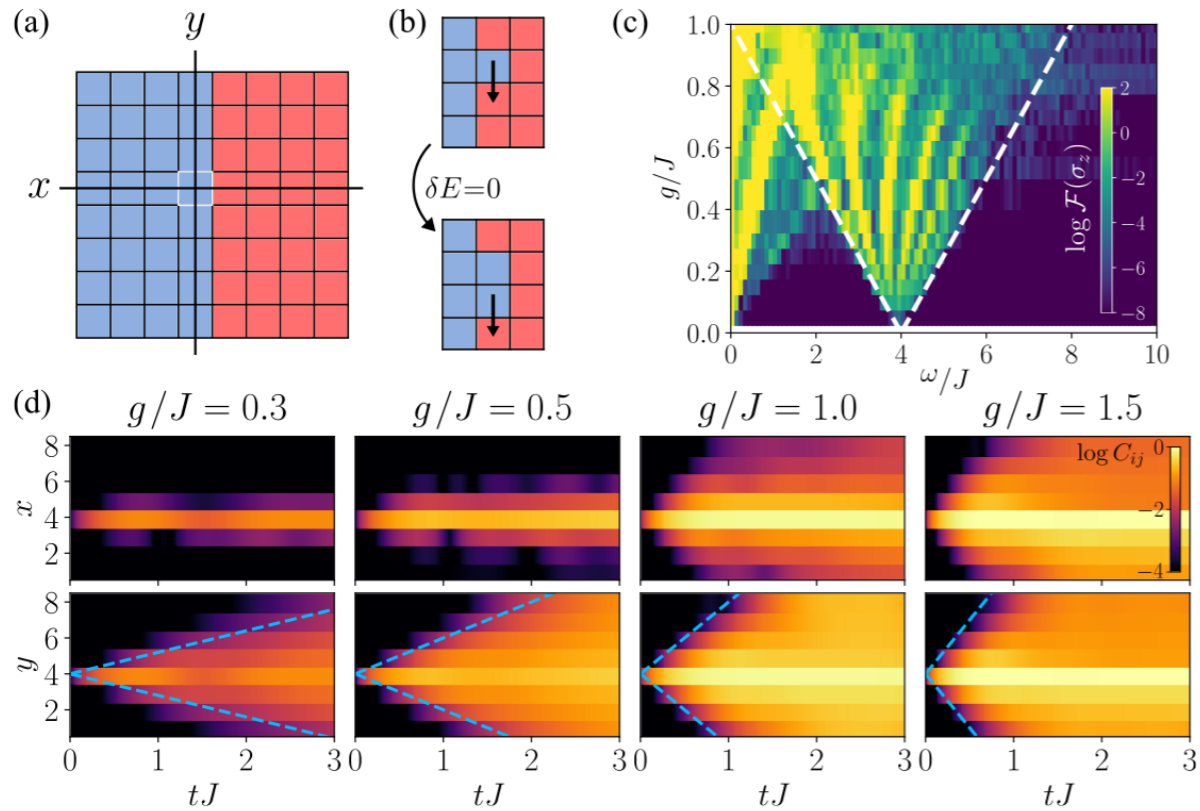


FIG. 3. Spread of correlations near an interface. (a) Sketch of the initial state, with blue representing \uparrow and red \downarrow spins. Black lines indicate the cuts shown in (d). (b) Sketch of the resonant process along the interface. (c) Heatmap of the spectral density of $\langle \sigma^z \rangle(t)$ for a spin at the interface for a range of g/J . White dashed lines correspond to the transition energies of a freely propagating edge mode. (d) Horizontal (x) and vertical (y) cuts of the connected correlations function C_{ij} with respect to the spin at $(4,4)$ (white square in (a)). Blue dashed lines are $\pm 4gt$, showing that the interface mode carries the correlations.

INTERFACE PHYSICS IN 2D ISING MODEL

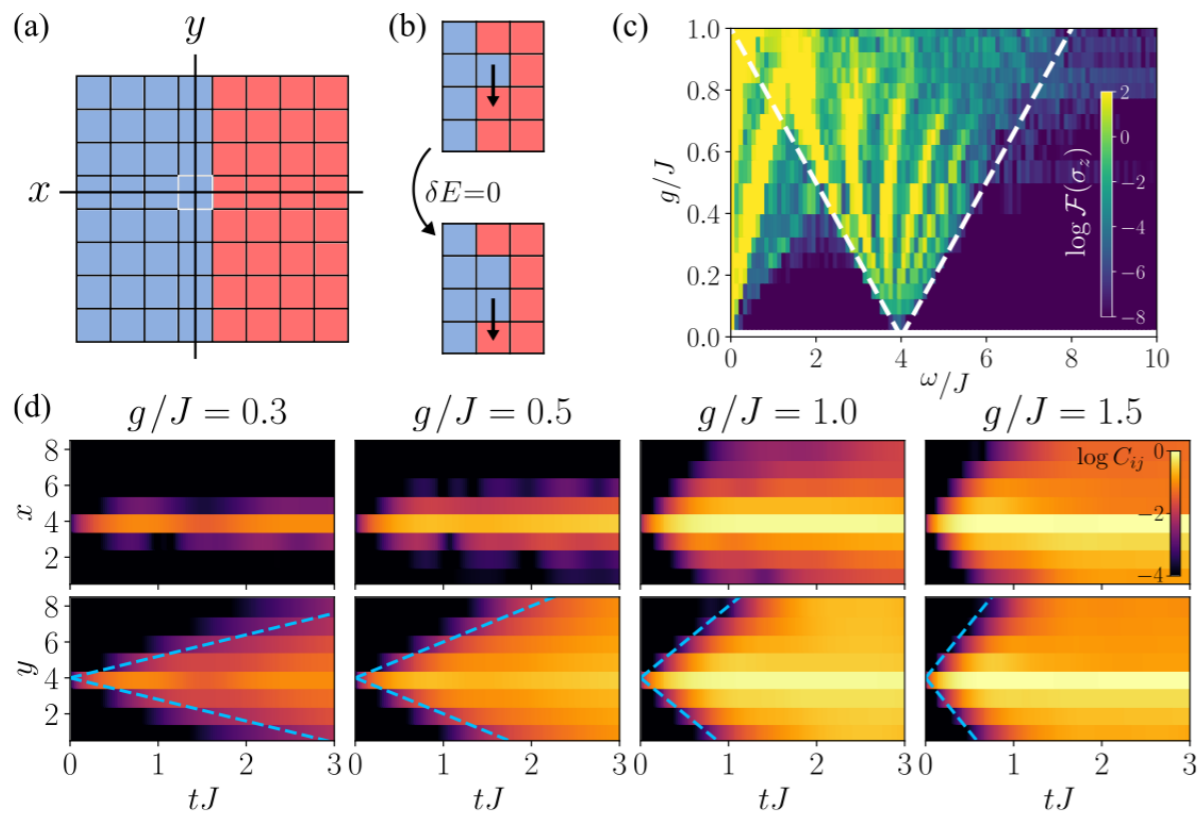
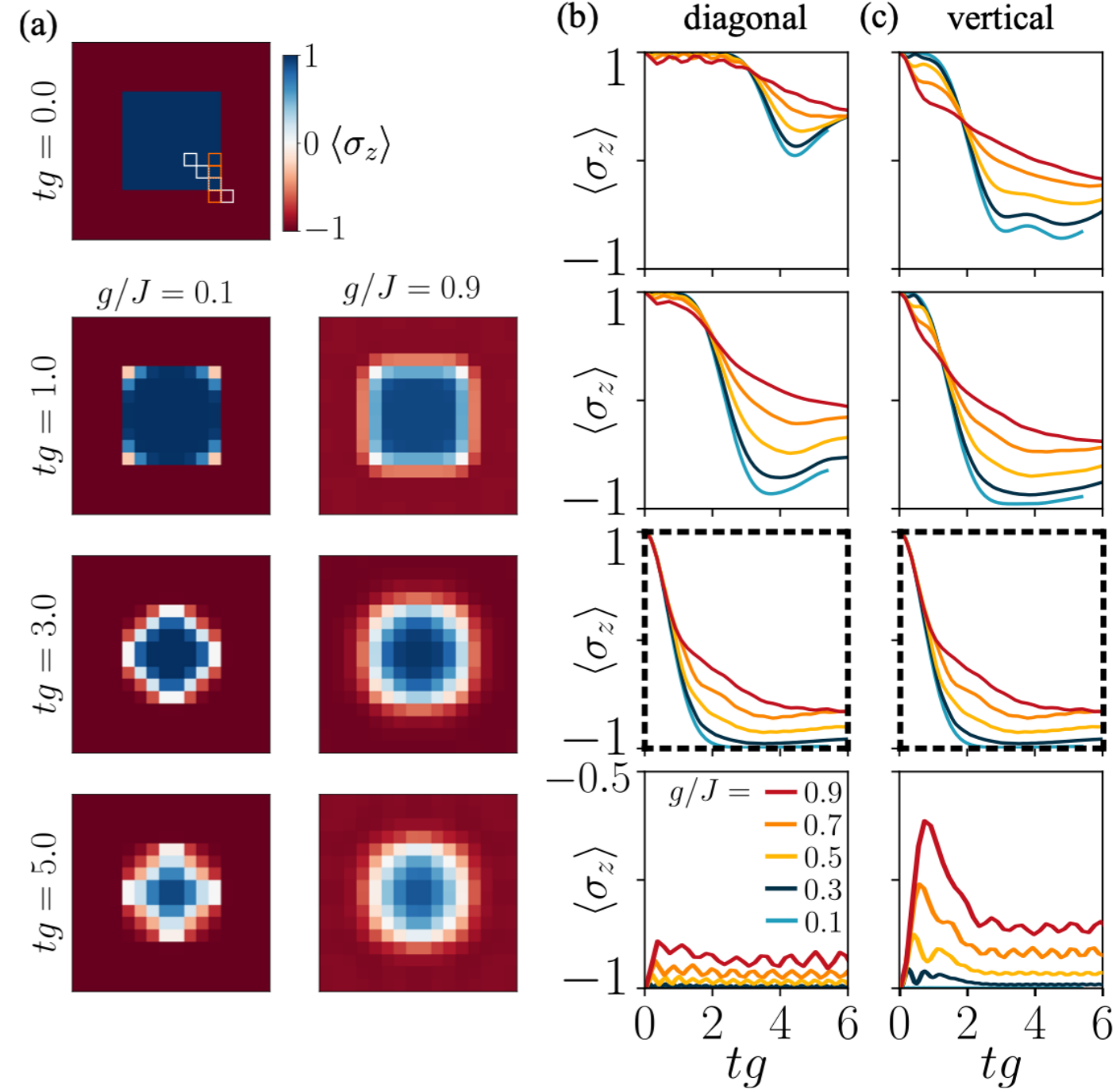
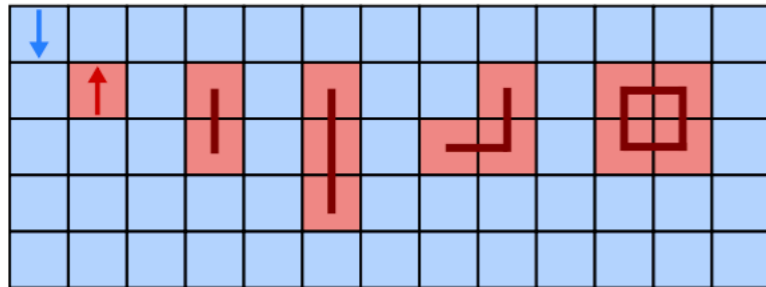


FIG. 3. Spread of correlations near an interface. (a) Sketch of the initial state, with blue representing \uparrow and red \downarrow spins. Black lines indicate the cuts shown in (d). (b) Sketch of the resonant process along the interface. (c) Heatmap of the spectral density of $\langle \sigma^z \rangle(t)$ for a spin at the interface for a range of g/J . White dashed lines correspond to the transition energies of a freely propagating edge mode. (d) Horizontal (x) and vertical (y) cuts of the connected correlations function C_{ij} with respect to the spin at (4,4) (white square in (a)). Blue dashed lines are $\pm 4gt$, showing that the interface mode carries the correlations.



STATE PREPARATION FOR SCATTERING SIMULATIONS

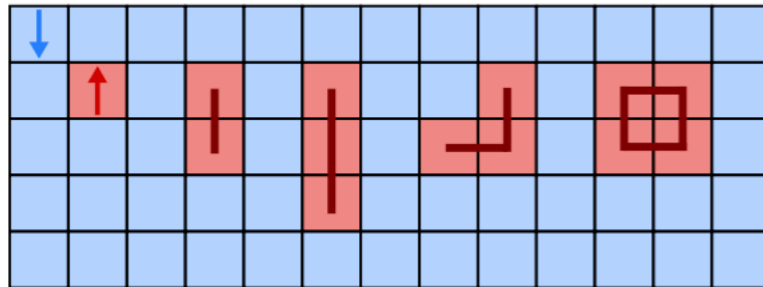
(a) magnon 2-spin 3-spin vertical kink 4-spin



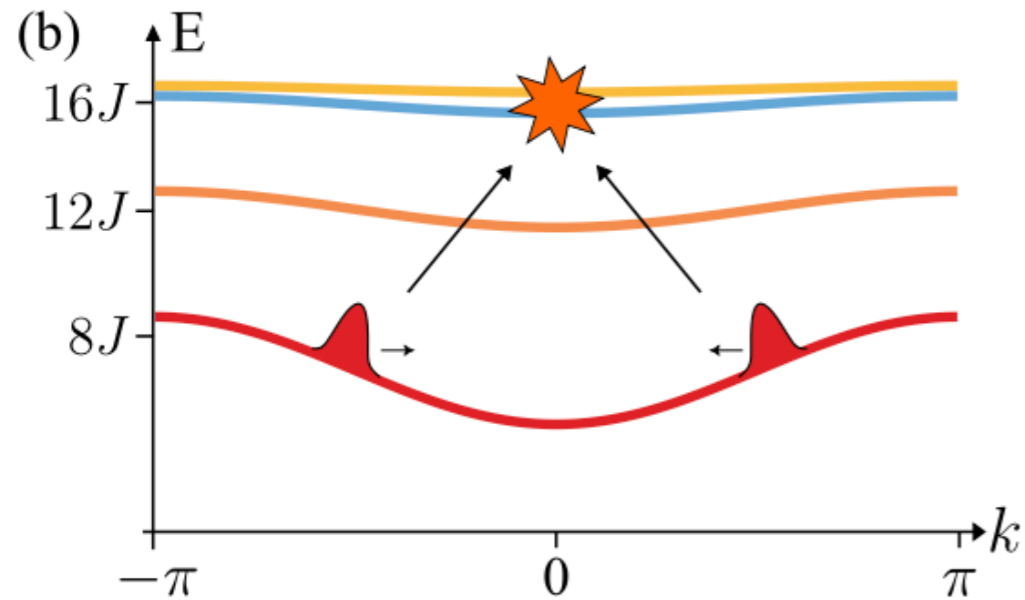
$$H = -J \sum_{\langle ij \rangle} Z_i Z_j - g \sum_i X_i - h \sum_i Z_i$$

STATE PREPARATION FOR SCATTERING SIMULATIONS

(a) magnon 2-spin 3-spin 4-spin
vertical kink

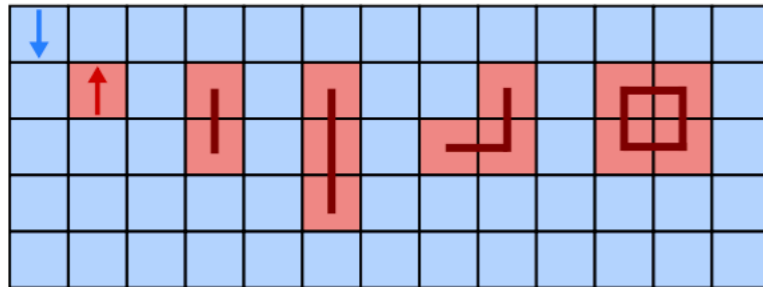


$$H = -J \sum_{\langle ij \rangle} Z_i Z_j - g \sum_i X_i - h \sum_i Z_i$$



STATE PREPARATION FOR SCATTERING SIMULATIONS

(a) magnon 2-spin 3-spin vertical kink 4-spin

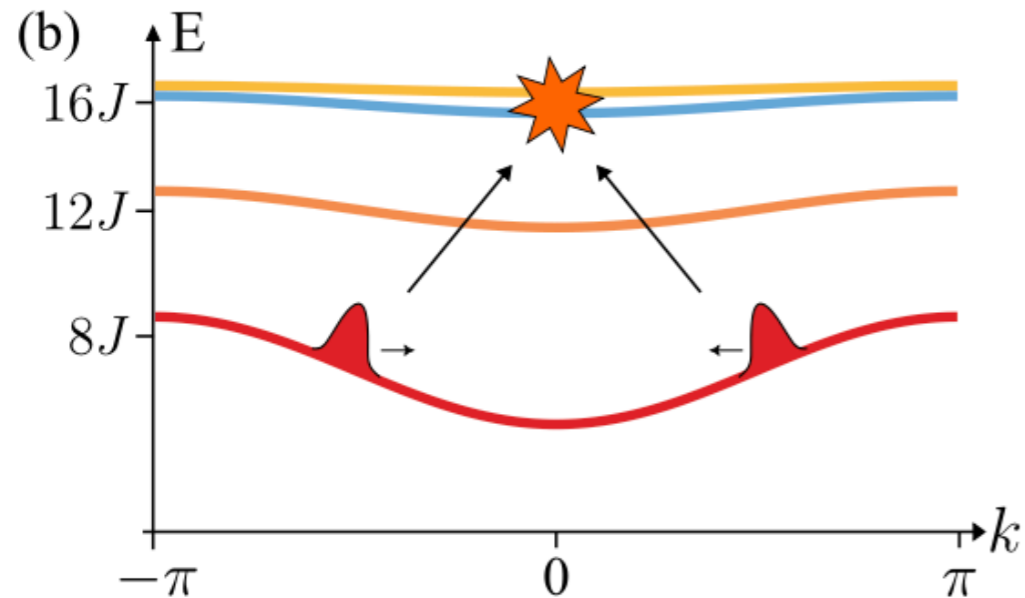


$$g = 0,$$

$$|\mathbf{r}_0, \mathbf{k}\rangle = \frac{1}{N} \sum_{\mathbf{r}} f(\mathbf{r}, \mathbf{r}_0) e^{i\mathbf{k}\cdot\mathbf{r}} X_{\mathbf{r}} |0\rangle$$

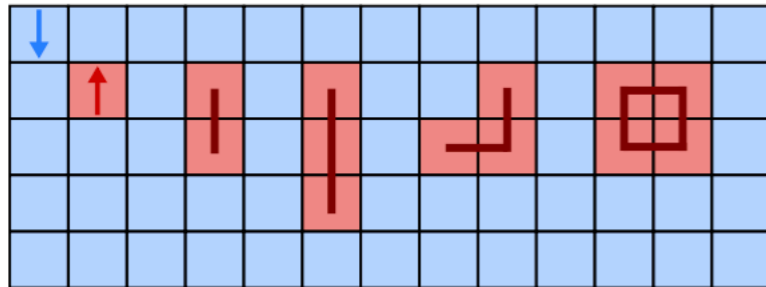
$$f(\mathbf{r}, \mathbf{r}_0) = \frac{1}{\sigma\sqrt{\pi}} e^{-\frac{(\mathbf{r}-\mathbf{r}_0)^2}{2\sigma^2}}$$

$$H = -J \sum_{\langle ij \rangle} Z_i Z_j - g \sum_i X_i - h \sum_i Z_i$$



STATE PREPARATION FOR SCATTERING SIMULATIONS

(a) magnon 2-spin 3-spin 4-spin
vertical kink



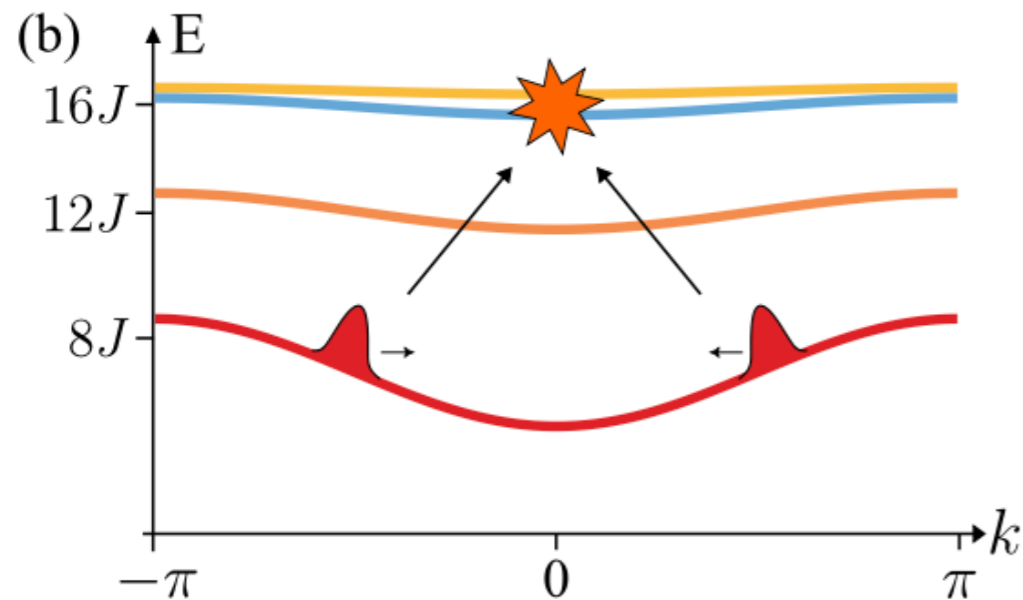
$$H = -J \sum_{\langle ij \rangle} Z_i Z_j - g \sum_i X_i - h \sum_i Z_i$$

$$g = 0,$$

$$|\mathbf{r}_0, \mathbf{k}\rangle = \frac{1}{N} \sum_{\mathbf{r}} f(\mathbf{r}, \mathbf{r}_0) e^{i\mathbf{k} \cdot \mathbf{r}} X_{\mathbf{r}} |0\rangle$$

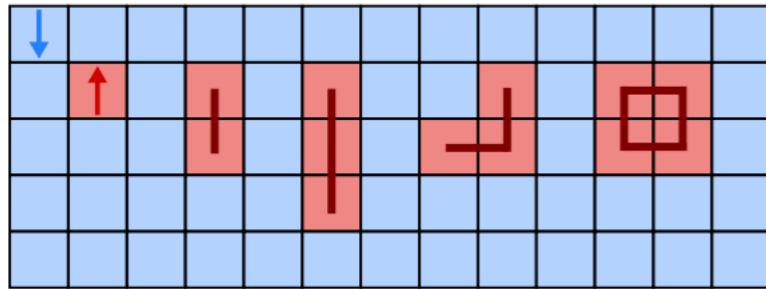
$$f(\mathbf{r}, \mathbf{r}_0) = \frac{1}{\sigma \sqrt{\pi}} e^{-\frac{(\mathbf{r}-\mathbf{r}_0)^2}{2\sigma^2}}$$

$$g(t) = g^* \sin^2 \left(\frac{\pi}{2} \sin^2 \left(\frac{\pi t}{2\tau} \right) \right)$$



STATE PREPARATION FOR SCATTERING SIMULATIONS

(a) magnon 2-spin 3-spin 4-spin
vertical kink



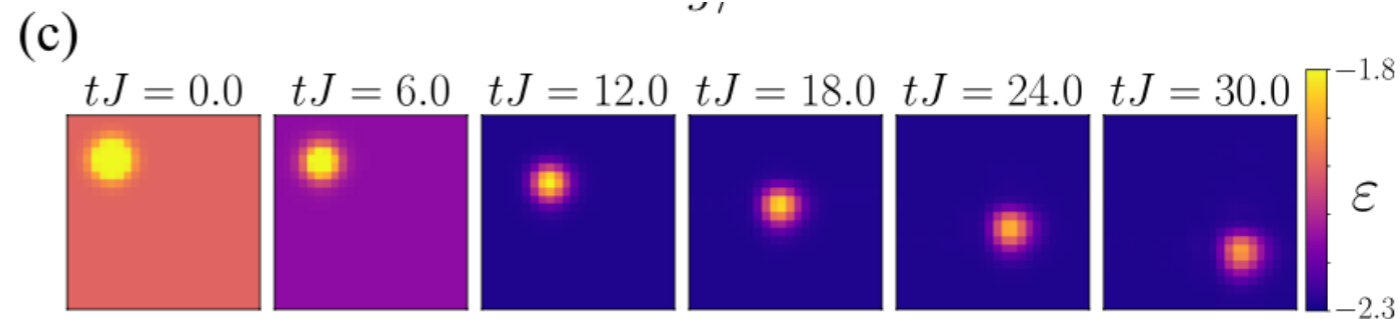
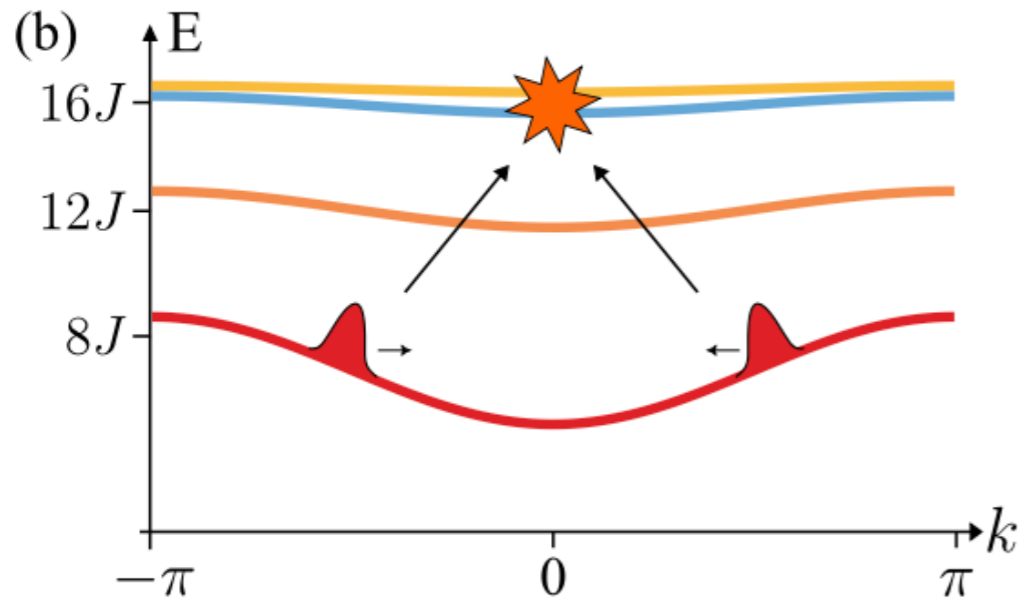
$$H = -J \sum_{\langle ij \rangle} Z_i Z_j - g \sum_i X_i - h \sum_i Z_i$$

$$g = 0,$$

$$|\mathbf{r}_0, \mathbf{k}\rangle = \frac{1}{N} \sum_{\mathbf{r}} f(\mathbf{r}, \mathbf{r}_0) e^{i\mathbf{k} \cdot \mathbf{r}} X_{\mathbf{r}} |0\rangle$$

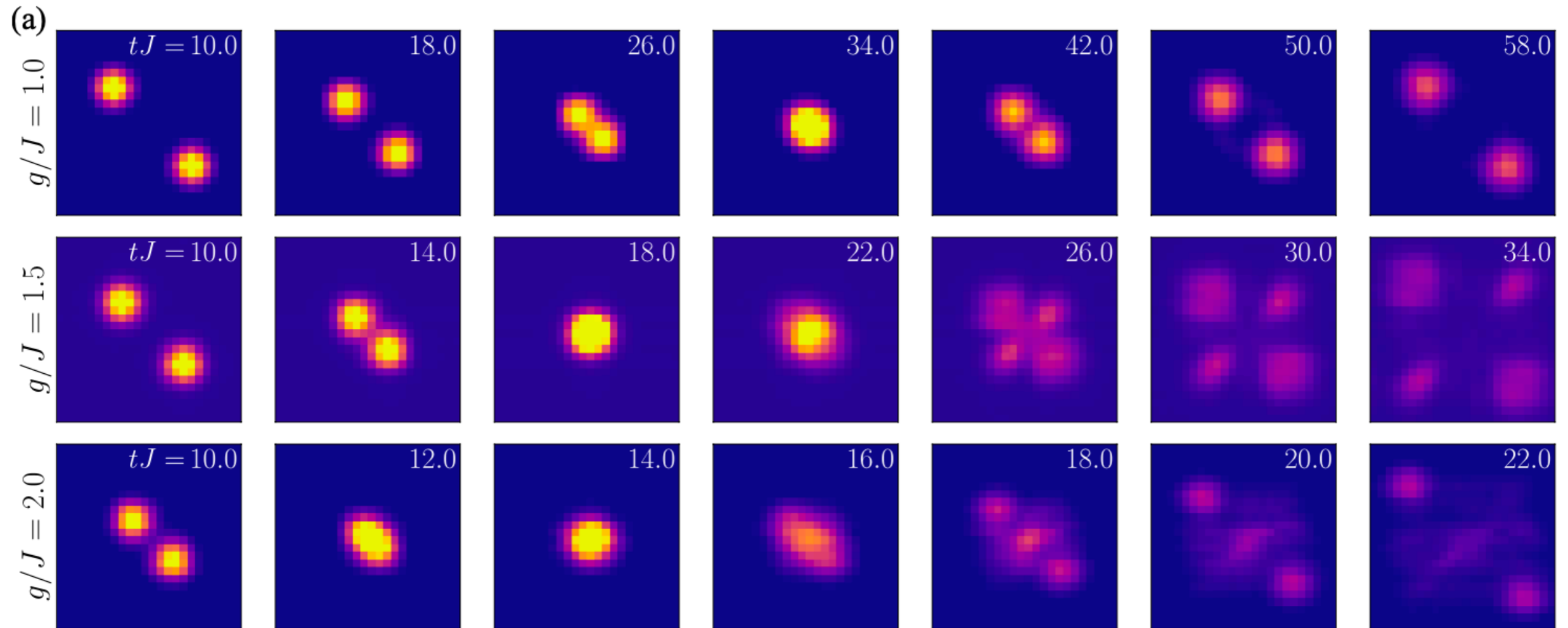
$$f(\mathbf{r}, \mathbf{r}_0) = \frac{1}{\sigma \sqrt{\pi}} e^{-\frac{(\mathbf{r}-\mathbf{r}_0)^2}{2\sigma^2}}$$

$$g(t) = g^* \sin^2 \left(\frac{\pi}{2} \sin^2 \left(\frac{\pi t}{2\tau} \right) \right)$$



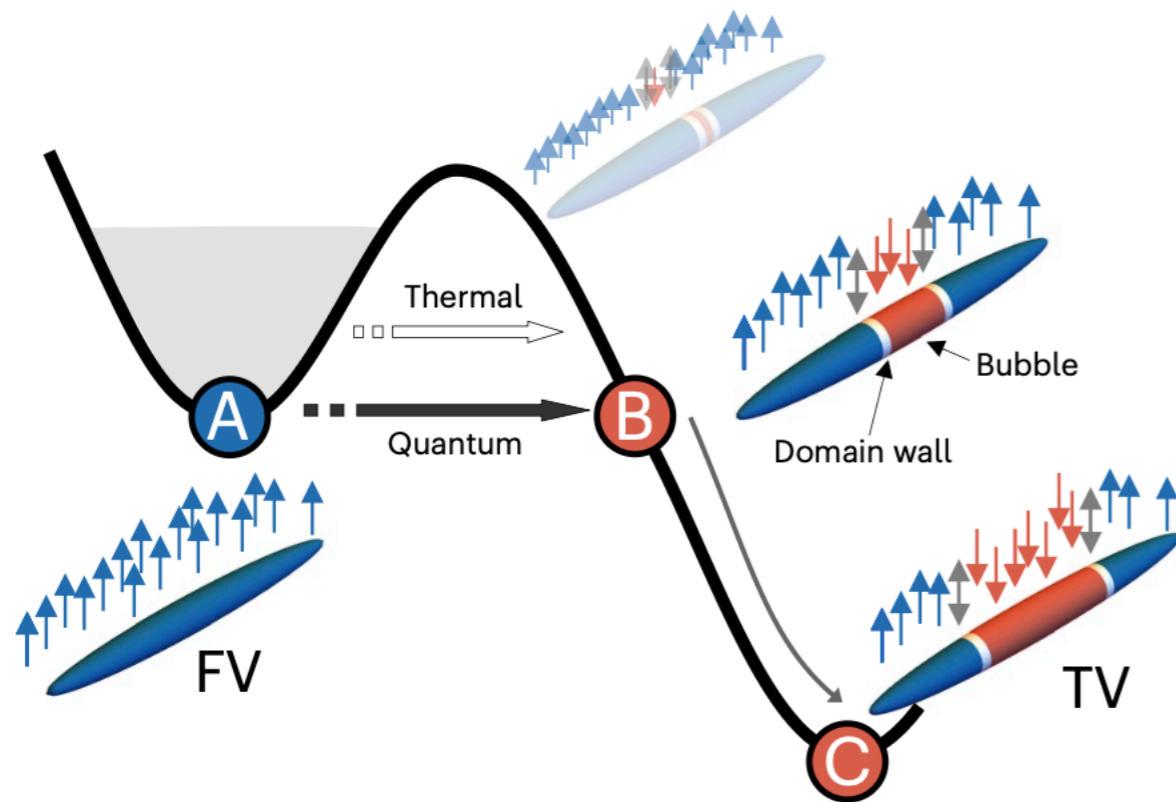
$$\tau J = 10, \mathbf{k} = \left(\frac{\pi}{2}, \frac{\pi}{2} \right) \text{ and } g/J = 1.5.$$

2D+1 SCATTERING IN ISING MODEL VIA TTN



$$H = -J \sum_{\langle ij \rangle} Z_i Z_j - g \sum_i X_i - h \sum_i Z_i$$

FALSE VACUUM DECAY



C. Callan; S. Coleman "Fate of the false vacuum. II. First quantum corrections". *Physical Review D*. **D16** (6): 1762–68 (1977)..

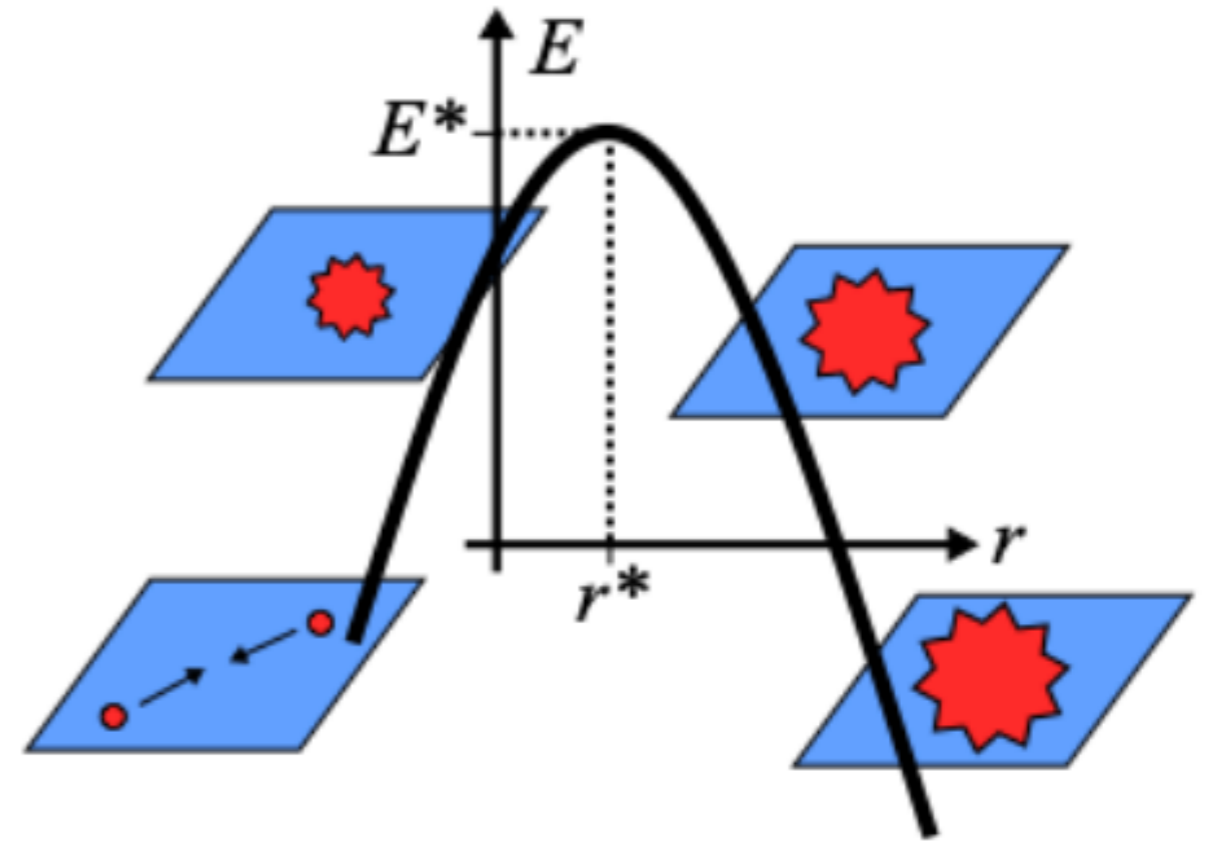
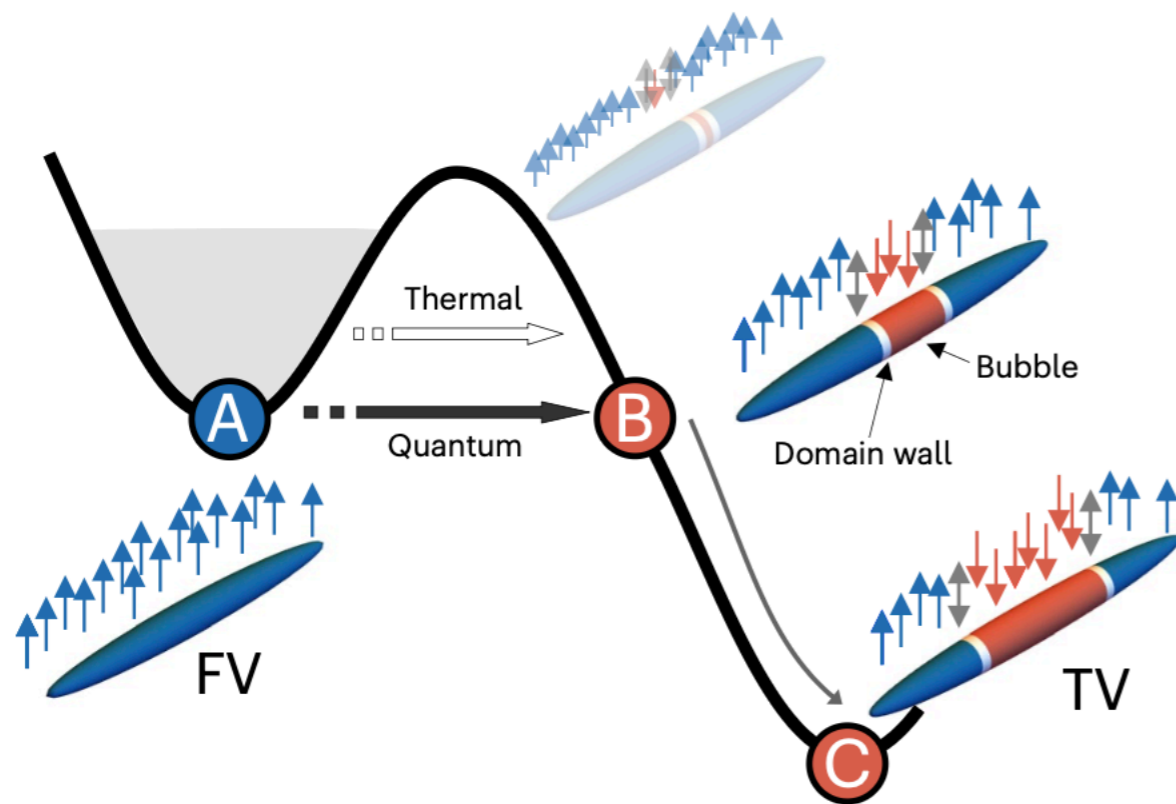
Turner, M. S.; Wilczek, F. "Is our vacuum metastable?" (PDF). *Nature*. 298 (5875): 633–634 (1982).

Abel, S; Spannowsky, M. "Quantum-Field-Theoretic Simulation Platform for Observing the Fate of the False Vacuum". *PRX Quantum*. 2: 010349 (2021).

Alessandro Zenesini, Anna Berti, Riccardo Cominotti, Chiara Rogora, Ian Moss, Tom Billam, Iacopo Carusotto, Giacomo Lamporesi, Alessio Recati, Gabriele Ferrari "False Vacuum decay via bubble formation in ferromagnetic superfluids", *Nature Physics* (2023),

....

FALSE VACUUM DECAY



C. Callan; S. Coleman "Fate of the false vacuum. II. First quantum corrections". *Physical Review D*. **D16** (6): 1762–68 (1977)..

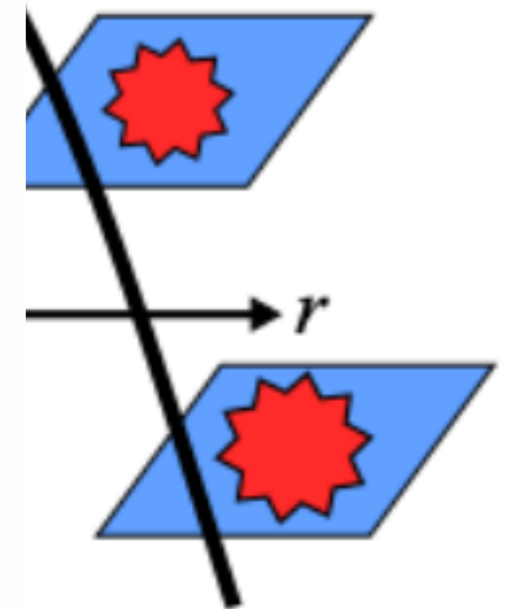
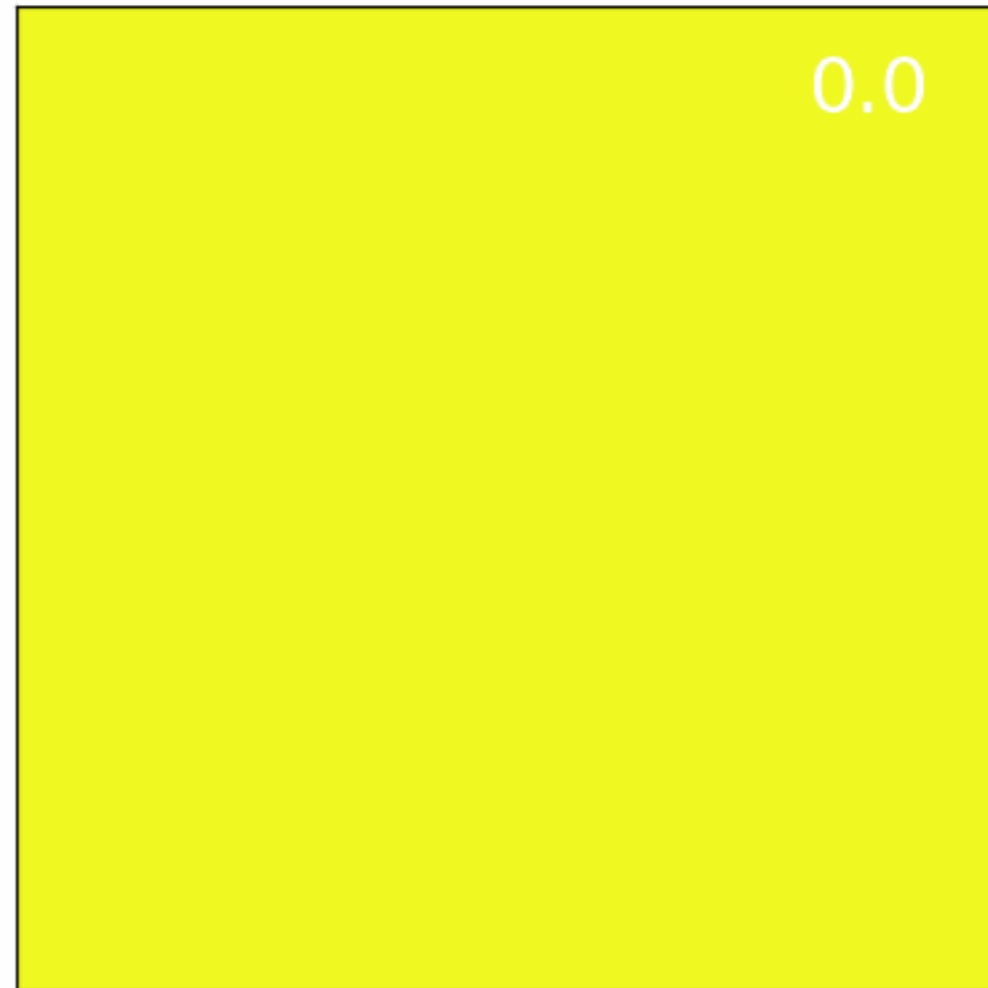
Turner, M. S.; Wilczek, F. "Is our vacuum metastable?" (PDF). *Nature*. 298 (5875): 633–634 (1982).

Abel, S; Spannowsky, M. "Quantum-Field-Theoretic Simulation Platform for Observing the Fate of the False Vacuum". *PRX Quantum*. 2: 010349 (2021).

Alessandro Zenesini, Anna Berti, Riccardo Cominotti, Chiara Rogora, Ian Moss, Tom Billam, Iacopo Carusotto, Giacomo Lamporesi, Alessio Recati, Gabriele Ferrari "False Vacuum decay via bubble formation in ferromagnetic superfluids", *Nature Physics* (2023),

....

FALSE VACUUM DECAY



C. Callan; S. Coleman "F

Turner, M. S.; Wilczek, F.

Abel, S; Spannowsky, M.

Quantum. 2: 010349 (2021).

Alessandro Zenesini, Anna Berti, Riccardo Cominotti, Chiara Rogora, Ian Moss, Tom Billam, Iacopo Carusotto, Giacomo Lamporesi, Alessio Recati, Gabriele Ferrari "False Vacuum decay via bubble formation in ferromagnetic superfluids", Nature Physics (2023),

....

FALSE VACUUM DECAY IN THE 2D+1 ISING MODEL

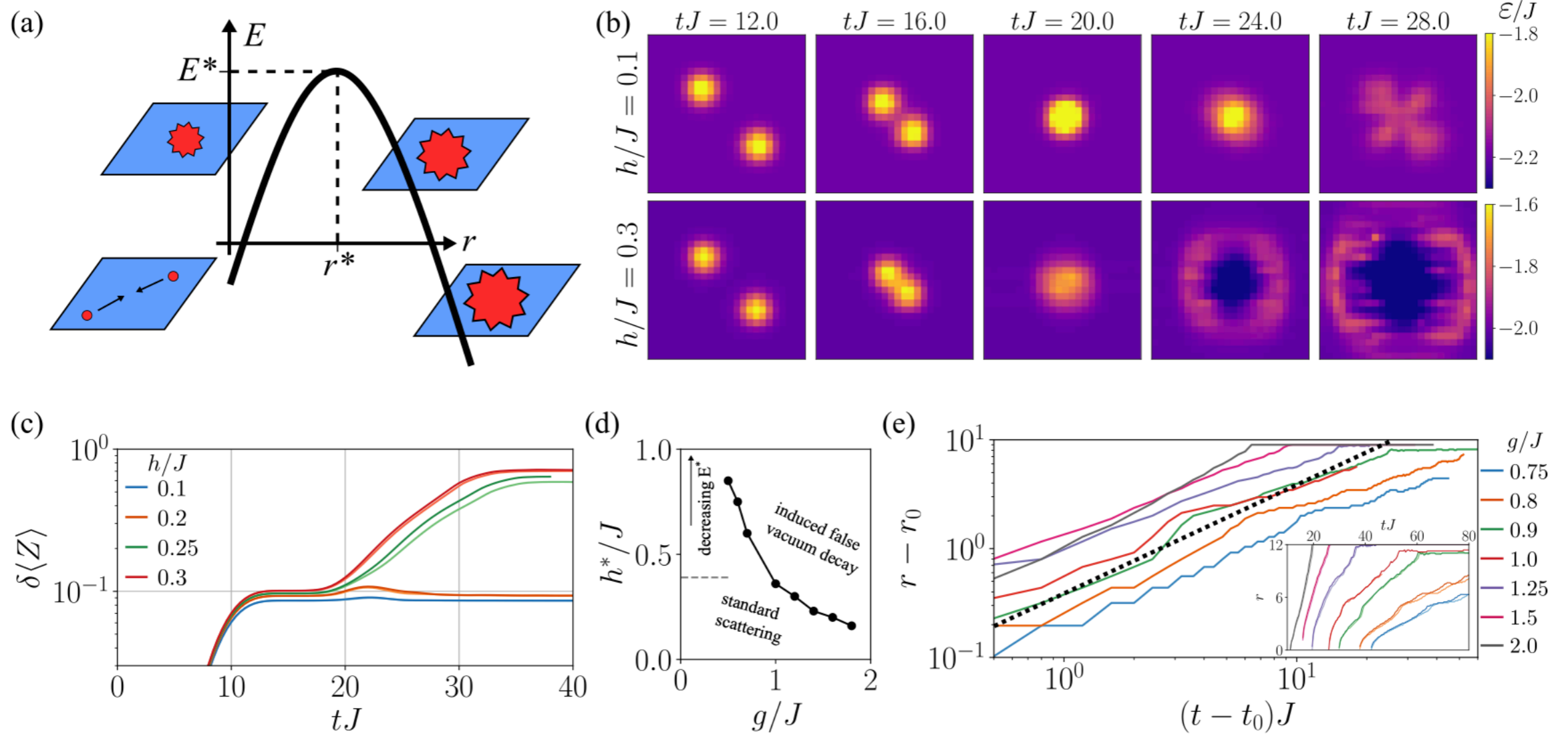
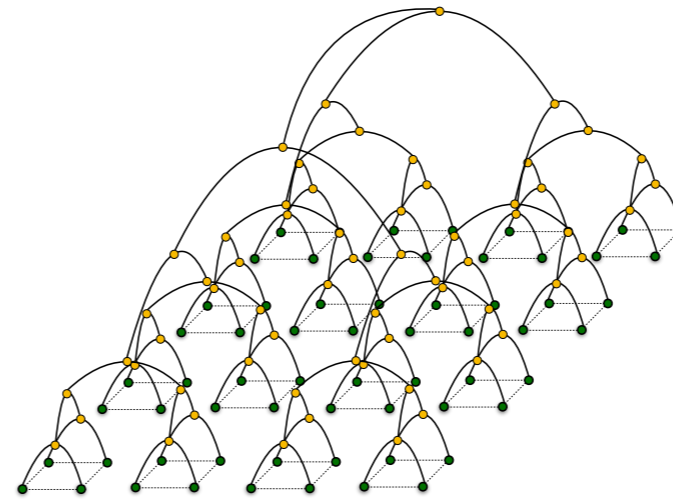
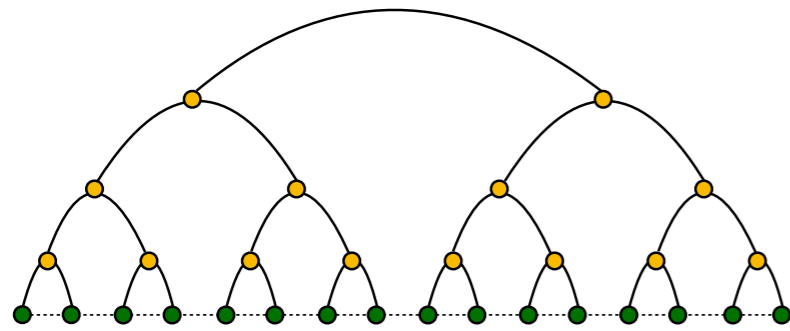


FIG. 3. Scattering in the false vacuum. (a) A sketch of the energy landscape of a true vacuum bubble with radius r . (b) The evolution of the energy density during scattering with $h/J = 0.1$ and $h/J = 0.3$, both with $g/J = 1.5$ and $\mathbf{k} = (\frac{\pi}{2}, \frac{\pi}{2})$. (c) The change in magnetization per site with varying h for $g/J = 1.5$ and $\mathbf{k} = (\frac{\pi}{2}, \frac{\pi}{2})$. (d) The dependence of the threshold value h^* on g/J . The gray dashed line corresponds to the threshold h^* expected for $g \rightarrow 0$. See text for details. (e) The evolution of the radius of the true vacuum bubble in log-log scale for varying g , with some longitudinal field larger than the threshold value. We subtract the time t_0 when the radius reaches $r_0 = 3$ on the horizontal, and r_0 on the vertical axis. The black dashed line corresponds to linear growth and acts as a guide to the eye. (Inset) The evolution of the radius in lin-lin scale. In (c) and (e), the curves with different shades of the same color correspond to simulations with different bond dimension, darker is bigger. Here we use 150 and 200.

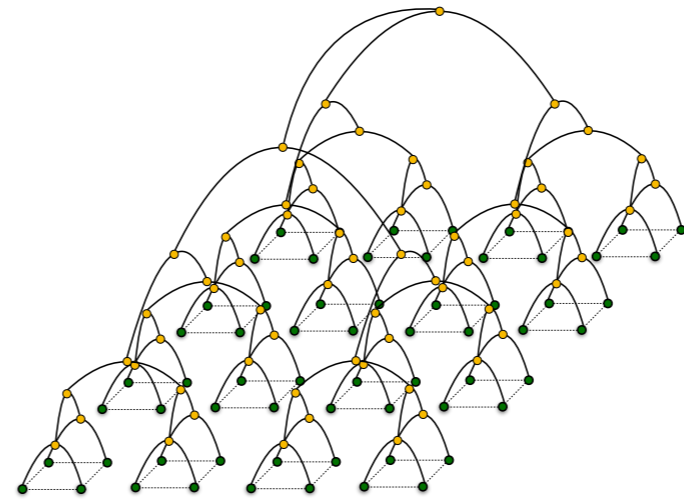
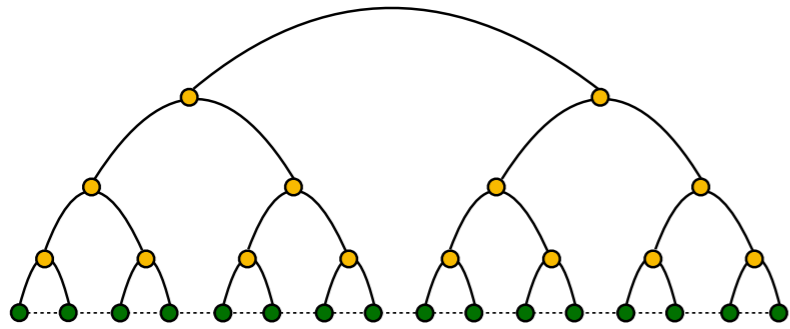
3D TREE TENSOR NETWORK



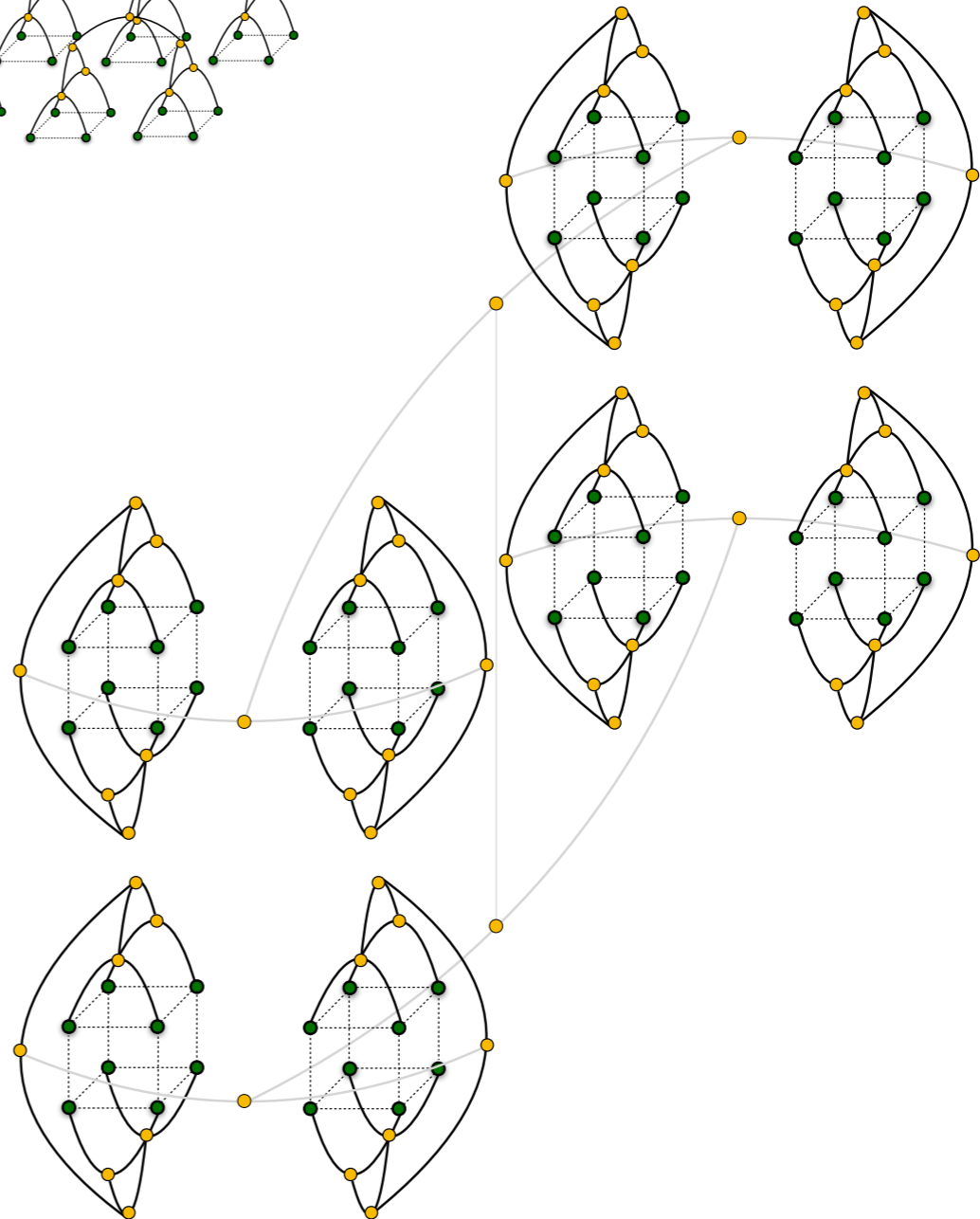
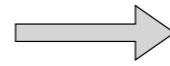
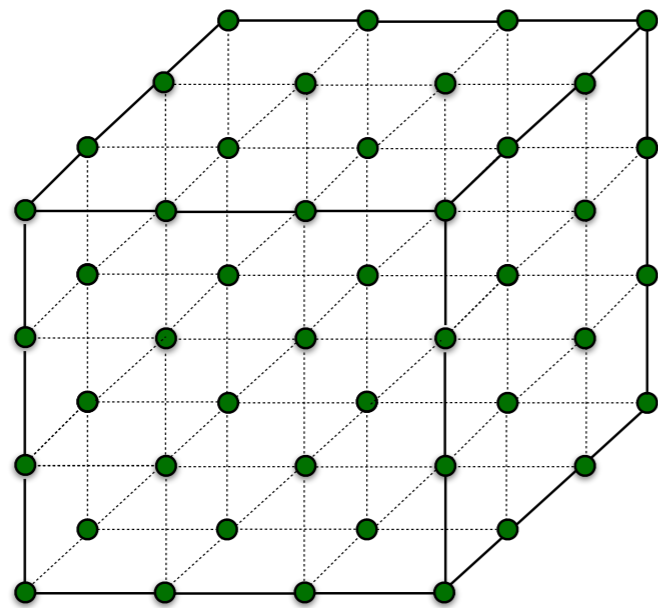
T. Felser, P. Silvi, M. Collura,
S. Montangero
PRX (2020)

*G. Magnifico, T. Felser, P. Silvi, and S. Montangero
Nat. Comm. (2021)*

3D TREE TENSOR NETWORK



T. Felser, P. Silvi, M. Collura,
S. Montangero
PRX (2020)

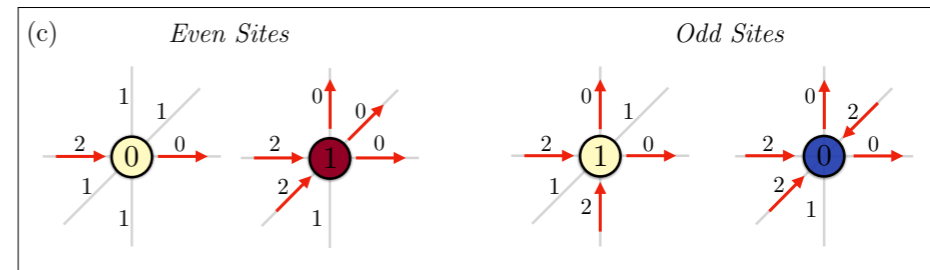
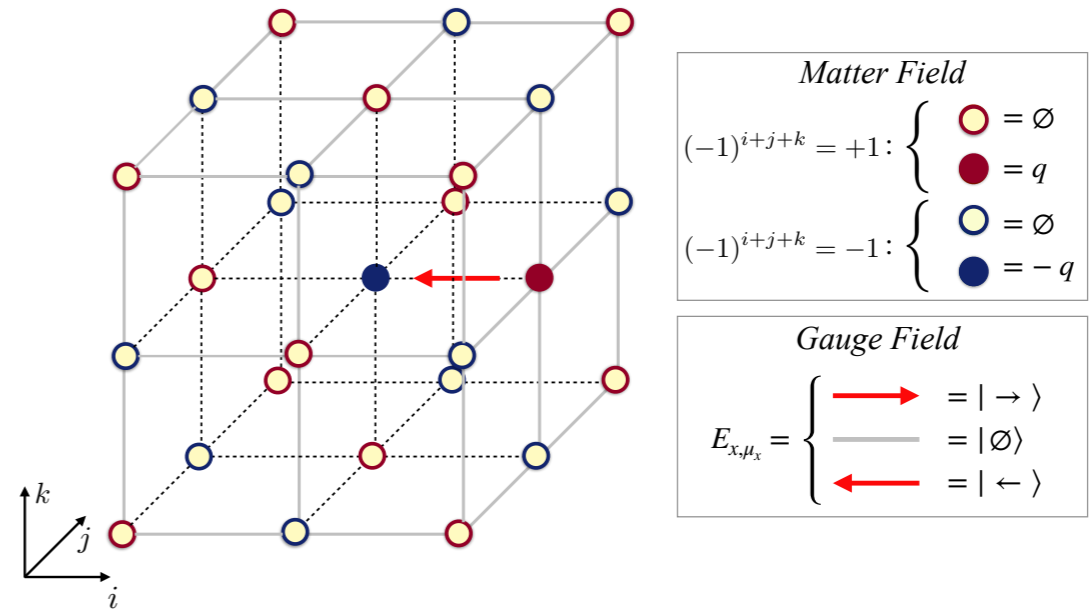


G. Magnifico, T. Felser, P. Silvi, and S. Montangero
Nat. Comm. (2021)

3D QUANTUM-LINK FORMULATION OF QED

$$\hat{H} = -t \sum_{x,\mu} \left(\hat{\psi}_x^\dagger \hat{U}_{x,\mu} \hat{\psi}_{x+\mu} + \text{H.c.} \right) \\ + m \sum_x (-1)^x \hat{\psi}_x^\dagger \hat{\psi}_x + \frac{g_e^2}{2} \sum_{x,\mu} \hat{E}_{x,\mu}^2 \\ - \frac{g_m^2}{2} \sum_x \left(\square_{\mu_x,\mu_y} + \square_{\mu_x,\mu_z} + \square_{\mu_y,\mu_z} + \text{H.c.} \right)$$

$$\hat{G}_x = \hat{\psi}_x^\dagger \hat{\psi}_x - \frac{1 - (-1)^x}{2} - \sum_{\mu} \hat{E}_{x,\mu}$$



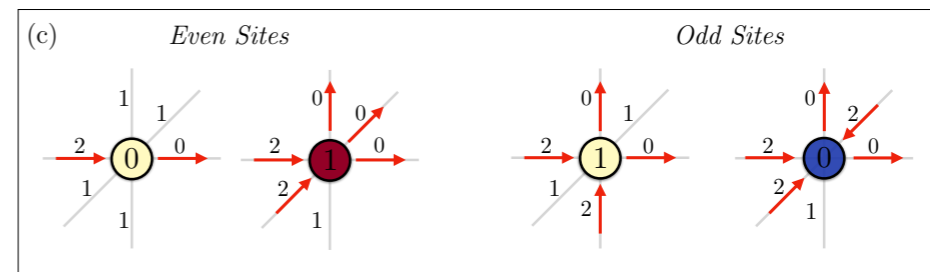
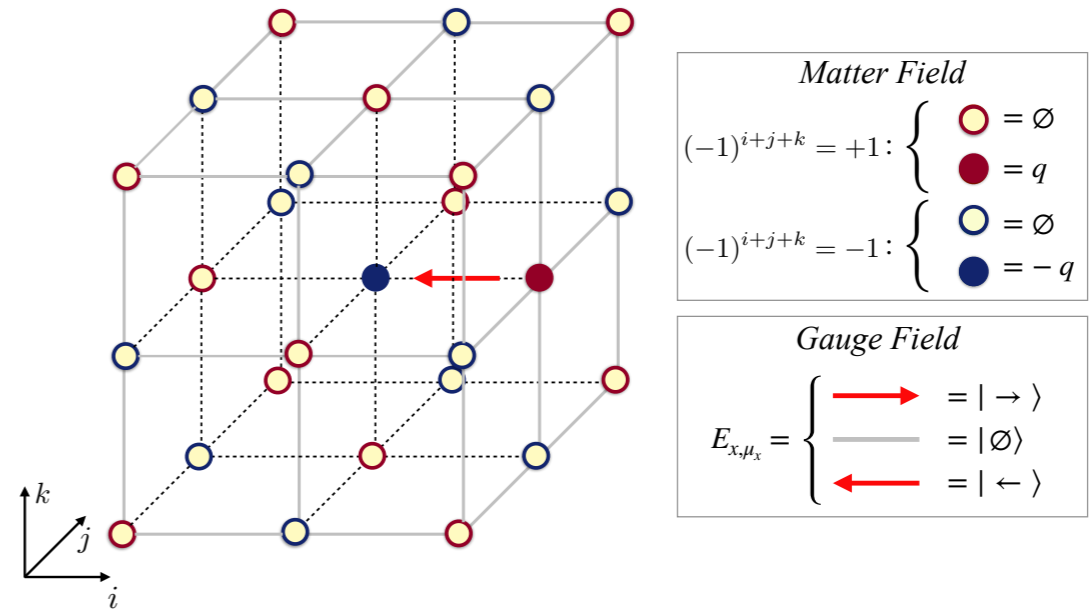
$$H_{pen} = \nu \sum_{x,\mu} \left(1 - \delta_{2,\hat{L}_{x,\mu}} \right)$$

3D QUANTUM-LINK FORMULATION OF QED

$$\hat{H} = -t \sum_{x,\mu} \left(\hat{\psi}_x^\dagger \hat{U}_{x,\mu} \hat{\psi}_{x+\mu} + \text{H.c.} \right) + m \sum_x (-1)^x \hat{\psi}_x^\dagger \hat{\psi}_x + \frac{g_e^2}{2} \sum_{x,\mu} \hat{E}_{x,\mu}^2 - \frac{g_m^2}{2} \sum_x \left(\square_{\mu_x,\mu_y} + \square_{\mu_x,\mu_z} + \square_{\mu_y,\mu_z} + \text{H.c.} \right)$$

$$\hat{G}_x = \hat{\psi}_x^\dagger \hat{\psi}_x - \frac{1 - (-1)^x}{2} - \sum_{\mu} \hat{E}_{x,\mu}$$

Local dimension 267, up to 12288 Hamiltonian operators



$$H_{pen} = \nu \sum_{x,\mu} \left(1 - \delta_{2, \hat{L}_{x,\mu}} \right)$$

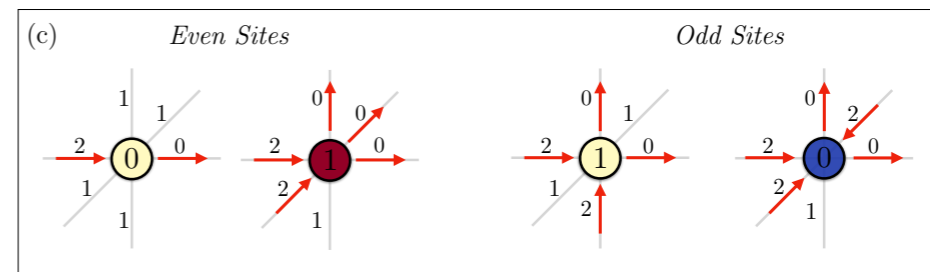
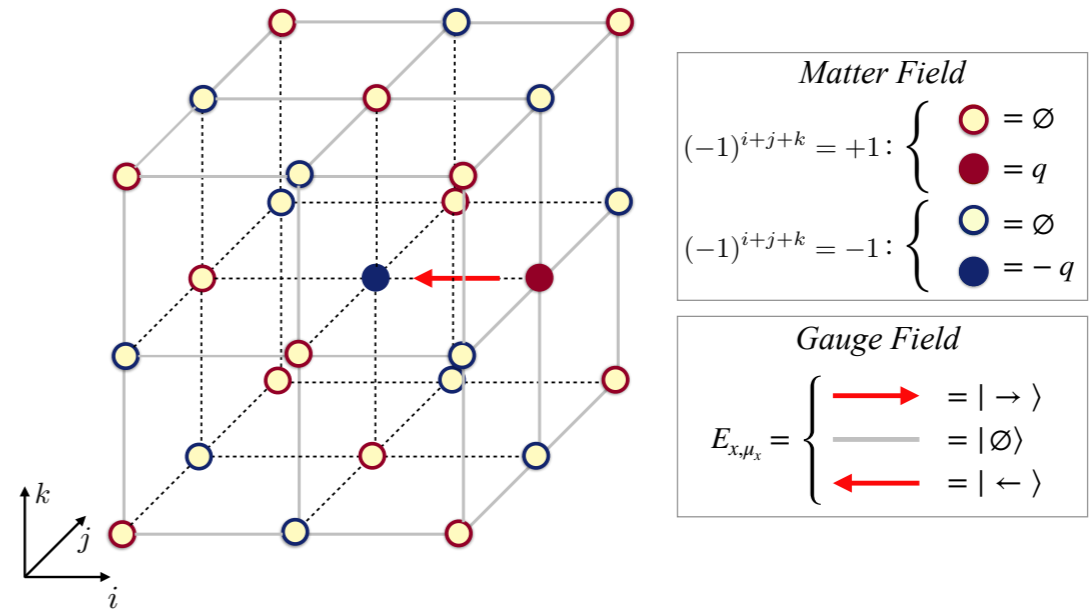
3D QUANTUM-LINK FORMULATION OF QED

$$\hat{H} = -t \sum_{x,\mu} \left(\hat{\psi}_x^\dagger \hat{U}_{x,\mu} \hat{\psi}_{x+\mu} + \text{H.c.} \right) + m \sum_x (-1)^x \hat{\psi}_x^\dagger \hat{\psi}_x + \frac{g_e^2}{2} \sum_{x,\mu} \hat{E}_{x,\mu}^2 - \frac{g_m^2}{2} \sum_x \left(\square_{\mu_x,\mu_y} + \square_{\mu_x,\mu_z} + \square_{\mu_y,\mu_z} + \text{H.c.} \right)$$

$$\hat{G}_x = \hat{\psi}_x^\dagger \hat{\psi}_x - \frac{1 - (-1)^x}{2} - \sum_{\mu} \hat{E}_{x,\mu}$$

Local dimension 267, up to 12288 Hamiltonian operators

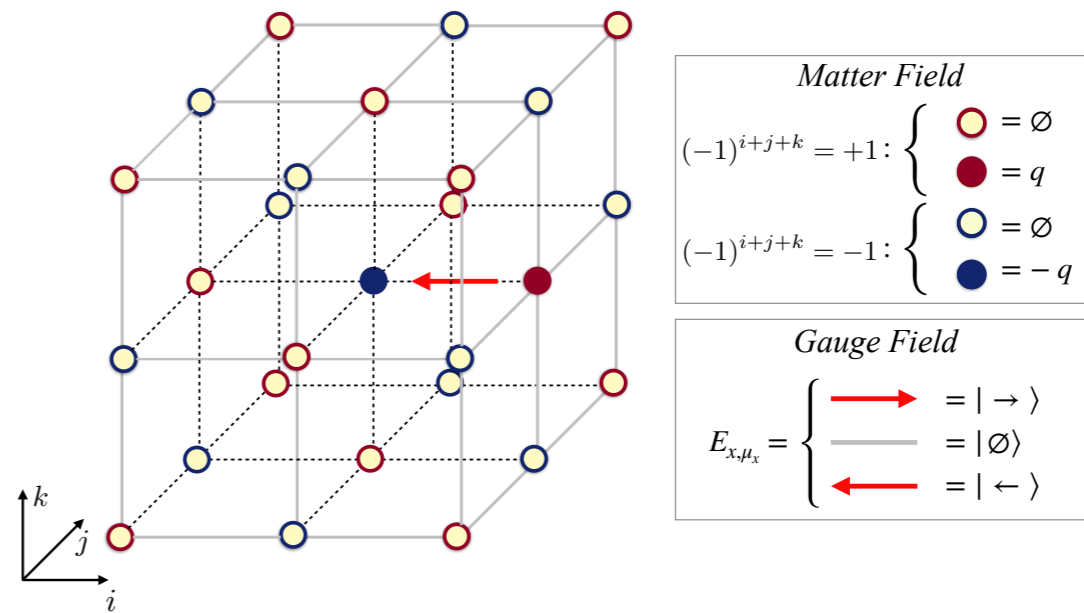
Up to 5 weeks x 64 cores of computational time



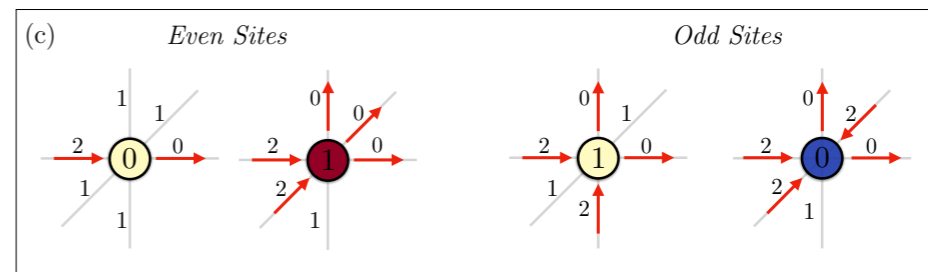
$$H_{pen} = \nu \sum_{x,\mu} \left(1 - \delta_{2, \hat{L}_{x,\mu}} \right)$$

3D QUANTUM-LINK FORMULATION OF QED

$$\hat{H} = -t \sum_{x,\mu} \left(\hat{\psi}_x^\dagger \hat{U}_{x,\mu} \hat{\psi}_{x+\mu} + \text{H.c.} \right) + m \sum_x (-1)^x \hat{\psi}_x^\dagger \hat{\psi}_x + \frac{g_e^2}{2} \sum_{x,\mu} \hat{E}_{x,\mu}^2 - \frac{g_m^2}{2} \sum_x \left(\square_{\mu_x,\mu_y} + \square_{\mu_x,\mu_z} + \square_{\mu_y,\mu_z} + \text{H.c.} \right)$$



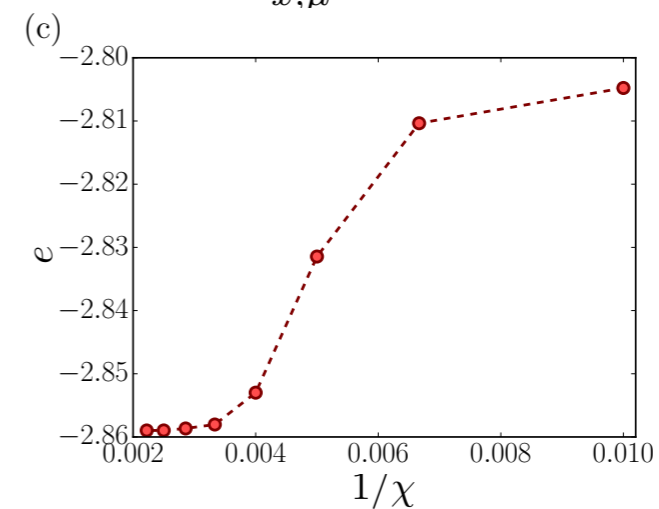
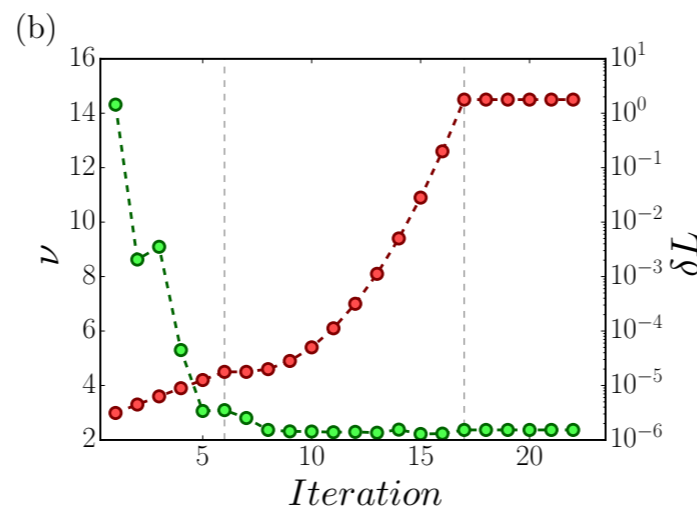
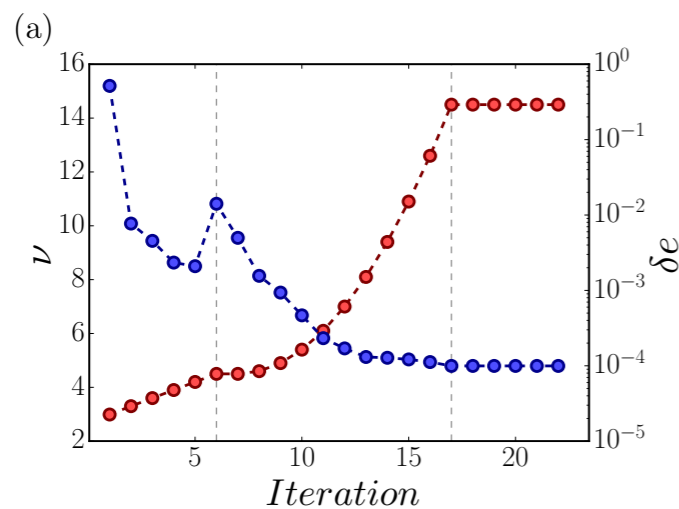
$$\hat{G}_x = \hat{\psi}_x^\dagger \hat{\psi}_x - \frac{1 - (-1)^x}{2} - \sum_{\mu} \hat{E}_{x,\mu}$$



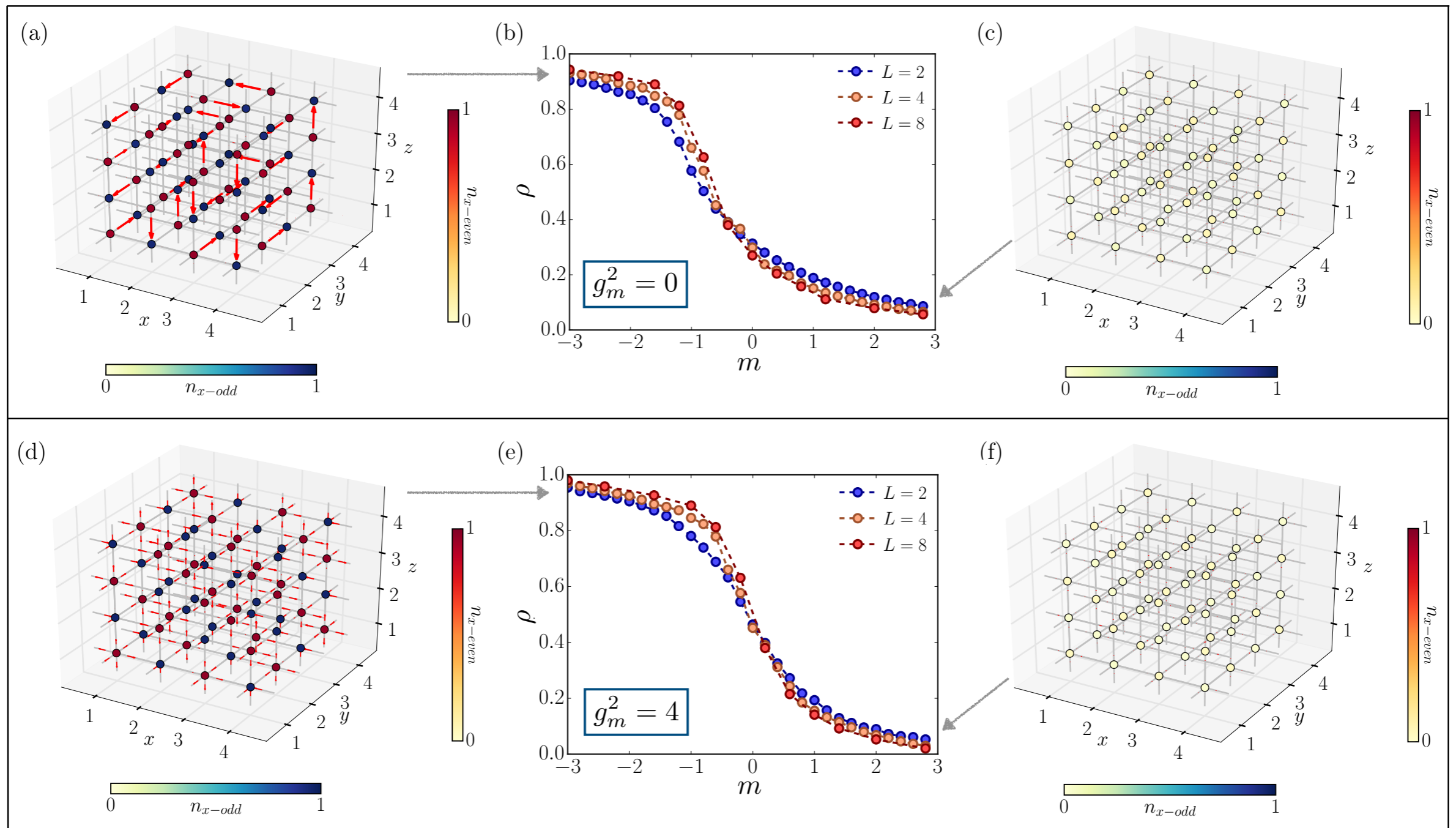
Local dimension 267, up to 12288 Hamiltonian operators

Up to 5 weeks x 64 cores of computational time

$$H_{pen} = \nu \sum_{x,\mu} \left(1 - \delta_{2, \hat{L}_{x,\mu}} \right)$$



QUANTUM PHASES



$$m_c \approx +0.22$$

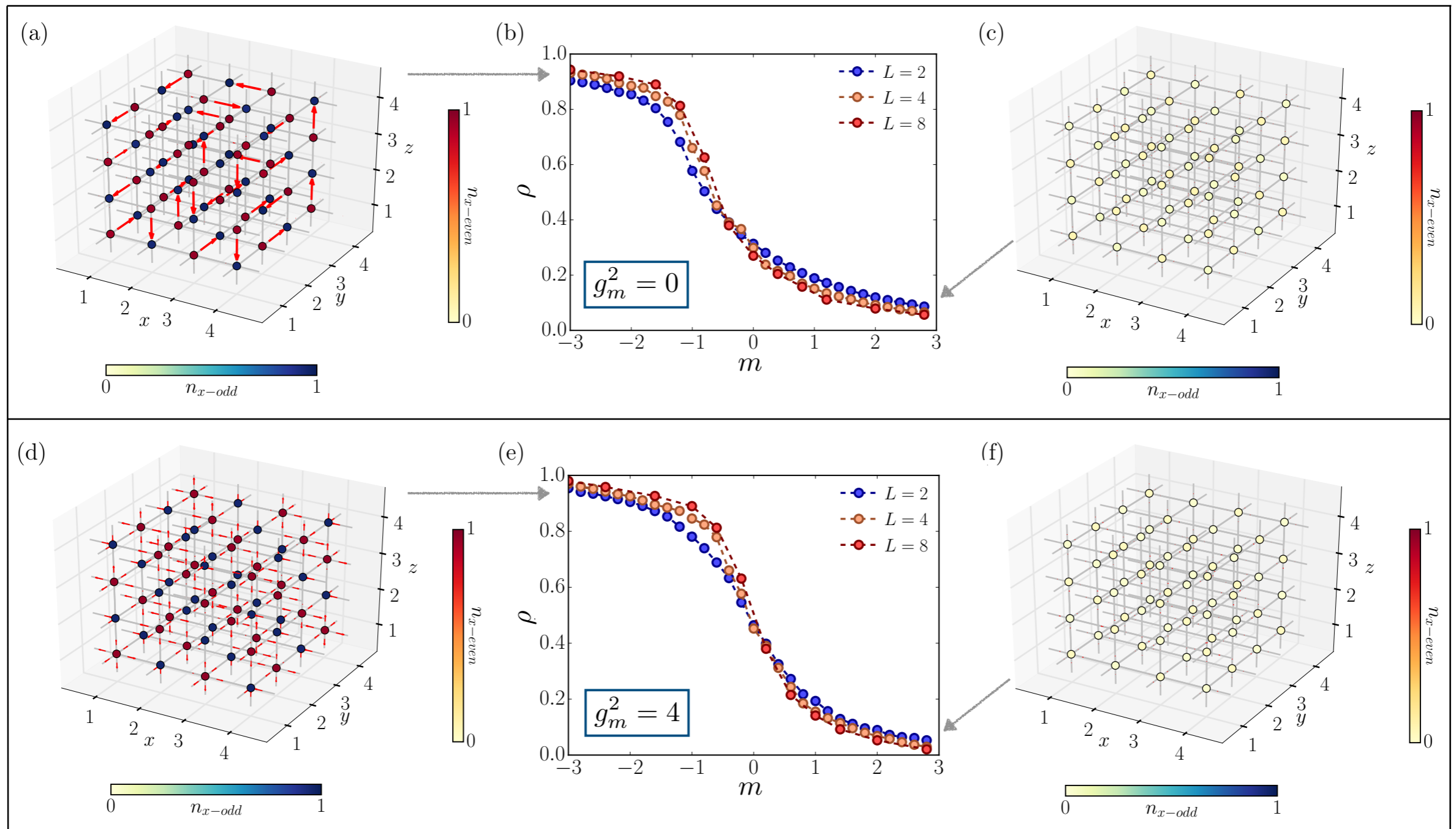
$$g_m^2 = 8/g_e^2$$

QUANTUM PHASES

Hilbert space of

4Kb QRAM

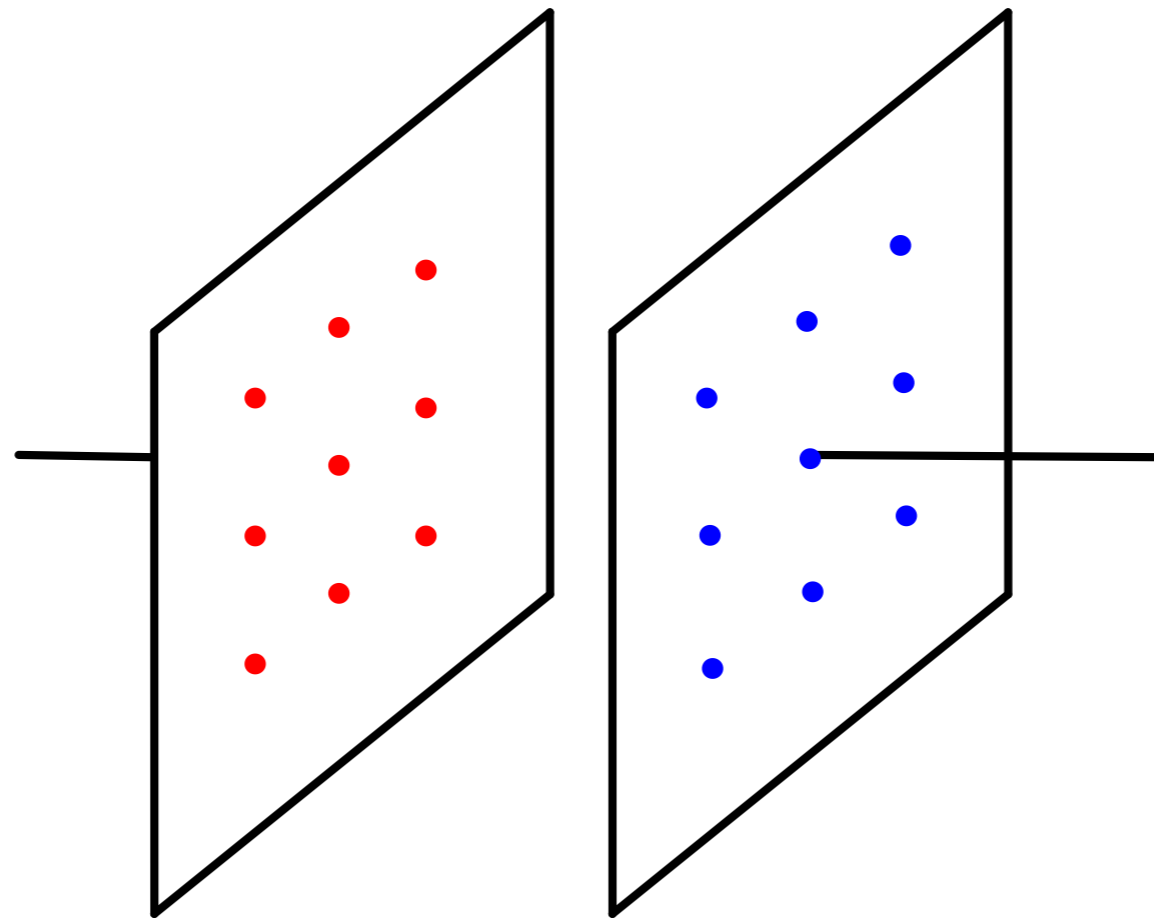
$\sim 8^4$ qubits!



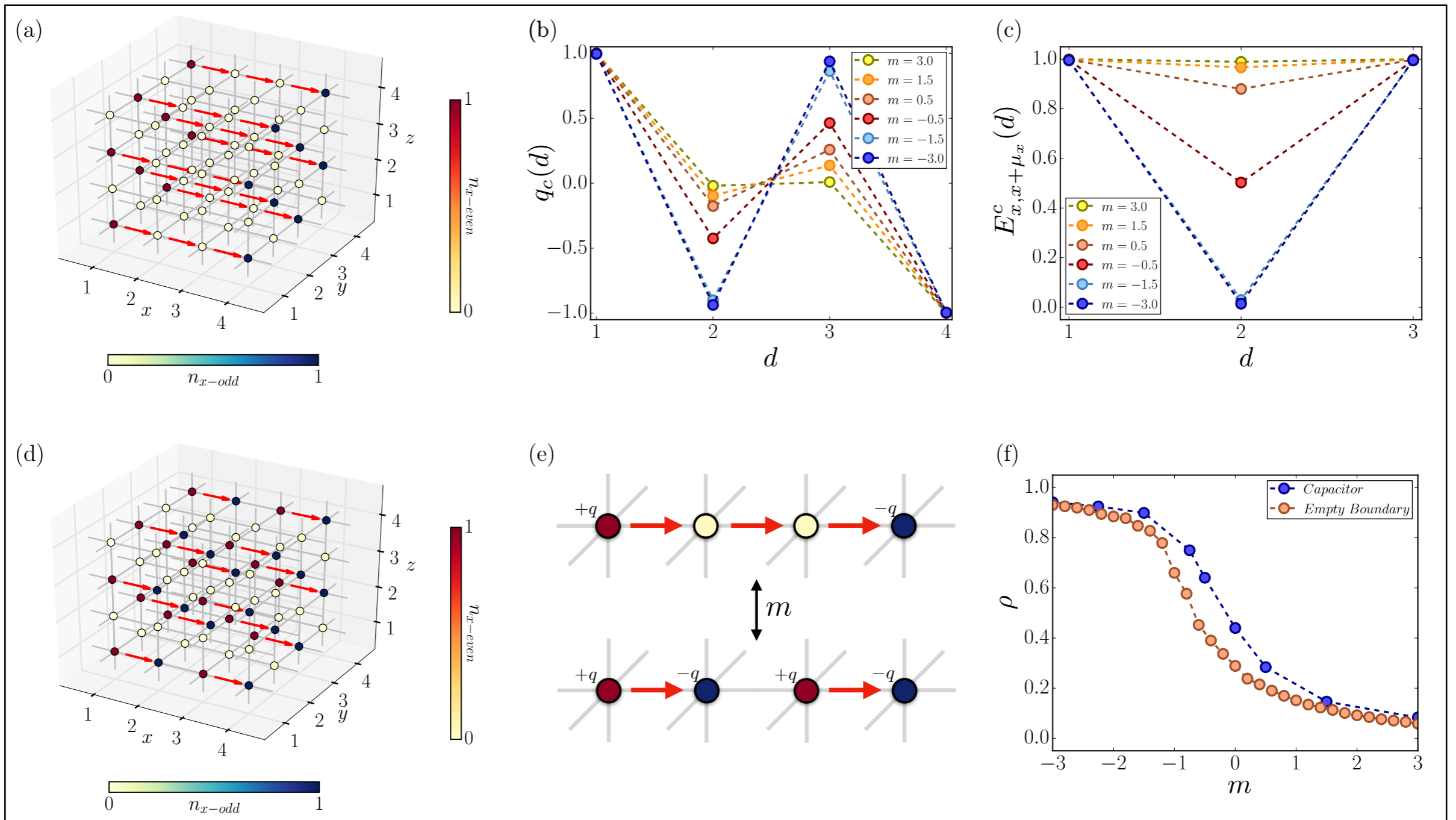
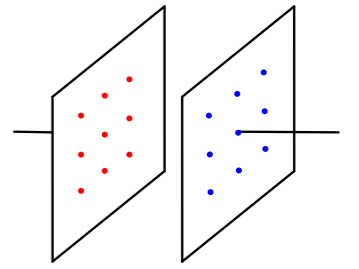
$$m_c \approx +0.22$$

$$g_m^2 = 8/g_e^2$$

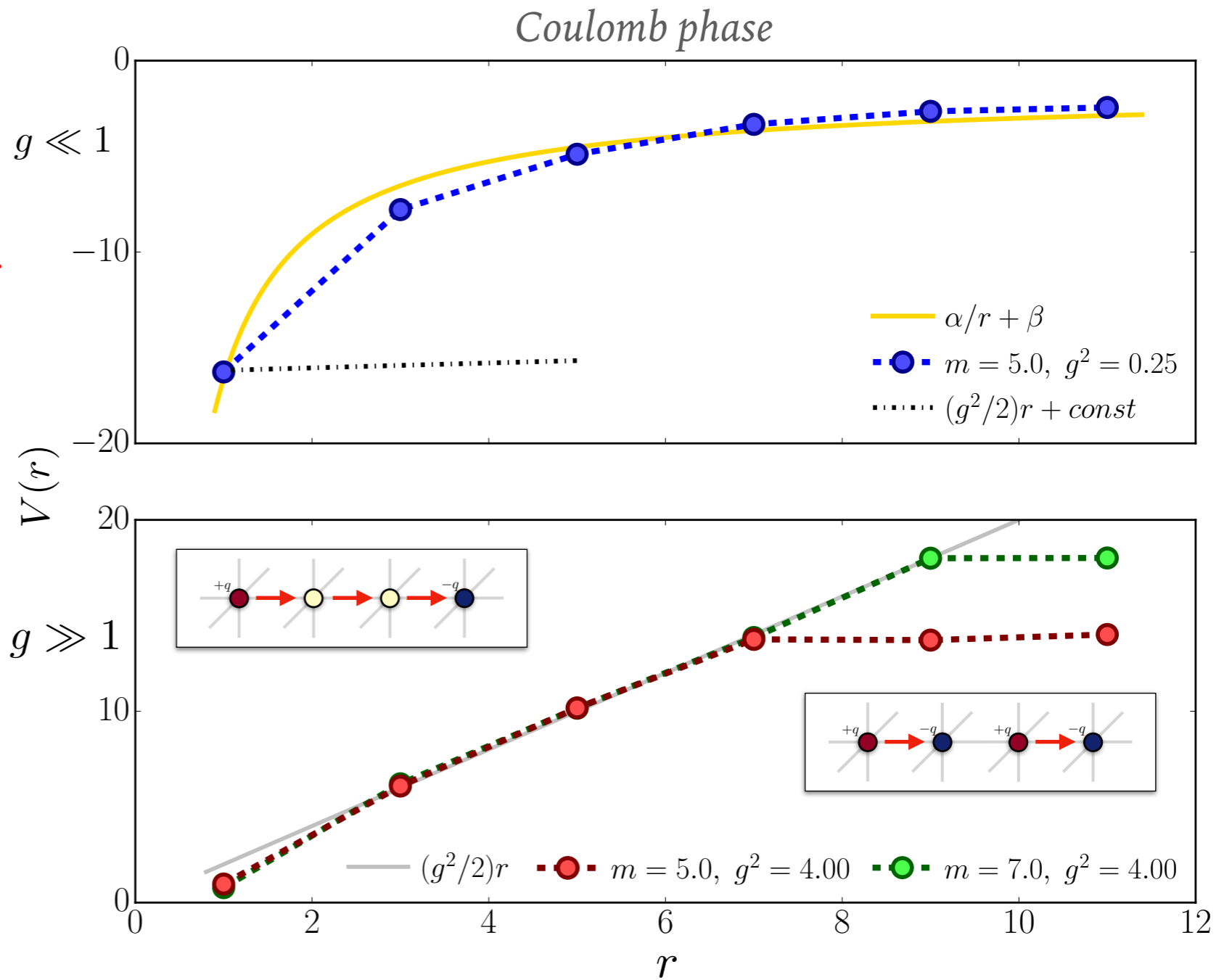
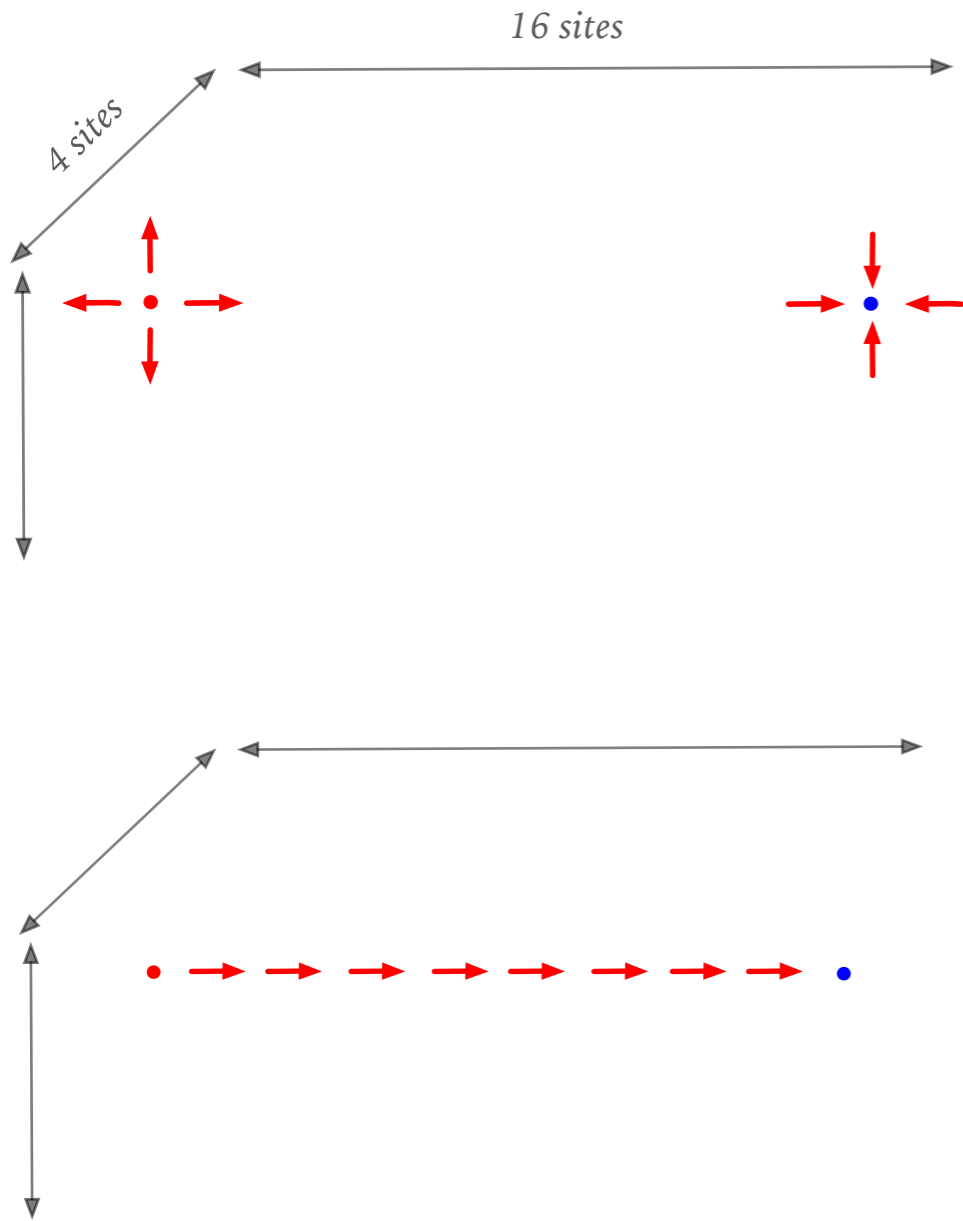
SCREENING



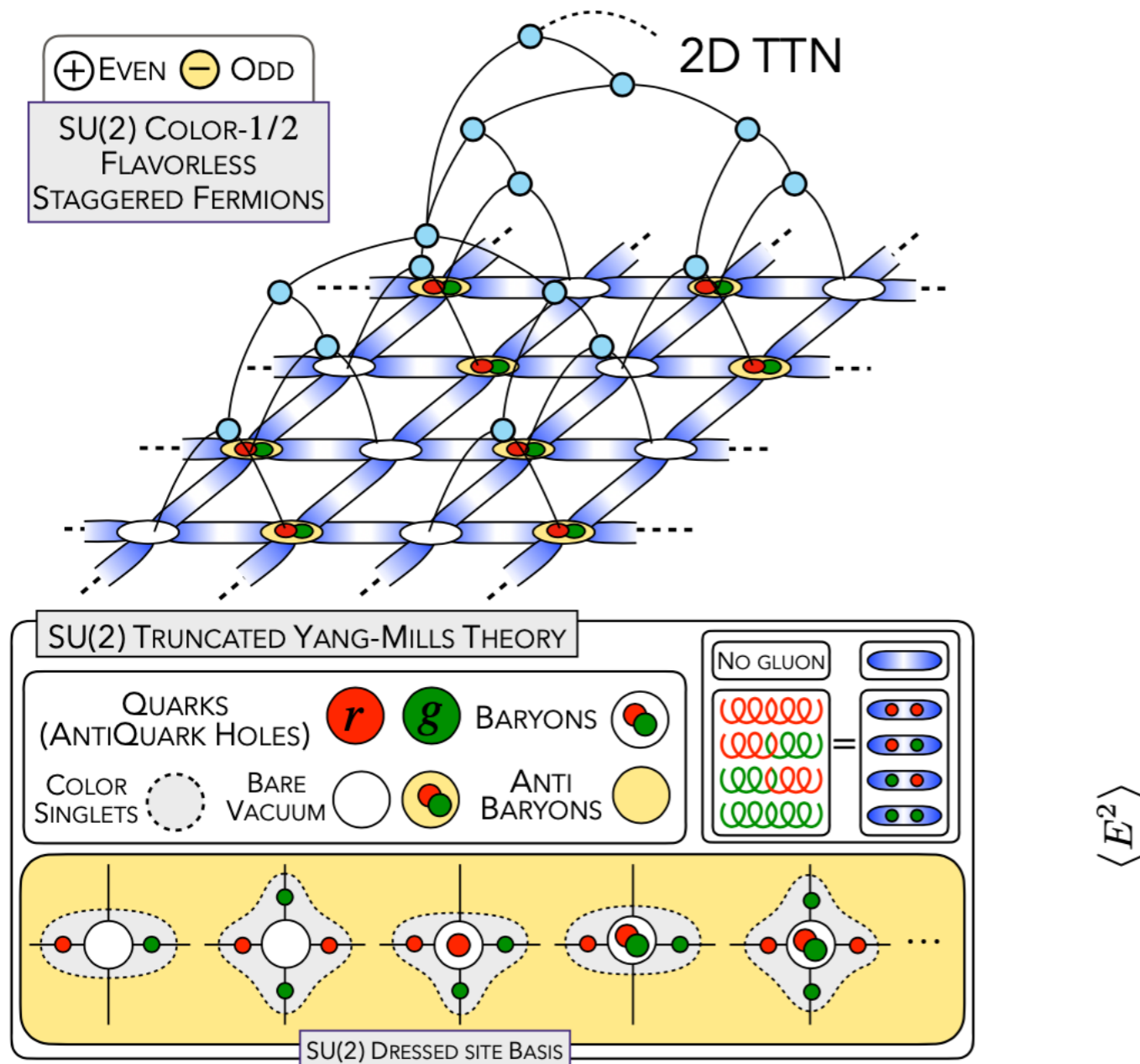
SCREENING



CONFINEMENT



2+1D NON-ABELIAN LGT

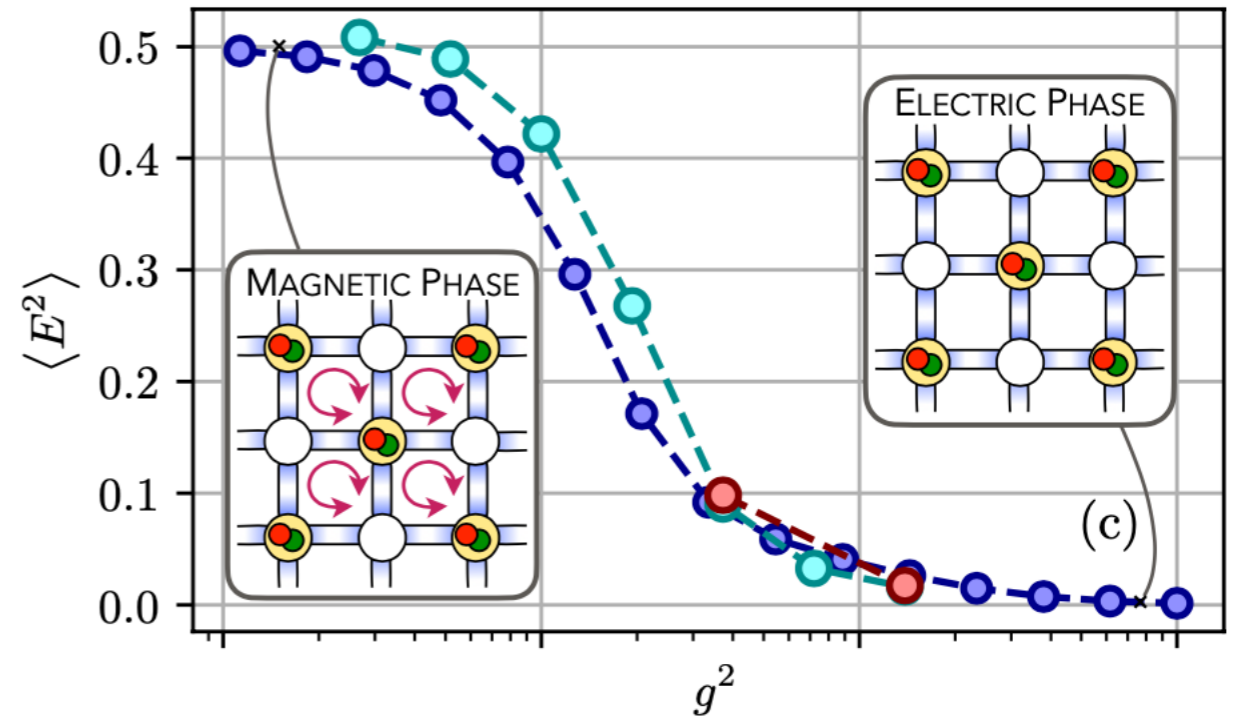
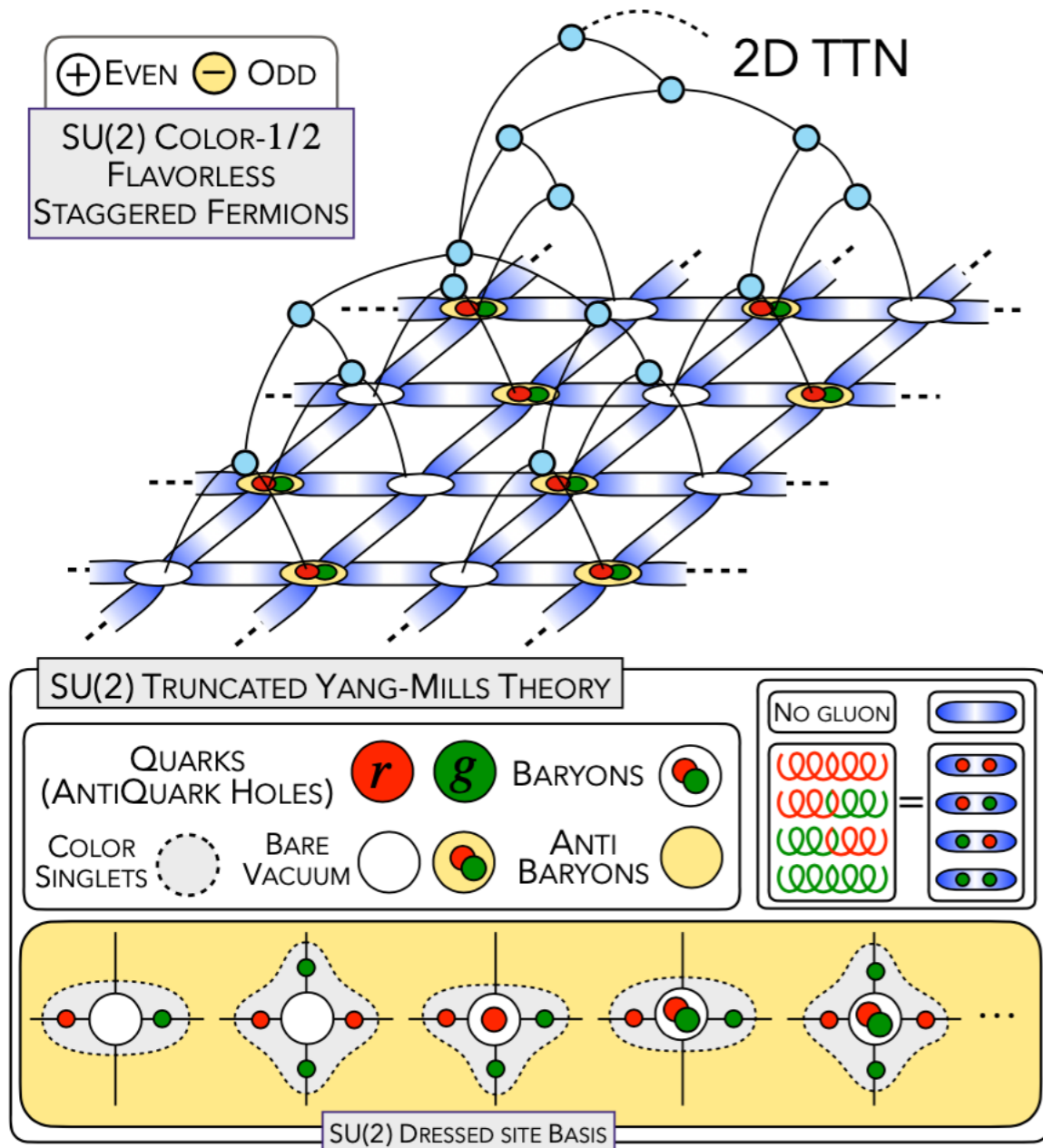


(2+1)D SU(2) Yang-Mills Lattice Gauge Theory at finite density via tensor networks

G. Cataldi, G. Magnifico, P. Silvi, SM

arXiv:2307.09396

2+1D NON-ABELIAN LGT

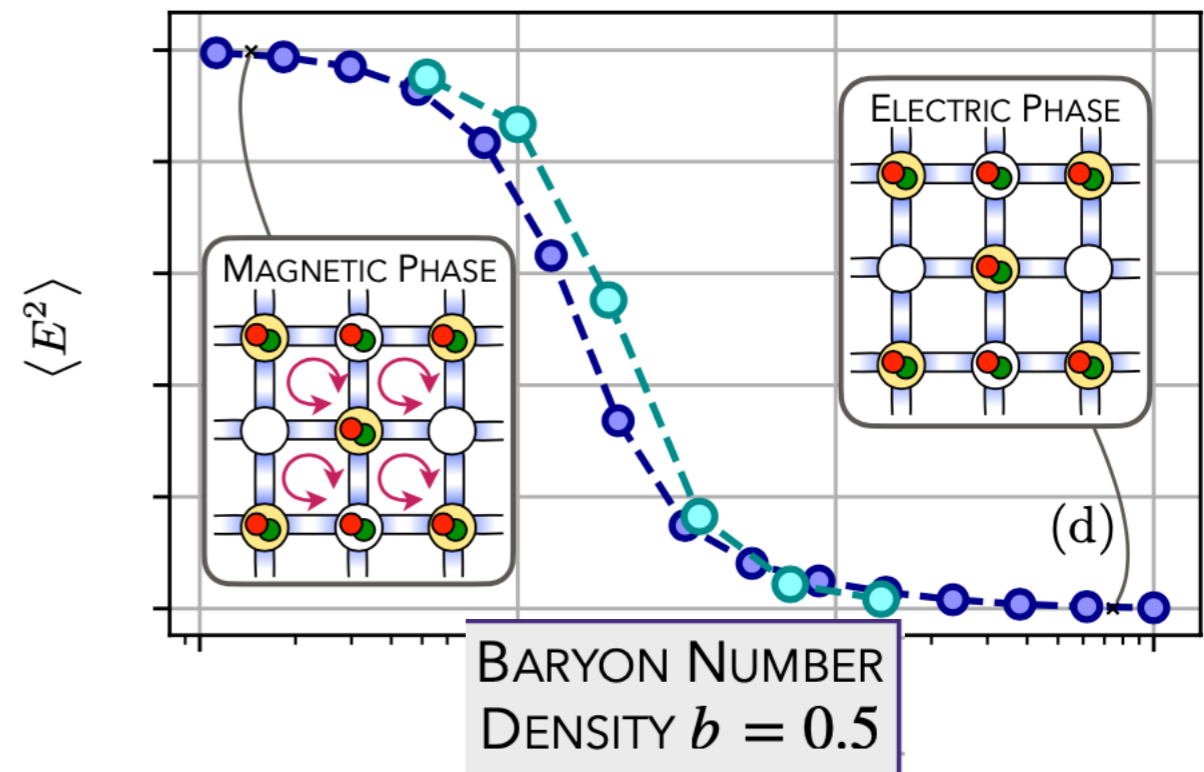
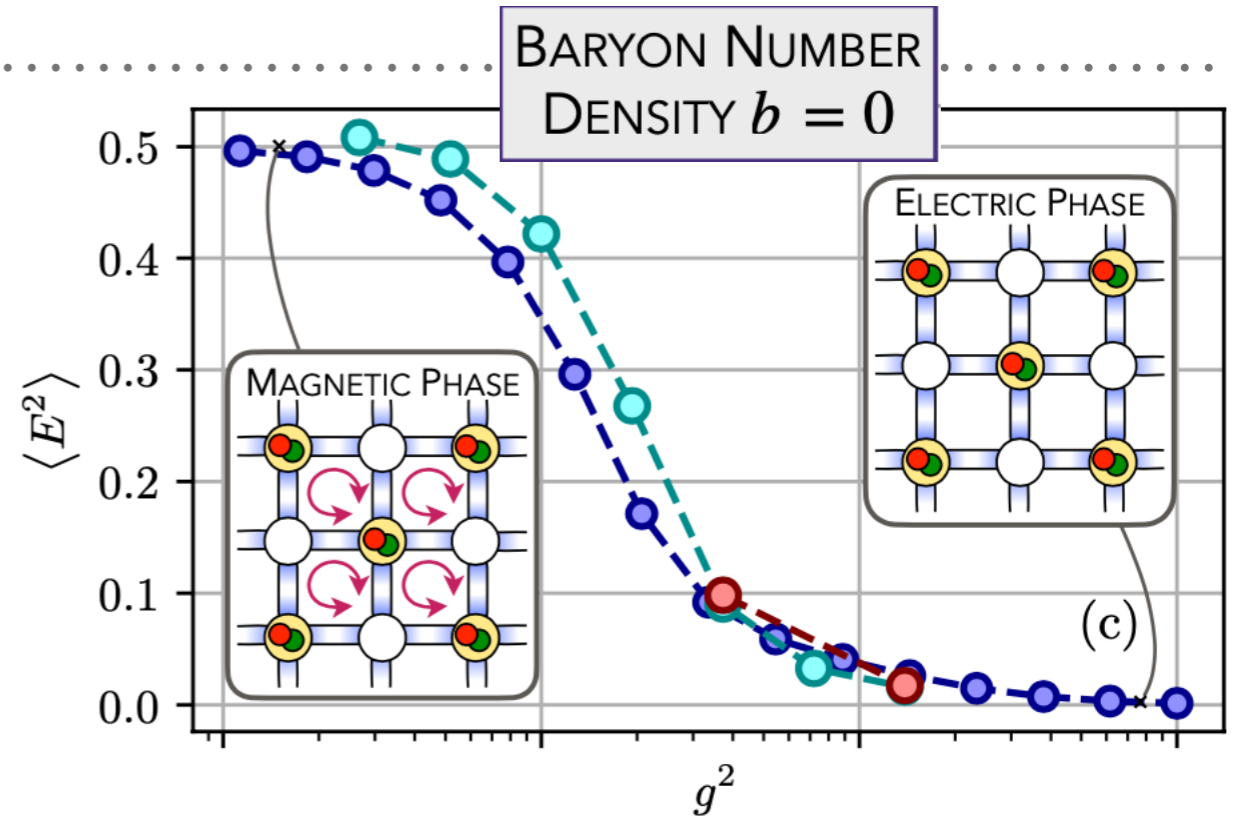
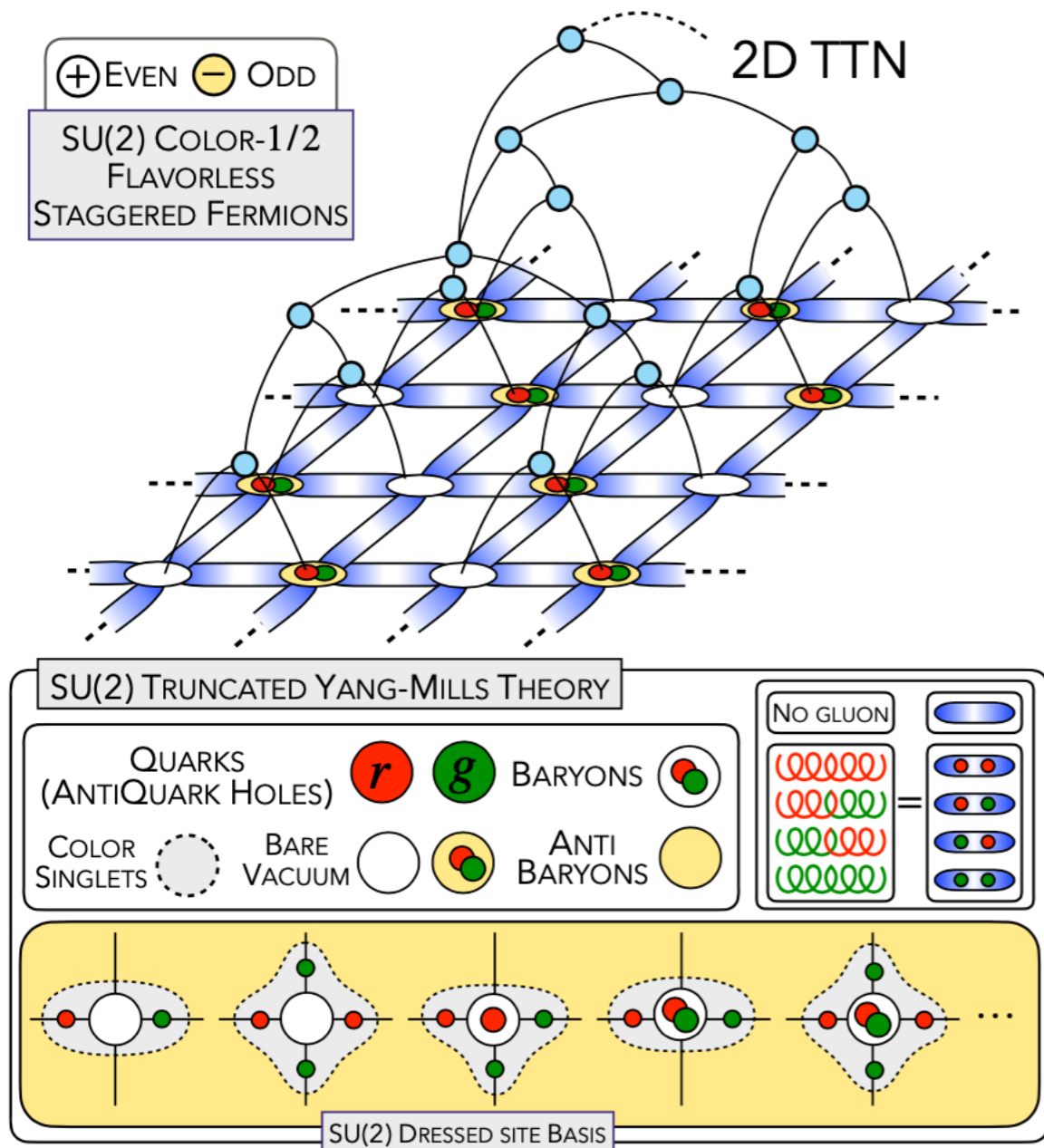


(2+1)D SU(2) Yang-Mills Lattice Gauge Theory at finite density via tensor networks

G. Cataldi, G. Magnifico, P. Silvi, SM

arXiv:2307.09396

2+1D NON-ABELIAN LGT

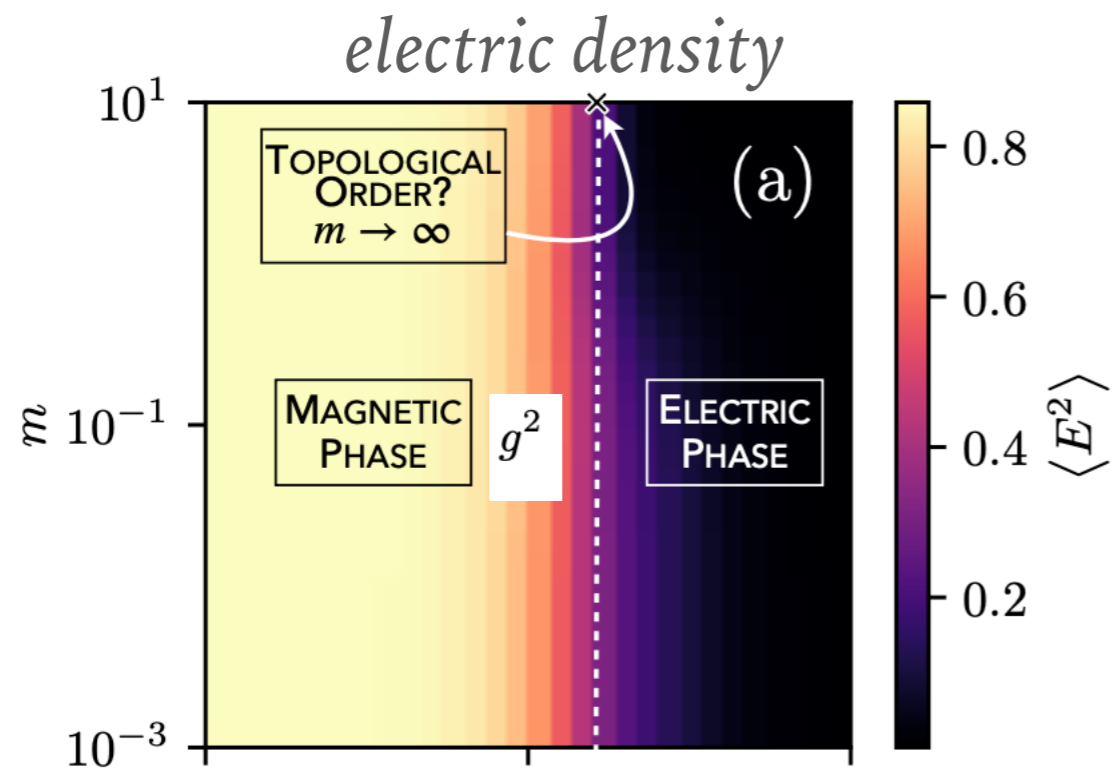


(2+1)D SU(2) Yang-Mills Lattice Gauge Theory at finite density via tensor networks

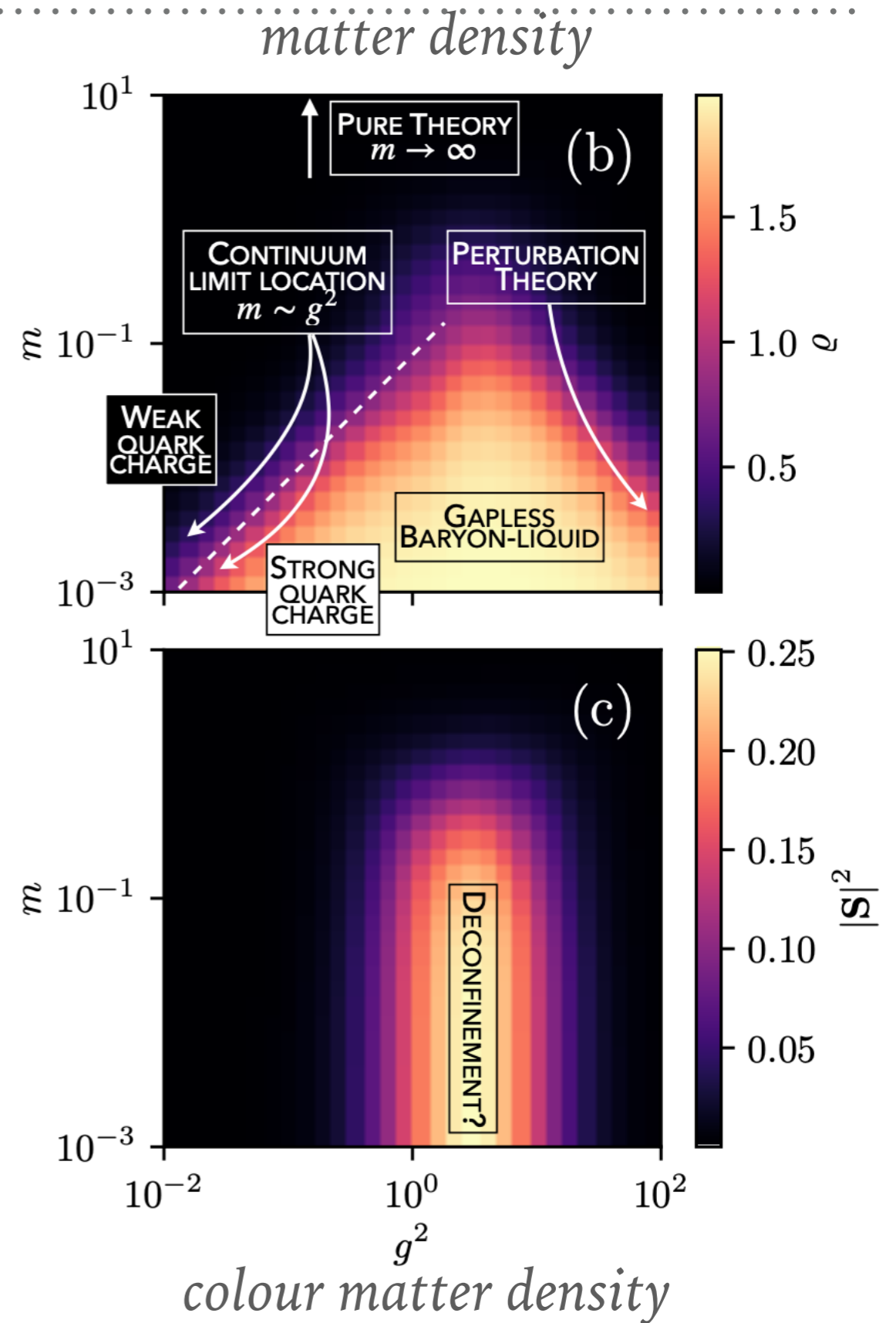
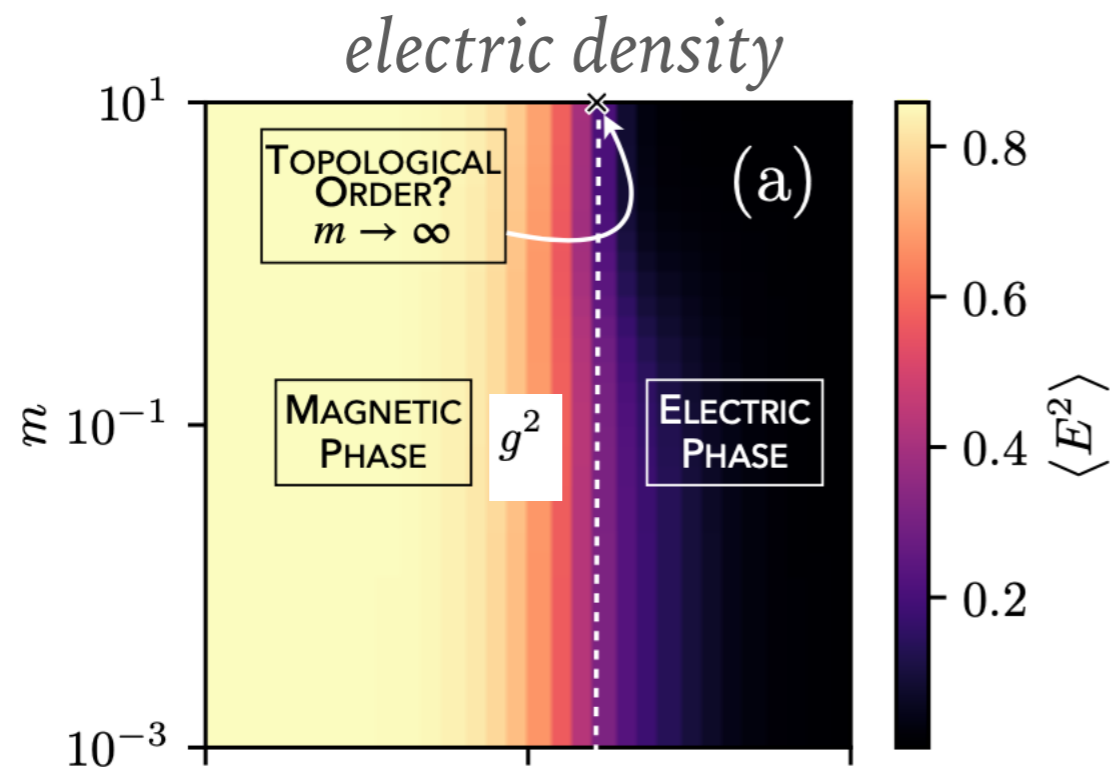
G. Cataldi, G. Magnifico, P. Silvi, SM

arXiv:2307.09396

2D+1 SU(2) FINITE-SIZE PHASE DIAGRAM



2D+1 SU(2) FINITE-SIZE PHASE DIAGRAM



ROADMAP FOR QUANTUM(-INSPIRED) LGT SIMULATION

ROADMAP FOR QUANTUM(-INSPIRED) LGT SIMULATION

3. [arXiv:2407.03058](#) [[pdf](#), [other](#)]

hep-lat

cond-mat.str-el

hep-th

physics.comp-ph

quant-ph

Tensor Networks for Lattice Gauge Theories beyond one dimension: a Roadmap

Authors: Giuseppe Magnifico, Giovanni Cataldi, Marco Rigobello, Peter Majcen, Daniel Jaschke, Pietro Silvi, Simone Montangero

ROADMAP FOR QUANTUM(-INSPIRED) LGT SIMULATION

3. [arXiv:2407.03058](https://arxiv.org/abs/2407.03058) [pdf, other]

hep-lat

cond-mat.str-el

hep-th

physics.cc

Tensor Networks for Lattice Gauge The Roadmap

Authors: Giuseppe Magnifico, Giovanni Cataldi, M. Pietro Silvi, Simone Montangero

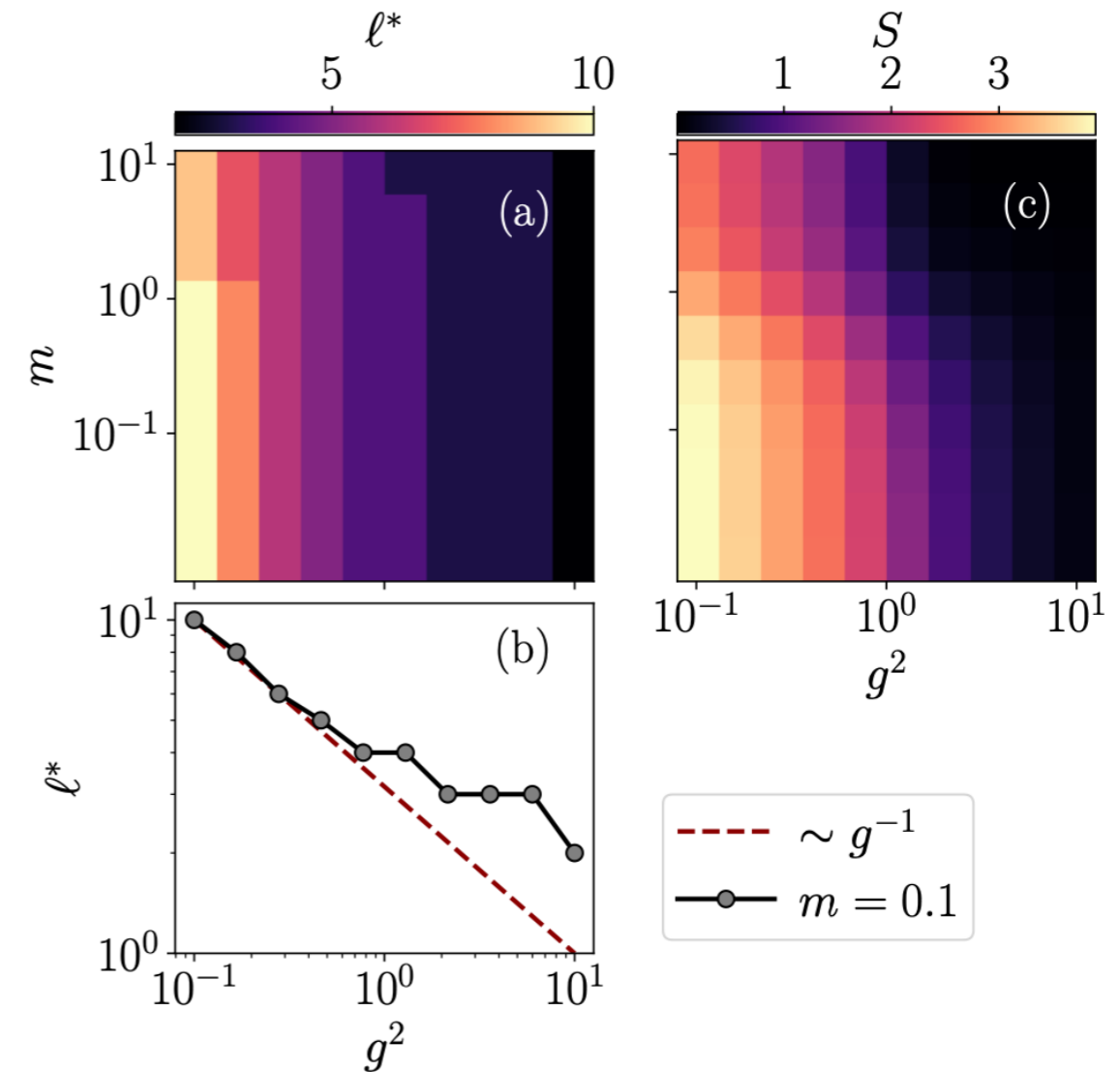


FIG. 4. Exact diagonalization of a QED plaquette for a grid of masses and couplings, $m \in [10^{-2}, 10^1]$ and $g^2 \in [10^{-1}, 10^1]$. (a,b) Minimal gauge truncation ℓ^* required to reach a precision $\epsilon_{\text{trunc}} = 10^{-5}$ in the magnetic energy $\langle \text{Re} \hat{U}_{\square} \rangle$. (c) Corresponding entanglement entropy S associated with a symmetric bipartition of the plaquette.

ROADMAP FOR QUANTUM(-INSPIRED) LGT SIMULATION

3. [arXiv:2407.03058](https://arxiv.org/abs/2407.03058) [pdf, other]

hep-lat

cond-mat.str-el

hep-th

physics.cc

Tensor Networks for Lattice Gauge The Roadmap

Authors: Giuseppe Magnifico, Giovanni Cataldi, M. Pietro Silvi, Simone Montangelo

ℓ	d					
	(2 + 1)-dimensions			(3 + 1)-dimensions		
	U(1)	SU(2)	SU(3)	U(1)	SU(2)	SU(3)
1	35	30	164	267	178	3096
2	165	168	752	3437	3670	52476
3	455	600	3738	18487	35280	813438
4	969	1650	19878	64953	214958	17490134
5	1771	3822	43698	177155	967466	69232482
6	2925	7840	82128	408421	3509062	228461186
7	4495	14688	212496	835311	10828494	1245755754
8	6545	25650	333538	1561841	29473038	2782999996

TABLE I. Dressed site Hilbert space dimension d for increasing number ℓ of allowed electric energy density levels in some 2- and 3-dimensional paradigmatic LGTs with dynamical matter and gauge groups U(1), SU(2), and SU(3).

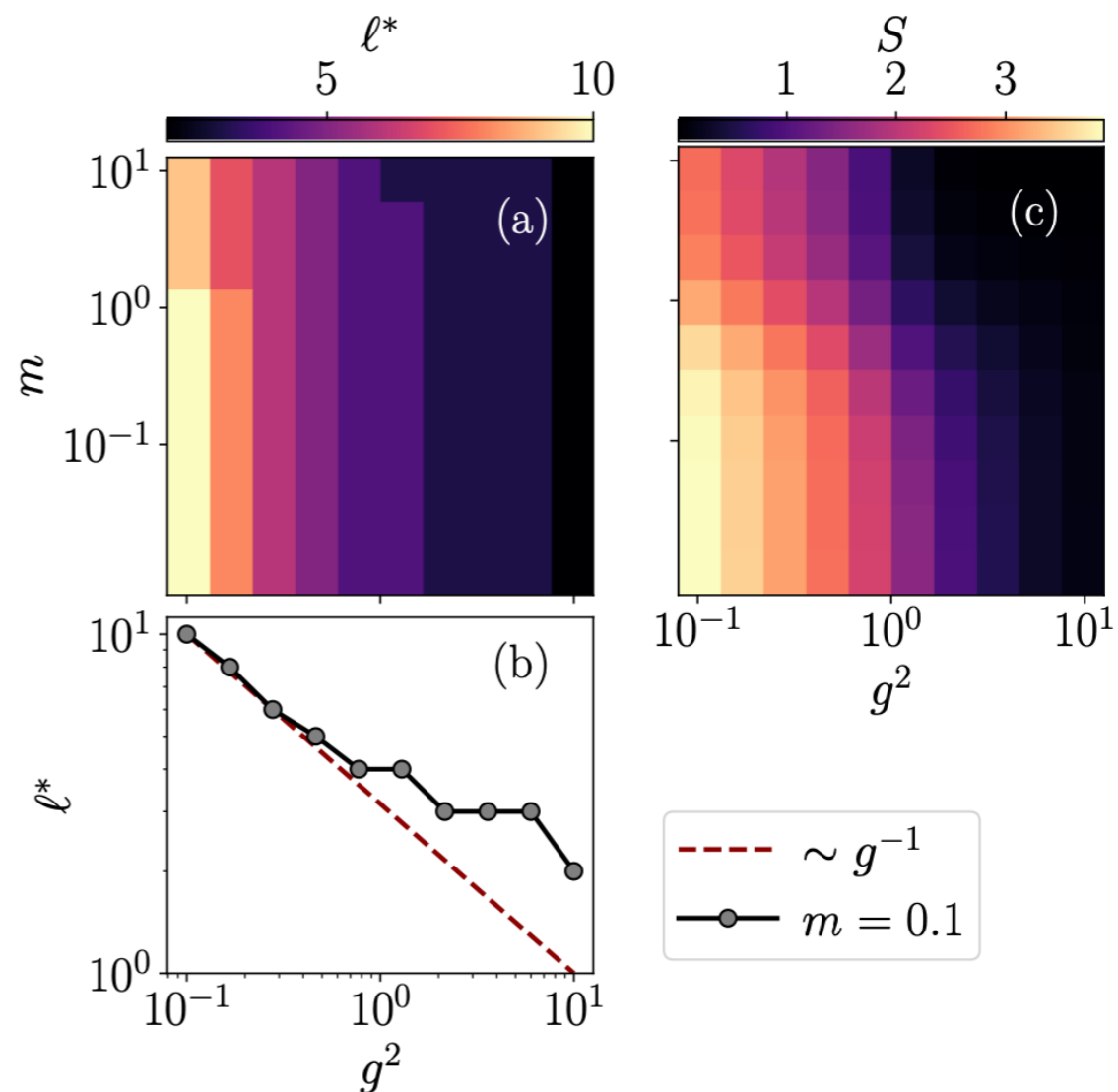


FIG. 4. Exact diagonalization of a QED plaquette for a grid of masses and couplings, $m \in [10^{-2}, 10^1]$ and $g^2 \in [10^{-1}, 10^1]$. (a,b) Minimal gauge truncation ℓ^* required to reach a precision $\epsilon_{\text{trunc}} = 10^{-5}$ in the magnetic energy $\langle \text{Re} \hat{U}_{\square} \rangle$. (c) Corresponding entanglement entropy S associated with a symmetric bipartition of the plaquette.

ROADMAP FOR QUANTUM(-INSPIRED) LGT SIMULATION

3. [arXiv:2407.03058](#) [[pdf](#) [other](#)]

hep-lat con

Tensor Net
Roadmap

Authors: Giuse
Pietro Silvi, Sim

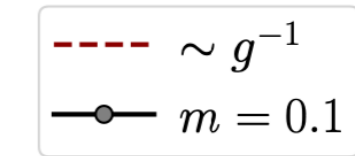
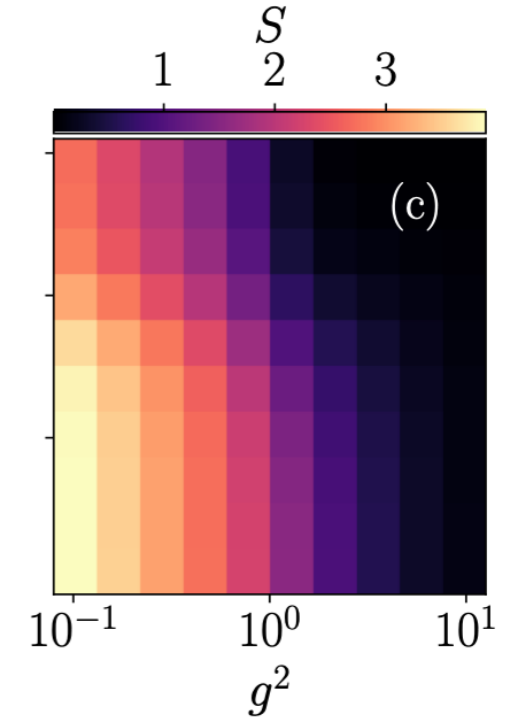
ℓ	(2 + 1)-dimensions		
	U(1)	SU(2)	SU(3)
1	35	30	16
2	165	168	75
3	455	600	375
4	969	1650	1987
5	1771	3822	4369
6	2925	7840	8212
7	4495	14688	21249
8	6545	25650	33359

TABLE I. Dressed site counts for increasing number ℓ of a tensor network in some 2- and 3-dimensional matter and gauge groups U(1), SU(2), and SU(3).

System size	χ	Factor	Estimated walltime
64×64	450	T_{base}	4.16 days
64×64	900	$16 \cdot T_{\text{base}}$	66.6 days
256×256	450	$28 \cdot T_{\text{base}}$	116.5 days
256×256	900	$448 \cdot T_{\text{base}}$	5.1 years
$16 \times 16 \times 16$	450	$4 \cdot T_{\text{base}}$	16.6 days
$16 \times 16 \times 16$	900	$64 \cdot T_{\text{base}}$	266 days
$64 \times 64 \times 64$	450	$1984 \cdot T_{\text{base}}$	23 years
$64 \times 64 \times 64$	900	$31744 \cdot T_{\text{base}}$	362 years

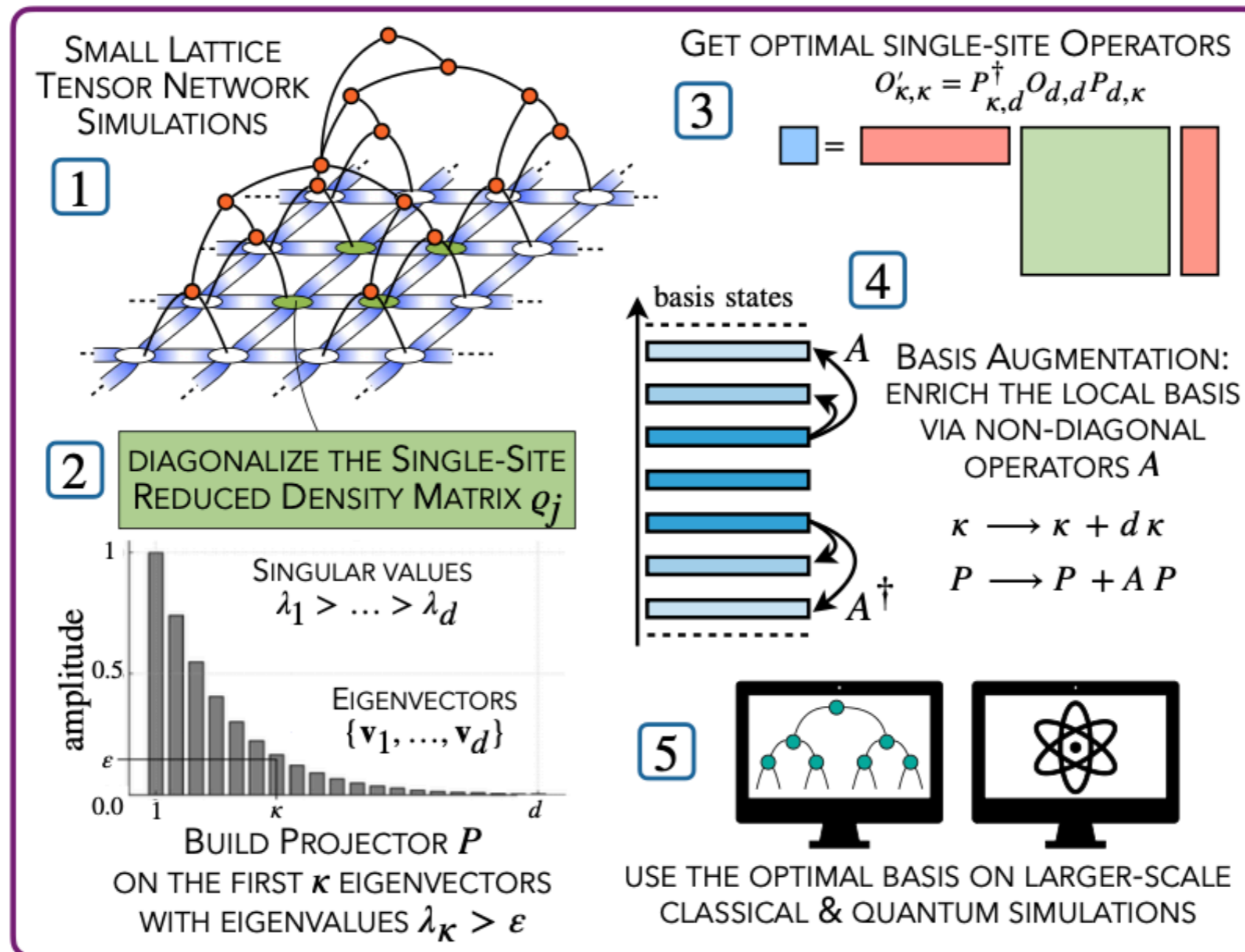
TABLE II. *Estimated simulation time.* We derive the baseline from a single-tensor optimization of a 64×64 quantum Ising simulation with \mathbb{Z}_2 symmetry taking 7192s on a A100 GPU. Further, we assume that single-tensor update, one tensor and one GPU per MPI thread, and 50 sweeps for the baseline. To extrapolate to larger systems, we assume a scaling with $\mathcal{O}(\chi^4 N^{D-1})$ as well as seven (thirty-one) tensors per MPI thread for 256×256 ($64 \times 64 \times 64$) systems. The empirical scalings are approximately a factor of 2.3 for doubling the system size and 13 for doubling the bond dimension, which we obtain from smaller simulations with $\chi = 225$ and for 32×32 qubits. The times are valid for any $d < \chi$.

ℓ^*

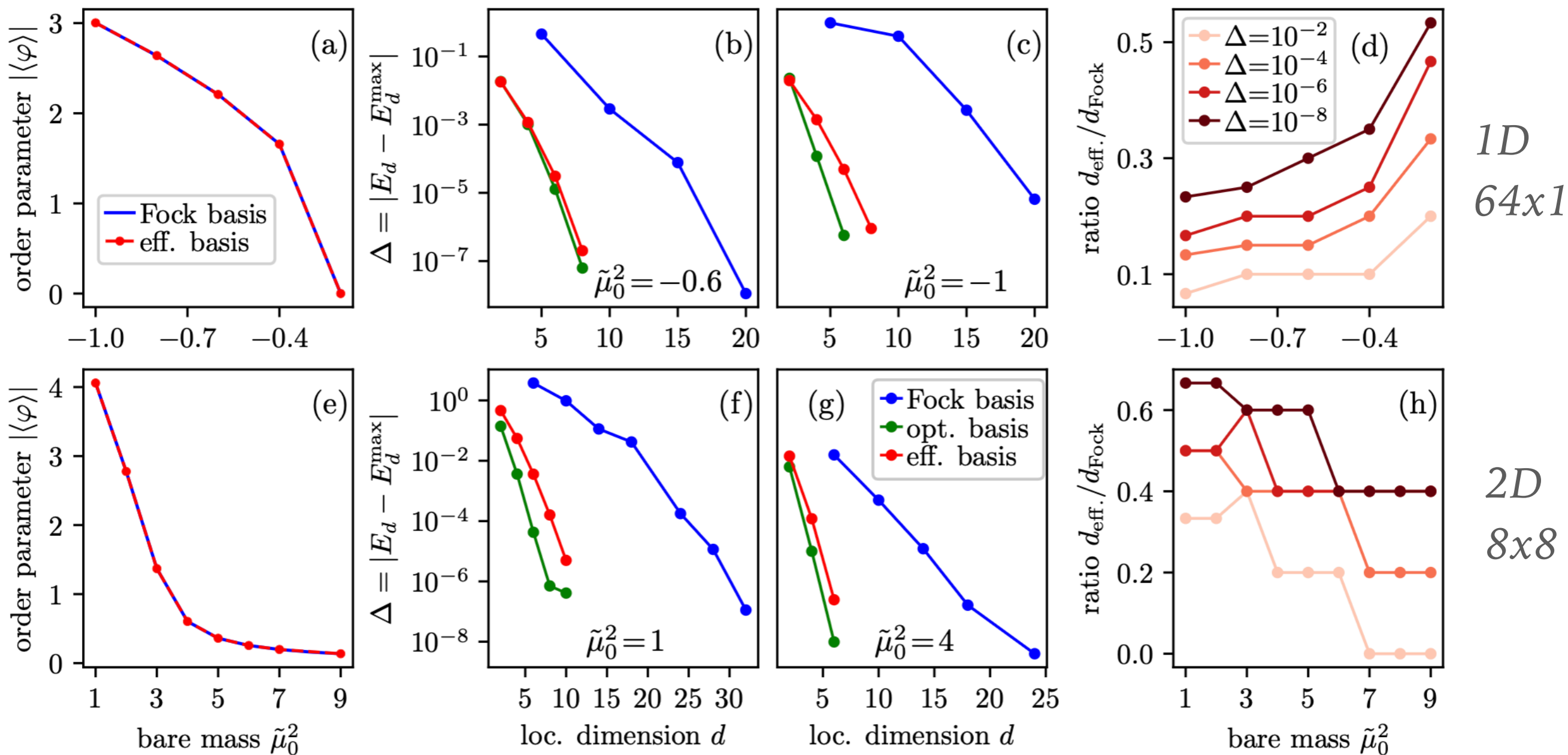


(c) Correlation length S associated with a symmetric bipartition of the plaquette. (d) A QED plaquette for a grid $[-2, 10^1]$ and $g^2 \in [10^{-1}, 10^1]$. ℓ^* required to reach a precise energy $\langle \text{Re} \hat{U}_{\square} \rangle$.

OPTIMAL TRUNCATED BASIS FOR QUANTUM SIMULATIONS



PHI4 MODEL



$$\hat{H} = \sum_{\mathbf{n}, k} \left[\frac{\hat{\pi}_{\mathbf{n}}^2}{2a} + \frac{(\hat{\varphi}_{\mathbf{n}+\mu_k} - \hat{\varphi}_{\mathbf{n}})^2}{2a} + \frac{a\mu_0^2}{2} \hat{\varphi}_{\mathbf{n}}^2 + \frac{a\lambda}{4!} \hat{\varphi}_{\mathbf{n}}^4 \right]$$

TAKE HOME MESSAGES

- Tensor network algorithms can be used to benchmark, verify, support and guide quantum simulations/computations
- High-dimensional tensor network simulations are becoming increasingly efficient and able to investigate interesting physics
- Entanglement of mixed many-body states can be quantified
- Scalability to full HPC will be necessary to produce quantitative results
- Interesting developments also in other directions (classical optimisers/annealers)
- Tensor network machine learning is competitive with DNN



Tensor Networks in Simulation of Quantum matter



QUANTUM
Information and Matter

quantum.dfa.unipd.it
qcsc.dfa.unipd.it



Dipartimento
di Fisica
e Astronomia
Galileo Galilei



UNIVERSITÀ
DEGLI STUDI
DI PADOVA

Thank you for your attention!

Simone Montangero
Marco di Liberto Pietro Silvi
Ilaria Siloi Carmelo Mordini
Daniel Jaschke Giuseppe Calajò
Giuseppe Magnifico Simone Notarnicola
Davide Rattacaso Francesco Campaioli
Flavio Baccari Darvin Wanish
Lorenzo Maffi Luka Pavešić
Marco Rigobello Giovanni Cataldi
Marco Ballarin Mattia Morgavi
Peter Majcen Alice Pagano
Nora Reinić Marco Tesoro
Asmita Datta Rocco Barač

Positions available!



Tensor Networks in Simulation of Quantum matter



QUANTUM
Information and Matter

quantum.dfa.unipd.it
qcsc.dfa.unipd.it



Dipartimento
di Fisica
e Astronomia
Galileo Galilei



UNIVERSITÀ
DEGLI STUDI
DI PADOVA